

**Dissertation zur Erlangung des Doktorgrades der Fakultät für Chemie und
Pharmazie der Ludwig-Maximilians-Universität München**

**The adaptor protein Migfilin is dispensable for mouse
development and homeostasis, but suppresses tetraploidy
and acts as a tumor suppressor in skin**

Daniel V. Moik

aus

Dortmund

2011

Erklärung

Diese Dissertation wurde im Sinne von § 13 Abs. 3 bzw. 4 der Promotionsordnung vom 29. Januar 1998 (in der Fassung der vierten Änderungssatzung vom 26. November 2004) von Herrn Prof. Dr. Reinhard Fässler betreut.

Ehrenwörtliche Versicherung

Diese Dissertation wurde selbständig, ohne unerlaubte Hilfe erarbeitet.

München, den 15. April 2011

.....

(Unterschrift des Autors)

Dissertation eingereicht am 19. April 2011

1. Gutachter: Prof. Dr. Reinhard Fässler

2. Gutachter: Prof. Dr. Angelika Vollmar

Mündliche Prüfung am 12. Mai 2011

Für meine Frau, meine Tochter, und meine ganze Familie.

Table of contents

Table of figures	VI
1. List of publications	1
2. Abbreviations	2
3. Summary.....	3
4. Introduction	5
Migfilin and the Zyxin family.....	5
Migfilin function in its sub-cellular compartments.....	7
Migfilin in focal adhesions	7
Migfilin in cell-cell adhesions.....	8
Nuclear functions of migfilin	9
Gene targeting of migfilin in mouse using Cre recombinase.....	9
Cre recombinase – a useful tool with routinely overlooked side-effects	10
General role and composition of skin.....	11
Epidermis	12
Dermis and subcutis.....	14
Skin appendages	15
Epidermis in development and homeostasis	15
Development of hair follicles	16
The inflammatory stress response in skin.....	16
Mouse mutants displaying reactive epidermal hyperplasia	17
Treatment of reactive epidermal hyperplasia	18
Cutaneous inflammation and skin cancer	19
Non-melanoma skin cancer	19
The DMBA/TPA skin cancer model.....	20

The cell cycle	22
Progression through mitosis.....	24
Tetraploidy, aneuploidy and cancer	26
Roads to tetraploidy	28
Mechanisms of CIN.....	30
Suppression of tetraploidy/aneuploidy	33
Mechanism of p53-mediated repression of tetraploidy/aneuploidy.....	35
5. Aim of the thesis	36
6. Brief summaries of the publications	37
7. References.....	39
8. Acknowledgements.....	49
9. Curriculum vitae	51
10. Supplements.....	52
Moik et al, 2011a	53
Supplementary Figure Legends – Moik et al. 2011a.....	62
Moik et al, 2011b	70

Table of figures

Figure 1: Domain architecture and sub-cellular localization of migfilin.	6
Figure 2: Architecture of mammalian skin and epidermis.....	12
Figure 3: p53-mediated epidermal tanning.....	14
Figure 4: 3-stage skin cancer model – initiation, promotion, progression.....	22
Figure 5: The cell cycle	26
Figure 6: Roads to tetraploidy.	29
Figure 7: Supernumerary centrosomes promote aneuploidy.....	32

1. List of publications

This thesis founds on the following manuscripts, which are referred to as **Moik et al. 2011a** or **b**, respectively.

Manuscript I (Moik et al., 2011a)

Daniel V. Moik, Vaibhao C. Janbandhu, Reinhard Fässler (2011). Loss of migfilin expression has no overt consequences on murine development and homeostasis, *J Cell Sci***124**, 414-21.

Manuscript II (Moik et al., 2011b)

Daniel V. Moik, Vaibhao C. Janbandhu, Christian Kuffer, Zuzana Storchova, Reinhard Fässler (2011). Migfilin represses tetraploidy and acts a tumor suppressor in skin, *manuscript in preparation*.

2. Abbreviations

+	wild-type allele
-	null allele
AJ	adherens junctions
AMP	adenosine-monophosphate
AMPK	AMP-activated protein kinase
ATM	ataxia telangiectasia mutated
ATR	ATM- and Rad3-related
BCC	basal cell carcinoma
xC	x chromosome complements
CDK	cyclin-dependent kinase
CIN	chromosomal instability
CSF	colony-stimulating factor
DMBA	7,12-Dimethylbenz(a)anthracene
DNA-PK	DNA-dependent protein kinase
ECM	extra-cellular matrix
ES cells	embryonic stem cells
FA	focal adhesion
Fblim1	filamin-binding LIM protein 1
fl	floxed allele
IFE	interfollicular epidermis
IL-1	interleukin-1
IL1RA	interleukin-1 receptor antagonist
IR	ionizing radiation
<i>Kn</i>	keratin <i>n</i>
LIM	Lin-11/Is1-1/Mec-3
xN	(x multiples of) the monoploid chromosome complement
NES	nuclear export signal
NMSC	non-melanoma skin cancer
ORS	outer root sheath
PPAR β/δ	peroxisome proliferator-activated receptor β/δ
SAC	spindle assembly checkpoint
SCC	squamous cell carcinoma
siRNA	short interfering RNA
Tnf(r)	tumor necrosis factor (receptor)
TPA	12-O-Tetradecanoylphorbol-13-acetate

3. Summary

Integrins are major cellular adhesion molecules that mediate binding to the extracellular matrix (ECM). Cell adhesion to the ECM is essential for the development and homeostasis of all multi-cellular organisms. The affinity of integrins for matrix ligands is increased by the β integrin tail binding proteins talin and kindlin, and decreased by filamin. Migfilin was found to interact both with kindlin-2 and filamins *in vitro*. siRNA-mediated depletion of migfilin was reported to interfere with cell adhesion and spreading, which made the study of migfilin *in vivo* an interesting case for increasing our understanding of integrin function. To this end, we disrupted its expression in mice using the gene ablation technology in embryonic stem (ES) cells.

To identify cell types and tissues that could be affected by the loss of migfilin expression, we investigated the expression of migfilin in cells, tissues and different developmental stages. In adult mice, migfilin was mainly expressed in heart, lung, skin, and in simple epithelia. In embryos migfilin was expressed throughout embryonic development. Migfilin-null mice had no detectable phenotypes. Moreover, integrin activation, cell adhesion and spreading were normal in primary migfilin-null cells. Migfilin-null skin keratinocytes, but not fibroblasts, had a slightly reduced migration velocity. This overall lack of defects could not be due to long-term compensatory defects, as transient siRNA-mediated depletion of migfilin also failed to produce any detectable defects in fibroblasts (these results are shown in Moik et al., 2011a).

In parallel to the analysis of the constitutive deletion of the migfilin gene in mice, we also restricted migfilin loss to the epidermis using the Cre/loxP system. Cre

expression is known to have cytotoxic off-target effects. Although migfilin-null skin was normal, the expression of Cre in migfilin-null epidermis induced a reactive inflammatory hyperplasia in the skin associated with lethality between 7-10 days after birth. Adhesion defects were not observed in the mutant epidermis. However, the Cre recombinase increased cellular ploidy and apoptosis when expressed in migfilin-null background. Apoptosis increased over time and correlated with the increasing morbidity. Since Cre-expressing wild-type epidermis was normal, these findings point to a dedicated role of migfilin as a suppressor of tetraploidy in epidermis.

A well-known suppressor of tetraploidy is p53. Deletion of p53 in Cre-expressing migfilin-null epidermis further increased morbidity, suggesting that migfilin is part of a novel tetraploidy-repression mechanism that functions independently of p53. Tetraploidy is an intermediate towards aneuploidy and promotes carcinogenesis and cancer progression *in vivo*. To test if migfilin suppresses tetraploidy-associated tumor formation independently of Cre recombinase, we exposed migfilin-null mice to the DMBA/TPA two-stage skin carcinogenesis protocol. Loss of migfilin led to significantly increased tumor incidence and number, confirming that migfilin is a *bona fide* tumor suppressor, probably by suppressing tetraploidy (these results are shown in Moik et al., 2011b).

4. Introduction

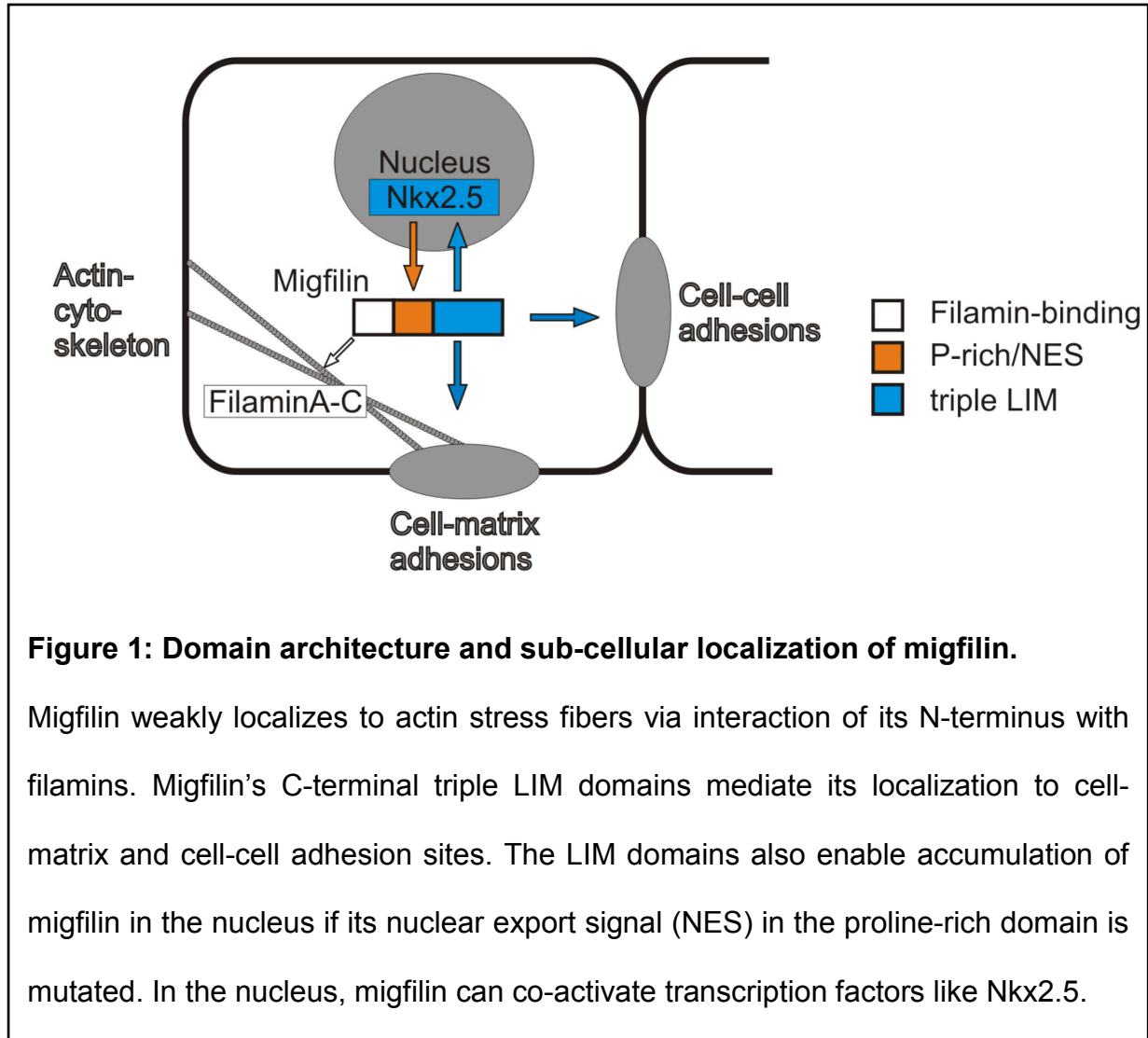
Migfilin and the Zyxin family

The zyxin gene family consists of seven highly conserved members in mammals. The genes code for adaptor proteins with a variable N-terminus, a proline-rich domain with a nuclear export signal (NES), and three C-terminal Lin-11/Isl-1/Mec-3 (LIM) domains, as shown for migfilin/Fblim1 (filamin-binding LIM protein 1) (Figure 1, p.6). LIM domains are tandem zinc finger protein interaction domains (Kadmas and Beckerle, 2004; Zheng and Zhao, 2007).

Like all zyxin family members, migfilin is found at cell-matrix adhesion sites, also called focal adhesions (FAs) (Takafuta et al., 2003; Tu et al., 2003), cell-cell adhesions (Gkretsi et al., 2005), and in the nucleus (Akazawa et al., 2004) (Figure 1, p.6). It is recruited to these compartments by its C-terminal LIM domains (Gkretsi et al., 2005). Migfilin is shuttled out from the nucleus by karyophorins recognizing the NES (Akazawa et al., 2004). The recruitment to FAs is tension-dependent for all zyxin family proteins, pointing to an important function as sensors and/or modulators of intracellular tension (Schiller et al., 2011).

In mouse, the genes of four members of the zyxin family have previously been ablated: *ajuba* (Pratt et al., 2005), *limd1* (Feng et al., 2007), *lpp* (Vervenne et al., 2009) and *zyxin* (Hoffman et al., 2003). Previous *in vitro* data suggested that their gene ablation should result in substantial defects. However, embryonic development and homeostasis were normal in their absence. When the mutant mice were exposed to specific stressors some of the proteins gave rise to defects including inflammation (*ajuba*, Feng and Longmore, 2005) and cancer (*limd1*, Sharp et al., 2008). This argues for molecular redundancy regarding adhesive functions, whereas

the specific stress response functions were not fully compensated. In fly, ablation of one of the two zyxin family members was pharate lethal, but also here there were no obvious adhesion defects (Das Thakur et al., 2010).



We chose to study the functional role of the zyxin family member migfilin, a putative interactor of the essential integrin adaptor Kindlin-2/Fermt-2 (fermitin family homolog-2) (Montanez et al., 2008). Biochemical and cell culture experiments suggested an important role for migfilin in integrin activation (Lad et al., 2008), cell adhesion (Gkretsi et al., 2005; Tu et al., 2003), migration (Zhang et al., 2006), transcriptional activation (Akazawa et al., 2004), and cell survival (Zhao et al., 2009). *In vivo*, we expected migfilin would have a role in cell-cell adhesion of cutaneous

epidermis, as kindlin-2 localizes exclusively to cell-cell, but not to cell-matrix adhesions in this tissue (Ussar et al., 2008).

Migfilin function in its sub-cellular compartments

Migfilin in focal adhesions

Cellular adhesion to the ECM is highly dependent on the integrin family of heterodimeric transmembrane receptors (Hynes, 2002). Integrins consist of 18 α - and 8 β -subunits. Integrin ligand-specificity depends on which α - and β -subunits dimerize. Keratinocytes for example adhere to laminins via the hemidesmosomal integrin $\alpha 6 \beta 4$ and the FA integrin $\alpha 3 \beta 1$, and to collagens via integrin $\alpha 2 \beta 1$ (Margadant et al., 2010). Disruption of integrin $\beta 1$ function is lethal during embryogenesis (Fässler and Meyer, 1995) or it results in blistering and organ defects if the disruption is organ restricted (Brakebusch et al., 2000; Lorenz et al., 2007).

Stable attachment of cells to their surrounding ECM provides not only mechanical stability, but also triggers downstream signaling events that regulate processes such as polarity, survival, proliferation and differentiation (“outside-in” signaling) (Legate et al., 2009). The extent of integrin signaling is not solely dependent on integrin surface expression levels, but also on their conformational activation state (Moser et al., 2009) and their recycling (Caswell et al., 2009): Integrin heterodimers are by default preferentially in an inactive conformation, and intracellular integrin ligands such as talins and kindlins shift integrins into an active conformation (“inside-out” signaling) (Moser et al., 2009). This adaptor-induced allostery effectively increases the amount of integrins available for matrix binding, in return enabling increased attachment and outside-in signaling. Other intracellular integrin ligands like filamin shift integrins back into an inactive conformation (Kiema

et al., 2006). In some cell types such as thrombocytes, integrins need to be kept in an inactive state and are activated following a specific stimulus by inside-out signaling to fulfill their biological function (Moser et al., 2008; Nieswandt et al., 2007). In other cell types such as keratinocytes, integrin activation modulates integrin turnover and the number/stability of FAs (Reinhard Fässler, personal communication).

Migfilin was shown to bind both kindlin-2 and filamins (Takafuta et al., 2003; Tu et al., 2003), making migfilin an attractive target for studying integrin activation. Migfilin was shown to enhance integrin activation *in vitro* by competing with β integrin cytoplasmic tails for filamin binding, and migfilin-derived peptides could activate thrombocytes (Ithychanda et al., 2009; Lad et al., 2008). Migfilin's possible role in integrin activation might explain adhesion defects observed after siRNA-mediated depletion of migfilin in cell lines (Tu et al., 2003). Defective integrin activation upon loss of migfilin expression could also account for defects in cell migration and survival (Zhang et al., 2006; Zhao et al., 2009). Migration was also defective after migfilin overexpression (Zhang et al., 2006).

Migfilin in cell-cell adhesions

Adhesion between cells is mediated by adherens junctions (AJ) and desmosomes and is established by homo-dimerization between cadherins on adjacent cells. AJ connect the cell-cell adhesion to the actin cytoskeleton via catenins, whereas desmosomes connect intracellularly to intermediate filaments. Abolishment of cell-cell interactions prohibits organogenesis and homeostasis (reviewed in Stepniak et al., 2009).

Immunoelectron microscopy in epithelial cells showed that migfilin localized to AJ (Gkretsi et al., 2005). siRNA-mediated depletion of migfilin in HT1080 cells diminished E-cadherin and β -catenin staining and weakened cell-cell adhesion, pointing to a possible function of migfilin in formation or maintenance of cell-cell contacts (Gkretsi et al., 2005).

Nuclear functions of migfilin

Migfilin is highly expressed in mouse heart and was found to interact with and transactivate the transcription factor Nkx2.5 (Akazawa et al., 2004). Migfilin is usually efficiently excluded from the nucleus, but high intracellular Ca^{2+} -levels were shown to enable nuclear localization of migfilin, as did deletion of the NES or inhibition of karyophorins. Deletion of the NES further increased Nkx2.5 transactivation, while deletion of the C-terminal LIM domains abolished it. Overexpression of a NES-deficient migfilin mutant increased cardiomyocyte-specific transcript levels in P19CL6 cells, an embryonic carcinoma cell line which can assume some characteristics of cardiomyocytes upon treatment with Dimethylsulfoxide. This indicates a potential role of migfilin in cardiac development and/or homeostasis.

Gene targeting of migfilin in mouse using Cre recombinase

To study the role of migfilin in development, homeostasis, and disease, we pursued a reverse genetics approach by targeting migfilin for genetic ablation. Specific genomic loci can be manipulated in ES cells by homologous recombination. These ES cells are then introduced into blastocysts and give rise to chimeras and to mutant mouse lines after germ line transmission. Commonly used genetic modification strategies include the introduction of point mutations to manipulate

protein function, delete genes, or introduce new genes into a specific locus. For inducible and/or tissue-specific gene targeting, genes are flanked with loxP sites (“floxing”, fl), consisting of a palindromic 34 base pair sequence of viral origin that is recognized by the Cre recombinase. Cre-mediated excision of floxed alleles allows time- and cell type-specific gene modification depending on the promoter used to drive Cre expression (Rajewsky et al., 1996).

Since we were interested in the role of migfilin *in vivo*, we wanted to analyze the consequences of constitutive and epidermis-specific ablation of migfilin. Keratin 5 (K5) or K14 promoters for Cre transgene expression enable gene targeting in the stratified epithelium of the epidermis when using male carriers, as the floxed migfilin allele is excised in basal layer keratinocytes that gives rise to all other epidermal layers (Hafner et al., 2004; Ramirez et al., 2004). Female carriers have constitutive null-offspring due to K5 and K14 promoter activity in oocytes, which results in oocytic Cre activity. These transgenes can thus be used to study the effects of both constitutive and stratified epithelium-specific ablation of a floxed gene in parallel.

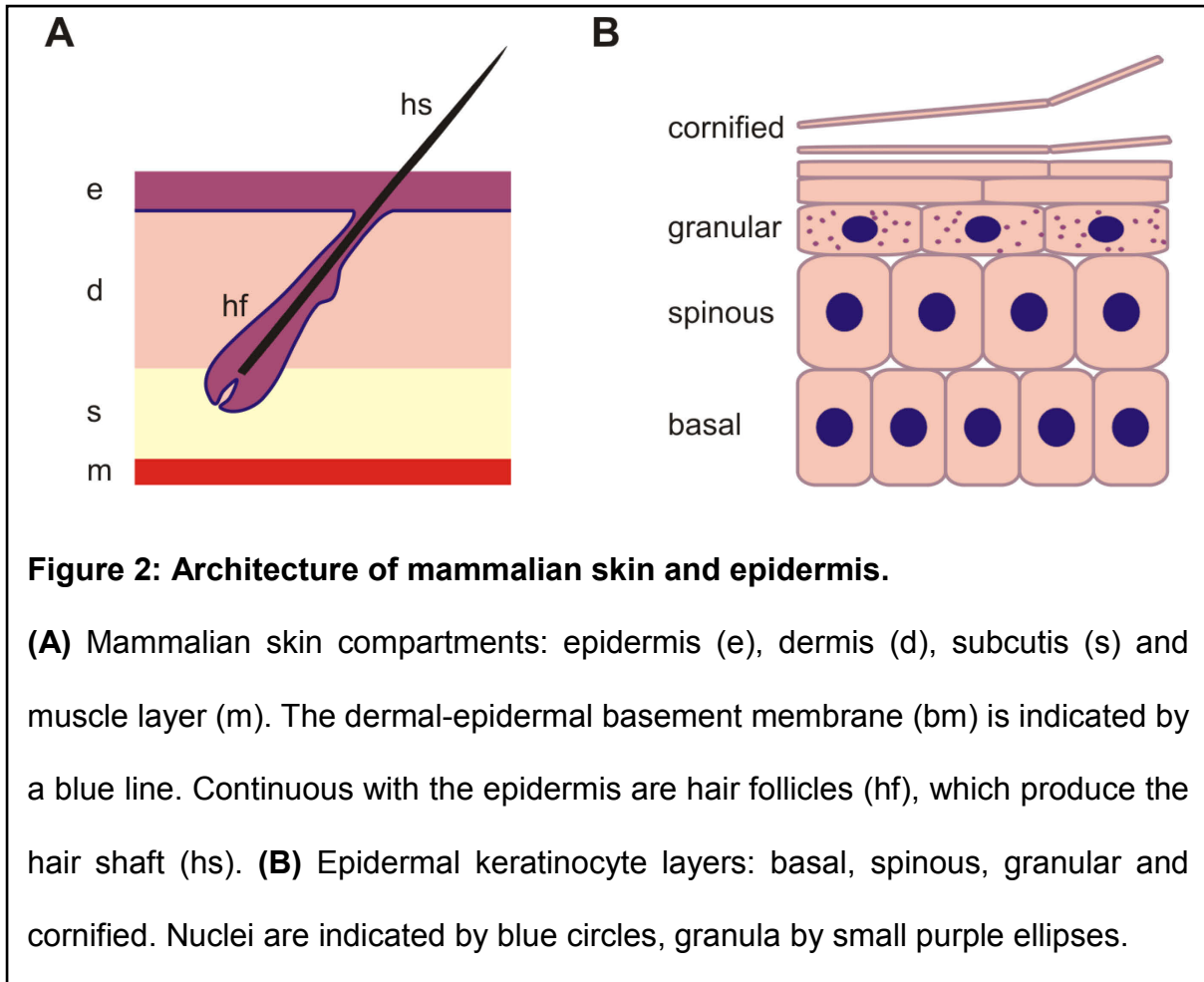
Cre recombinase – a useful tool with routinely overlooked side-effects

One caveat when using Cre recombinase is its off-target activity, which presumably results from nonspecific recognition of genomic sequences that distantly resemble loxP sites (Thyagarajan et al., 2000). These are present at a frequency of 1 per 1.2 mega base pairs in the mouse genome (Semprini et al., 2007). In cells, nonspecific Cre recombinase activity inhibits proliferation and results in increased fractions of cells with 4 or more chromosomal complements (C) and chromosomal aberrations (Loonstra et al., 2001; Pfeifer et al., 2001; Silver and Livingston, 2001). In mice, Cre can nonspecifically induce apoptosis and chromosomal instability (CIN)

(Higashi et al., 2009; Naiche and Papaioannou, 2007) and damage post-mitotic DNA (Schmidt et al., 2000). This necessitates proper controls to avoid conclusions that may potentially be based on Cre-mediated toxicity (Lee et al., 2006; Schmidt-Supprian and Rajewsky, 2007). Such possibilities, however, are not routinely discussed in publications employing Cre-mediated gene ablation.

General role and composition of skin

Establishment and maintenance of a firm barrier to the environment is essential for all organisms. This barrier ranges in complexity from the bacterial cell envelope to mammalian skin, a complex organ derived from several germ layers. Some tasks are universal to all these barriers: defining a clear boundary between the organism and its environment, maintaining homeostasis of water and other compounds, protecting against harm e.g. from radiation, trauma, and pathogens. Some highly developed organisms like mammals additionally need to maintain a constant body temperature for survival. Mammalian skin therefore also needs to insulate against cold and heat. Skin is thus the most exposed organ to various forms of stress, and studying the stress response of skin can provide useful knowledge for treatment of a variety of human diseases (e.g. Segre, 2006; Wagner et al., 2010). Mouse and human skin are similar, making mouse skin a useful model for human skin development and diseases despite macroscopic differences such as a reduced thickness of mouse skin, its near-lack of sweat glands, and its increased density of hair follicles compared to most parts of human skin (Wagner et al., 2010).



Epidermis

The architecture of skin is composed of distinct compartments (Figure 2A, p.12) (McGrath et al., 2008). The outmost compartment is the epidermis, a squamous stratified epithelium that predominantly consists of keratinocytes. Epidermal keratinocytes are organized in histologically well-distinguishable layers (Figure 2B). First, there are basal keratinocytes attached to a basement membrane. Above them are three suprabasal keratinocyte layers: spinous, granular and cornified. All epidermal layers contribute to mechanical stability, which depends on expression and intra- and intercellular cross-linking of keratins and secreted matrix proteins (Elias, 2005; Proksch et al., 2008).

Passage of liquids or pathogens is averted by the outside-in barrier, which is maintained by highly cross-linked protein and lipid complexes in the cornified layer (Segre, 2006). Protection against radiation (e.g. ambient UV radiation) is also provided by the cornified layer (Denecker et al., 2007). Water loss from the inside is partially prevented by this barrier and mainly by tight-junctions in the granular layer (inside-out barrier) (Brandner et al., 2006). Furthermore, keratinocytes function as non-professional antigen presenting cells, stimulate innate immunity and produce anti-microbial peptides – for these reasons, epidermis is often viewed as a primary immune organ (Nestle et al., 2009).

Epidermis is not innervated or vascularized, receiving nutrients from the underlying dermal layers. It also contains melanocytes, which leave mouse epidermis shortly after birth in pelagic skin to colonize hair follicles (Okura et al., 1995). This is in contrast to human melanocytes, which persist in the epidermis throughout life and are replenished by dermal melanoblasts (Costin and Hearing, 2007). Melanocytes produce melanin-containing melanosomes that are transferred to keratinocytes and protect against UV irradiation (Box and Terzian, 2008). This process is regulated by the tumor suppressor and stress sensor p53 (Figure 3, p.14): p53 is activated in irradiated keratinocytes and induces the expression of melanogenic cytokines like Kit ligand (Kitl), which stimulates proliferation of melanocytes and leads to an increased production of melanosomes (Cui et al., 2007; McGowan et al., 2008; Murase et al., 2009).

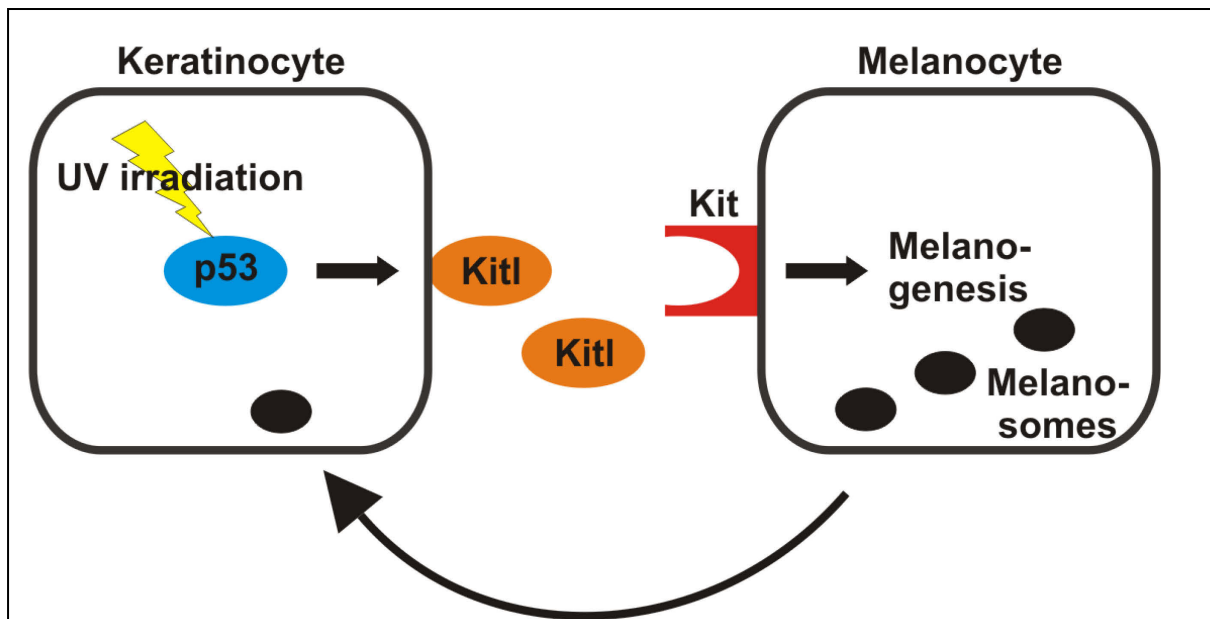


Figure 3: p53-mediated epidermal tanning

Upon UV irradiation, p53 is activated in keratinocytes and upregulates melanogenic factors like Kit ligand (Kitl), which stimulates melanocyte proliferation and melanosome production by binding to the receptor tyrosine kinase Kit. Melanosomes are consequently transferred to keratinocytes and increase protection against further UV irradiation.

Dermis and subcutis

The dermis is a collagen-rich mesenchyme mostly composed of fibroblasts and resident macrophages (Dupasquier et al., 2004). It is connected to the epidermis at the basement membrane and is continuous with the subcutis, containing white adipose tissue connected to a subcutaneous muscle layer underlying the whole skin. These layers also contain lymphatic vessels, blood vessels and nerves (McGrath et al., 2008; Wagner et al., 2010).

Skin appendages

The appendages of the skin fulfill additional tasks beyond barrier function. Especially hair is very versatile and serves a variety of uses: pelagic hair ensures thermal homeostasis, as it insulates the body, while e.g. the hair of whiskers has sensory functions. Thermal insulation is further increased when the arrector pili muscle pulls at the hair follicle and erects the hair. Colored pelagic hair can also provide camouflage or serve in signaling/warning purposes. Sweat glands can provide cooling. Sebaceous glands grease hair and epidermis, decreasing wear and tear on hair and increasing epidermal barrier efficiency, and have important anti-microbial and endocrine functions (Zouboulis et al., 2008). Specialized skin appendages like nails or claws can serve as weapons and assist in movement.

Epidermis in development and homeostasis

Epidermis is derived from ectodermic progenitor cells and forms a single layered simple epithelium by E8.5 in mouse. After formation of a transient second cell layer, the peridermis, by E10.5, suprabasal cell layers develop and stratify between the basal layer and peridermis. With establishment of epidermal barrier function between E16 and E18, the peridermis is lost and stratification is complete (Mack et al., 2005).

During homeostasis, epidermis is constantly renewed by p63-mediated programmed differentiation of basal keratinocytes, which in turn are constantly replenished by a pool of epidermal stem cells (Kaur, 2006) (Figure 2B, p.12). Upon differentiation, basal epidermal keratinocytes stop proliferating, down regulate integrin expression and delaminate from the basement membrane (Watt, 2002). They consequently undergo programmed differentiation while progressing upward through the spinous and granular layer into the cornified layer. Differentiation status

can be assessed by specific markers: e.g. basal keratinocytes express the keratin dimers K5 and K14, spinous cells express K1 and K10, and granular and early cornified cells express loricrin. In the cornified layer, keratinocytes undergo a specialized form of programmed cell death resulting in the loss of nucleus and cell membrane, and fuse into cornified sheets (Lippens et al., 2005). Eventually, these sheets are shed and replaced from underneath, completing epidermal turn-over.

Development of hair follicles

Crosstalk between epidermis and the underlying dermis first induces development and later maintenance of hair follicles (Schneider et al., 2009). Hair follicles are highly complex mini-organs, undergoing cyclic growth and regression, and are empowered by a distinct pool of hair follicle stem cells. The outermost layer of hair follicles, the outer root sheath (ORS), is continuous with basal keratinocytes of the epidermis, which is also termed interfollicular epidermis (IFE) to distinguish it from the ORS. Hair follicle stem cell compartments are supportive in, but not essential for, post-natal lateral skin expansion (Heath et al., 2009) and regeneration of interfollicular epidermis after wounding (Langton et al., 2008; Levy et al., 2007).

The inflammatory stress response in skin

Damage to the skin triggers a wound healing response to repair the damage and re-establish barrier function. Simultaneously, harmful irritants, toxins or pathogens that crossed the barrier have to be neutralized by activating an immune response. These two processes are linked as keratinocyte proliferation is regulated through inflammatory cytokines (Eming et al., 2007) such as interleukin-1 (IL-1): keratinocyte-derived IL-1 induces dermal fibroblasts to secrete keratinocytes growth factor (KGF)

and Colony stimulating factor 2 (CSF2). They support homeostatic keratinocyte proliferation, creating a paracrine feed-forward loop (Angel et al., 2001). Negative feedback regulation of this loop is provided by IL-1–mediated up-regulation of peroxisome proliferator–activated receptor β/δ (PPAR β/δ) in dermal fibroblasts leading to the activation of IL-1 receptor antagonist (IL1RA), which in turn inhibits IL-1 activity (Chong et al., 2009).

Thus, increased IL-1 secretion during wound healing promotes keratinocyte proliferation, but it also activates the immune response together with CSF2 (Hanada and Yoshimura, 2002): neutrophils are rapidly recruited to wounding sites and release toxins to battle pathogens (Eming et al., 2007). Macrophages subsequently remove dead and apoptotic cells by phagocytosis and resolve inflammation by release of anti-inflammatory cytokines (Serhan and Savill, 2005). As a corollary, a local activation of the immune response will induce epidermal hyperthickening independently of barrier breaches due to release of pro-inflammatory cytokines.

Mouse mutants displaying reactive epidermal hyperplasia

Thus, hyperactivation of the immune system in the skin can lead to hyperproliferative skin diseases, as seen after transgenic overexpression of inflammatory cytokines like IL-1 (Groves et al., 1995) or manipulation of immune regulators like nuclear factor kappa B (NF- κ B) (Descargues et al., 2008; Gareus et al., 2007; Klement et al., 1996; Nenci et al., 2006; Pasparakis et al., 2002; Schmidt-Supprian et al., 2000). Epidermal damage activates the immune system irrespective of the cause of damage, e.g. blistering at the basement membrane (Brakebusch et al., 2000; Lorenz et al., 2007), defective cell-cell adhesion (Tinkle et al., 2004), compromised barrier function (Demehri et al., 2008; Yang et al., 2010), or damage

by ultraviolet radiation (Clydesdale et al., 2001; Feldmeyer et al., 2007). Due to this intensive cross-talk, many phenotypes resulting from gene mutations in mouse skin are macroscopically similar, differing mainly in the degree of severity.

This entwinement of inflammation and epidermal stress response led to intense discussion in the past regarding whether keratinocytes or immune cells are the primary triggers of chronic skin diseases like psoriasis and atopic dermatitis (Bowcock and Krueger, 2005; Lowes et al., 2007; Nickoloff et al., 2007). An emerging synthetic view acknowledges that irrespective of the trigger, epidermal stress can lead to hyperproliferative pathogenesis (Nestle et al., 2009).

Treatment of reactive epidermal hyperplasia

Interestingly, phenotypes arising from a dysregulated immune response can often be fully rescued by immune suppression, e.g. by treatment with glucocorticoids or deletion of the tumor necrosis factor receptor (Tnfr) (Nenci et al., 2006; Pasparakis et al., 2002). These measures were proposed to protect keratinocytes against tumor necrosis factor (Tnf)-mediated apoptosis, which otherwise would escalate inflammation and further increase apoptosis in a possibly lethal feed-forward loop (Omori et al., 2006). For treatment of non-immune based defects, immune-suppression can be expected to worsen the phenotype as this also attenuates the beneficial wound healing response. Rather, the primary defect has to be treated, e.g. amelioration of barrier defects by treatment with moisturizing crème (Yang et al., 2010).

Cutaneous inflammation and skin cancer

There is extended overlap between molecular pathways involved in wound healing and non-melanoma skin carcinogenesis (Schafer and Werner, 2008), but the relationship between inflammation and carcinogenesis in the skin is complex and not entirely understood. On the one hand, early-stage cancer is suppressed by immune surveillance (Bui and Schreiber, 2007). Therefore, suppression or defects of the immune response increase cancer risk, in addition to carcinogenesis caused by opportunistic viral infections (Hofbauer et al., 2010; Nindl et al., 2007). Also, some chronic inflammatory hyperproliferative skin conditions like psoriasis have no increased associated cancer risk, but rather suppress tumorigenesis (de Visser et al., 2006; Nickoloff et al., 2005). On the other hand, chronic inflammatory milieus are also well-known to stimulate carcinogenesis (Allavena et al., 2008). In skin, wound-associated inflammation increases the risk to develop cancer (Eming et al., 2007). Also, cancer generates its own inflammatory niche, which has been shown to drive carcinogenesis as it increases genetic instability (Colotta et al., 2009).

Non-melanoma skin cancer

The development of cancer depends on the acquisition of somatic mutations and can be roughly divided into three stages (Figure 4, p.22) (Hanahan and Weinberg, 2000; Hanahan and Weinberg, 2011): an initiating event activates an oncogene (A). Under growth promoting conditions, initiated cells can grow into pre-cancerous lesions and accumulate additional genetic hits that promote the development of a benign tumor (B). Finally, additional mutations allow tumor cells to metastasize (C).

There are two major mechanisms how cancer cells can acquire somatic mutations: microsatellite instability (MIN) and CIN. MIN results from defective DNA

damage repair (e.g. mismatch repair defects). CIN describes gains or losses of whole chromosomes (e.g. by chromosome missegregation), or structural changes of chromosomes (e.g. translocations, deletions, inversions, duplications) (Lengauer et al., 1998).

Non-melanoma skin cancer (NMSC) is the cancer with the highest incidence worldwide, e.g. at about 0.1% per annum in northern Germany (Katalinic et al., 2003), but fortunately prognosis and therapy are usually non-problematic (Boukamp, 2005). While melanoma diagnoses are nearly 10-fold lower (Katalinic et al., 2003), the prognosis is usually worse due to a high propensity to metastasize (Gray-Schopfer et al., 2007). Nonetheless, the sheer number of NMSC cases warrants study to improve prevention, prognosis and treatment.

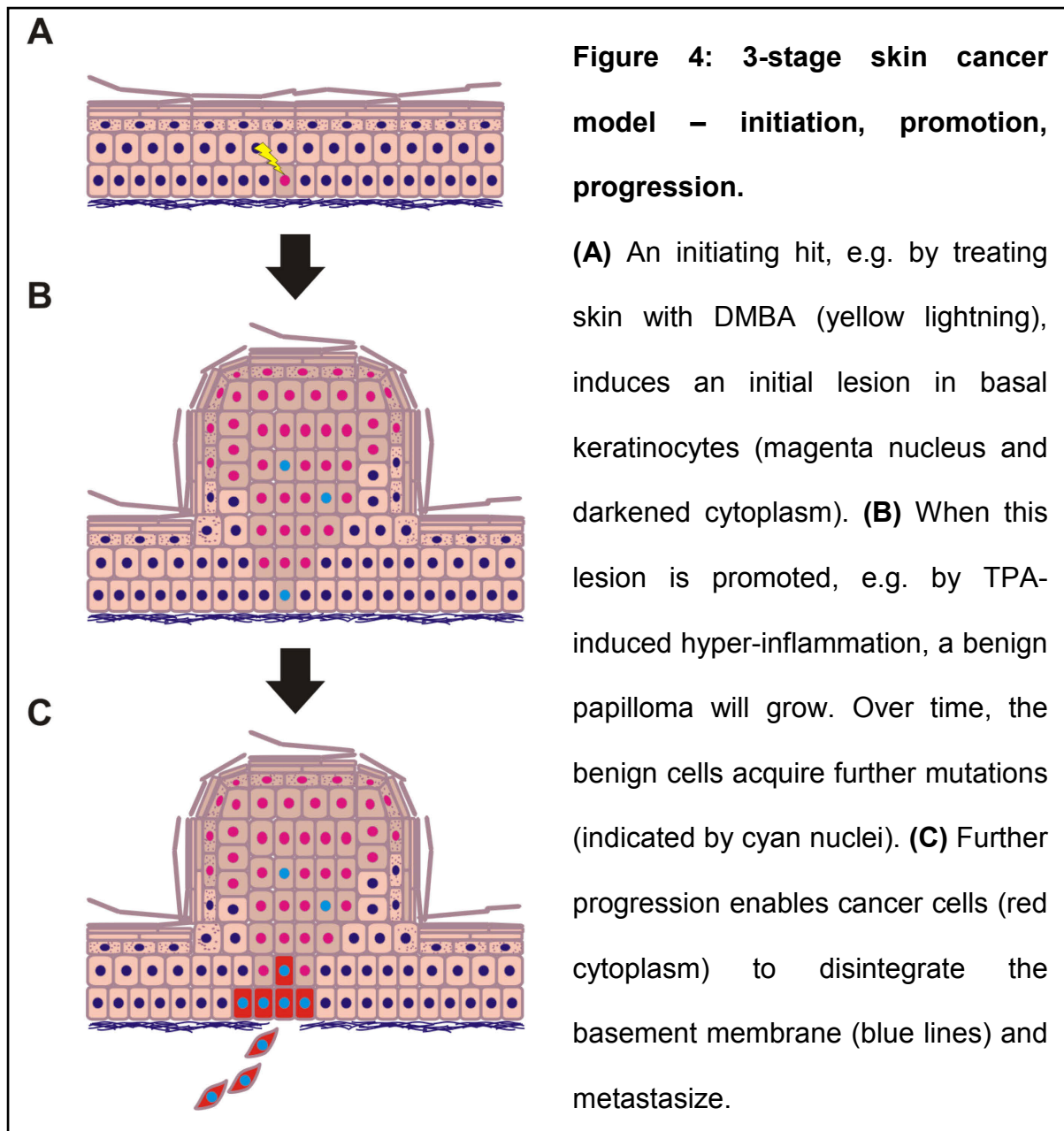
Human NMSC can be differentiated into basal cell carcinoma (BCC) and squamous cell carcinoma (SCC) (Boukamp, 2005): BCC is derived from hair follicles and is thought to develop de novo in otherwise normal epidermis driven by mutated Sonic Hedgehog pathway components. SCC is derived from IFE keratinocytes, which accumulates mutations and develops into a malignancy in a step-wise manner. A well-established model for NMSC is the two-stage DMBA/TPA protocol (reviewed by Kemp, 2005).

The DMBA/TPA skin cancer model

In the DMBA/TPA skin cancer model, application of 7,12-Dimethylbenz(a)anthracene (DMBA) to the skin of 6 weeks old mice induces amongst other an activating K-Ras mutation and initiates carcinogenesis. Two weeks later, 12-O-Tetradecanoylphorbol-13-acetate (TPA) treatment starts, which induces a hyperproliferative inflammatory response that promotes the growth of the

immortalized cell. Cancer progression is rare in this model and can usually only be observed in mouse models that have an increased propensity to develop metastasis. DMBA/TPA-treated mice usually develop benign, endophytically growing papillomas. Endophytic growth indicates tumor progression to SCC. Other possible tumors observed with this treatment regime are sebocyte-derived adenomas.

The laboratory mouse strain C57BL/6 is highly resistant to towards skin carcinogenesis compared to other strains (e.g. FVB/N), and is therefore well suited to discover tumor suppressive gene functions (Hennings et al., 1993; Wakabayashi et al., 2007).



The cell cycle

A hallmark of cancer cells is their aberrant growth. Study of the mechanistic details of the cell cycle can therefore provide insight into carcinogenesis (Figure 5, p. 26). Mitosis or M phase is the process of cell division (Alberts, 2002). In interphase between two mitoses (Figure 5A), a cell grows until it doubles its volume. Interphase is divided into G₀/G₁, S, and G₂ phase. A senescent/non-cycling cell is designated

as a G₀ phase cell. Mitogenic stimulus triggers entry into the cell cycle (G₁ phase). A G₁ phase cell proceeds to S phase, at which point it replicates its genome. Diploid cells have two complements of sister chromatids in G₀/G₁ phase and at the onset of S phase (2N;2C). In S phase each sister chromatid is replicated, thus the cell enters G₂ phase with 4 chromosomal complements (2N;4C). The duplication of the centrosome/microtubule-organizing center also starts in S phase and is completed in the following G₂ phase. When cellular growth is completed, a cell undergoes mitosis and divides into two identical G₁ phase daughter cells.

Cell cycle progression is driven by specific activated cyclin-dependent kinases (CDK) in complex with cyclins (Alberts, 2002). Proper completion of a given phase of the cycle results in proteosomal degradation of its specific cyclin. Entry into G₁ phase by mitogenic stimulus results in expression of cyclin D and formation of a complex with CDK4/6. This complex releases retinoblastoma-mediated inhibition of the transcription factor E2F, which in turn upregulates cyclin E and A expression. The cyclin E-CDK2 complex mediates entry into S phase, and cyclin E is consequently degraded to prevent DNA re-replication. Cyclin A-CDK2 assists progression through S phase (Woo and Poon, 2003). Cells with undamaged DNA directly proceed through G₂ phase into mitosis, which is regulated by cyclin A-CDK2 and cyclin B-CDK1 (Sullivan and Morgan, 2007).

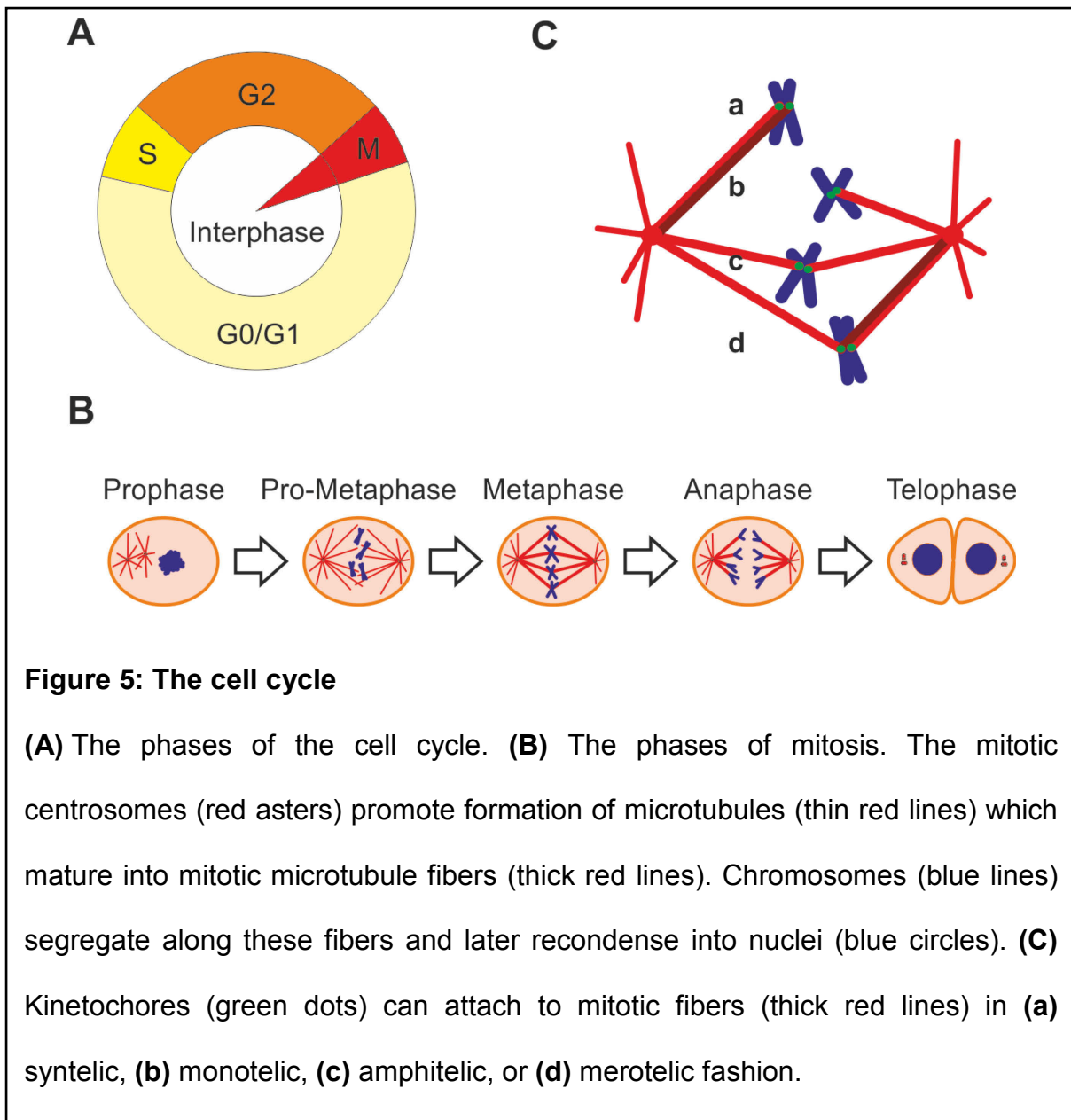
DNA damage triggers checkpoints in G₁ phase, at the G₁-S phase boundary, intra-S phase, or at the G₂/M boundary (Bartek et al., 2004; Kastan and Bartek, 2004). The master regulators of the DNA damage response are the apical kinases ATM (ataxia telangiectasia mutated), ATR (ATM- and Rad3-related), and DNA-PK (DNA-dependent protein kinase), which are activated by damaged DNA and trigger a signaling cascade that initiates DNA damage repair and activates p53. The ubiquitin

ligase Mdm2 ubiquitinates p53 and thereby maintains low cytosolic concentrations through its proteosomal degradation. Inhibition of Mdm2 binding to p53 e.g. by phosphorylation at residues S15 and S20 by activated ATM increases and stabilizes p53 protein levels (Vousden, 2002). Activated p53 then induces expression of cell cycle inhibitors like p21 to prevent cell cycle progression before DNA damage can be repaired, or pro-apoptotic proteins if the damage is beyond repair.

Progression through mitosis

Mitosis (Figure 5B) (Alberts, 2002; Sullivan and Morgan, 2007) starts with prophase, during which time the nuclear envelope breaks down and the chromosomes start to condense. The microtubule polymerizing activity of the centrosomes increases and leads to formation of an interdigitating mitotic microtubule spindle. Motor proteins push the centrosomes apart towards opposite ends of the cell, the mitotic poles. In the subsequent pro-metaphase, the DNA completes condensation into chromosomes. Astral microtubules anchor the centrosomes to the cortex, and mitotic spindle microtubules start capturing the kinetochores, specialized protein complexes that attach mitotic microtubules to the chromosomes. Mitotic microtubules can initially be attached to kinetochores in monotelic, syntelic or merotelic fashion (Figure 5C). With the transition to metaphase, the chromosomes convene at the equatorial metaphase plate while the microtubules attached to the kinetochores mature into thick mitotic fibers. The spindle assembly checkpoint (SAC) prevents progression into anaphase until all kinetochores are stably attached (Figure 5C). The release of the SAC results in the degradation of cyclin B and progression to anaphase (Glotzer, 2009; Sullivan and Morgan, 2007).

In anaphase, the sister chromatids of the chromosomes segregate along the mitotic fibers towards the mitotic poles and an equatorial contractile ring circumscribing the metaphase plate forms at the cell membrane. When the chromosomes reach the mitotic poles, telophase begins: the nuclear envelope reforms around the decondensed chromosomes, and the cell initiates cytokinesis (Steigemann and Gerlich, 2009): the cell membrane constricts at the contractile ring, leading to the formation of a cleavage furrow. The mitotic spindle compacts into a central spindle during ingression of the cleavage furrow (not shown on Figure 5). Finally, only a cytokinetic bridge remains between the two daughter cells, and this is pinched off in a process termed abscission. Successful cytokinesis depends on a large and diverse number of participants, involving cell cycle regulators, actomyosin- and microtubule-associated proteins, vesicle transport and targeting, (reviewed in Eggert et al., 2006), integrins and their regulators (Pellinen et al., 2008), and AJ constituents like APC (Caldwell et al., 2007).



Tetraploidy, aneuploidy and cancer

More than a century ago, cancer cells were noted to be strikingly heterogeneous in nuclear and cellular size, and they often underwent abnormal mitoses and cell death. Hansemann and Boveri found that abnormal mitoses result in aneuploidy, and they attributed the observed cell death to nullisomy (lack of a chromosome) after an abnormal mitosis (Bignold et al., 2006). They proposed that aneuploidy could confer

growth advantages in the cases where it is not lethal, and drive carcinogenesis. Boveri further pointed out that tetraploid cells underwent tetrapolar mitoses due to supernumerary centrosomes, resulting in severe aneuploidy and thus increasing the chance to acquire tumor promoting characteristics (Boveri, 2008). Tetraploidy would accordingly be an intermediate towards aneuploidy.

Since then, many aspects of their theory could be formally proven. Karyotyping confirmed substantial genomic and chromosomal abnormalities in malignant tumors (Mitelman et al., 2011), explaining heterogeneity in cell and nuclear size since both depend on DNA content (Epstein, 1967; Huber and Gerace, 2007). Tetraploid cells promote carcinogenesis *in vivo* (Fujiwara et al., 2005) and are associated with high CIN (Ganem et al., 2007; Storchova and Kuffer, 2008). It was confirmed that tetraploidy is an intermediate state between diploidy and aneuploidy (Vitale et al., 2010): tetraploid cell clones acquired near-diploid aneuploidy with chromosomal rearrangements upon cultivation or *in vivo* inoculation, and this correlated with tumorigenic aggressiveness. These experimental findings could be confirmed in human cancer, where tetraploid and aneuploid cells are often found in precancerous lesions, e.g. chronically inflamed esophagus and cervical dysplasia, and serve as potent predictors for cancer progression (Maley et al., 2004; Olaharski et al., 2006). Tetraploidy was also found in precancerous intraepithelial lesions in human epidermis, while malignant SCC were diploid or possibly near-diploid aneuploid (Smits et al., 2007). Furthermore, tetraploidy/aneuploidy in head and neck squamous cell carcinoma (HNSCC) and NMSC indicated increased propensity to recur and to metastasize (Hass et al., 2008; Robinson et al., 1996).

In light of these findings, answers to the following questions can help to better understand the fundamental processes that promote carcinogenesis and cancer

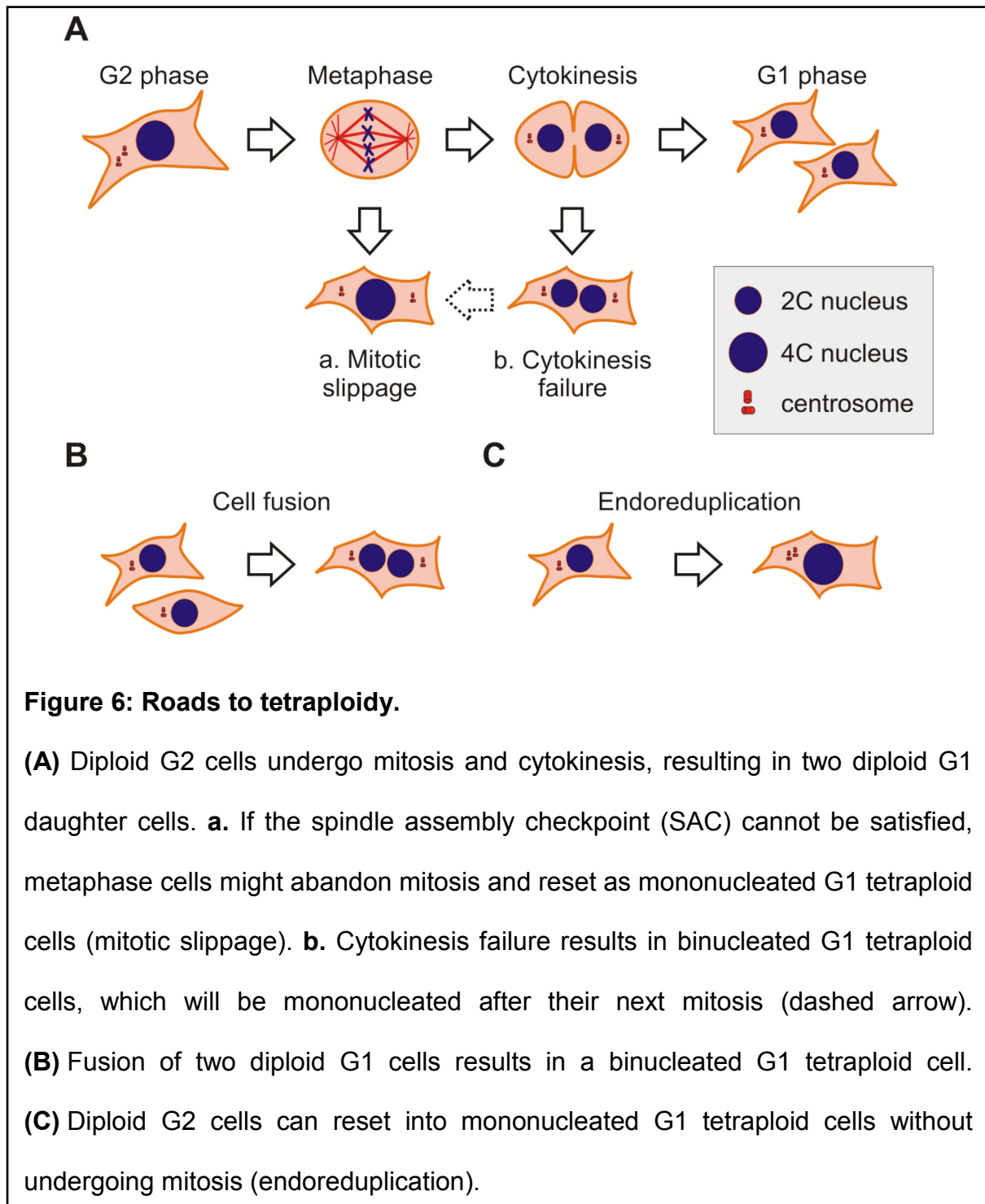
progression, which could in turn lead to more efficient prevention, prognosis and treatment of cancer: how does tetraploidy arise? Why are tetraploid cells prone to CIN and become aneuploid? How are tetraploidy and aneuploidy repressed?

Roads to tetraploidy

When a G2 phase diploid cell (2N;4C) undergoes mitosis (Figure 6, p.29), the condensed chromosomes align at the mitotic cleavage plane in metaphase until the SAC is satisfied. When the SAC cannot be satisfied, cells can escape mitotic arrest by a process termed mitotic slippage to become G1 mononucleated tetraploid cells (4N;4C) (Figure 6Aa) (Musacchio and Salmon, 2007). Mitotic slippage depends on nonspecific degradation of cyclin B, which is necessary for cell cycle progression into anaphase (Brito and Rieder, 2006). After progression into anaphase, the cell has to successfully complete cytokinesis. Incomplete cytokinesis results in binucleated G1 tetraploid cells that produce mononucleated daughter cells after another round of mitosis (Figure 6Ab) (Glotzer, 2009). Cytokinesis defects can also be caused by lagging chromosomes caught in the cytokinetic bridge (Steigemann et al., 2009).

Binucleated tetraploid cells also arise after fusion of two diploid cells (Figure 6B). Cell fusion is part of normal physiology e.g. in muscle development as part of terminal differentiation and will give rise to multinucleated giant cells, the muscle fibers (Ogle et al., 2005). Non-physiological cell fusion was observed after viral infection (Duelli et al., 2005) or after transplantation of hematopoietic stem cells (Vassilopoulos et al., 2003; Wang et al., 2003). Finally, during endoreduplication (also termed endomitosis) mitosis is skipped and a diploid G2 phase cell resets to G1 as a tetraploid and mononucleated cell (Figure 6C). This has been shown in connection with insufficient capping of telomeres, which triggers continuous DNA

damage signaling and interferes with commencement of mitosis, but not with DNA replication (Davoli et al., 2010). Megakaryocytes, the progenitors of thrombocytes, employ endomitosis to acquire highly polyploid genomes under physiological conditions (Geddis et al., 2007; Lordier et al., 2008).



Mechanisms of CIN

In the scenarios discussed above, the cells end up with 4 centrosomes. The loss or gain of whole chromosomes is highly increased by supernumerary centrosomes, which increase the likelihood of multipolar mitoses or chromosome missegregation.

A cell with supernumerary centrosomes can initiate multipolar mitoses, as each centrosome can serve as a mitotic pole (Figure 7, p.32). During a multipolar mitosis, chromosomes segregate near-randomly to the daughter cells, and a large percentage of these mitoses result in nullisomy for at least one daughter cell (48% tetraploid/tetrapolar, 92% diploid/tetrapolar) (Gisselsson et al., 2008) (Figure 7a). Nullisomy is thought to be inescapably lethal, viable nullisomic cells cannot be detected (Roumier et al., 2005). Notably, surviving progeny of a multipolar mitosis could end up with a single centrosome, increasing the likelihood of stable propagation in subsequent mitoses. Furthermore, multipolar mitoses are prone to defective cytokinesis, where two or more daughters fuse back into a highly aneuploid cell (Ganem et al., 2009; Gisselsson et al., 2010), and take several times longer than bipolar mitoses to complete (Gisselsson et al., 2008; Yang et al., 2008).

The extended duration of multipolar mitosis depends on SAC components and allows for centrosome clustering (Kwon et al., 2008; Yang et al., 2008). Centrosome clustering depends on specialized kinesins, actin-dynamics and interphase attachment patterns, and will reduce the number of mitotic poles (Ganem et al., 2009; Kwon et al., 2008). Unless a pseudo-bipolar spindle can be achieved, there remains a high risk for severe CIN (Ganem et al., 2009; Gisselsson et al., 2010). But even after centrosome clustering, a pseudo-bipolar mitosis can result in CIN caused by merotelic kinetochore attachment (Figure 5, p.26) and resulting lagging chromosomes (Ganem et al., 2009): lagging chromosomes could be caught in the

cytokinetic bridge, preventing cytokinesis (Figure 7b1) (Steigemann et al., 2009), or alternatively be trapped with one daughter cell during cytokinesis, resulting in CIN (Figure 7b2). Aneuploidy can only be avoided if amphitelic chromosome attachment is achieved before anaphase onset (Figure 7c).

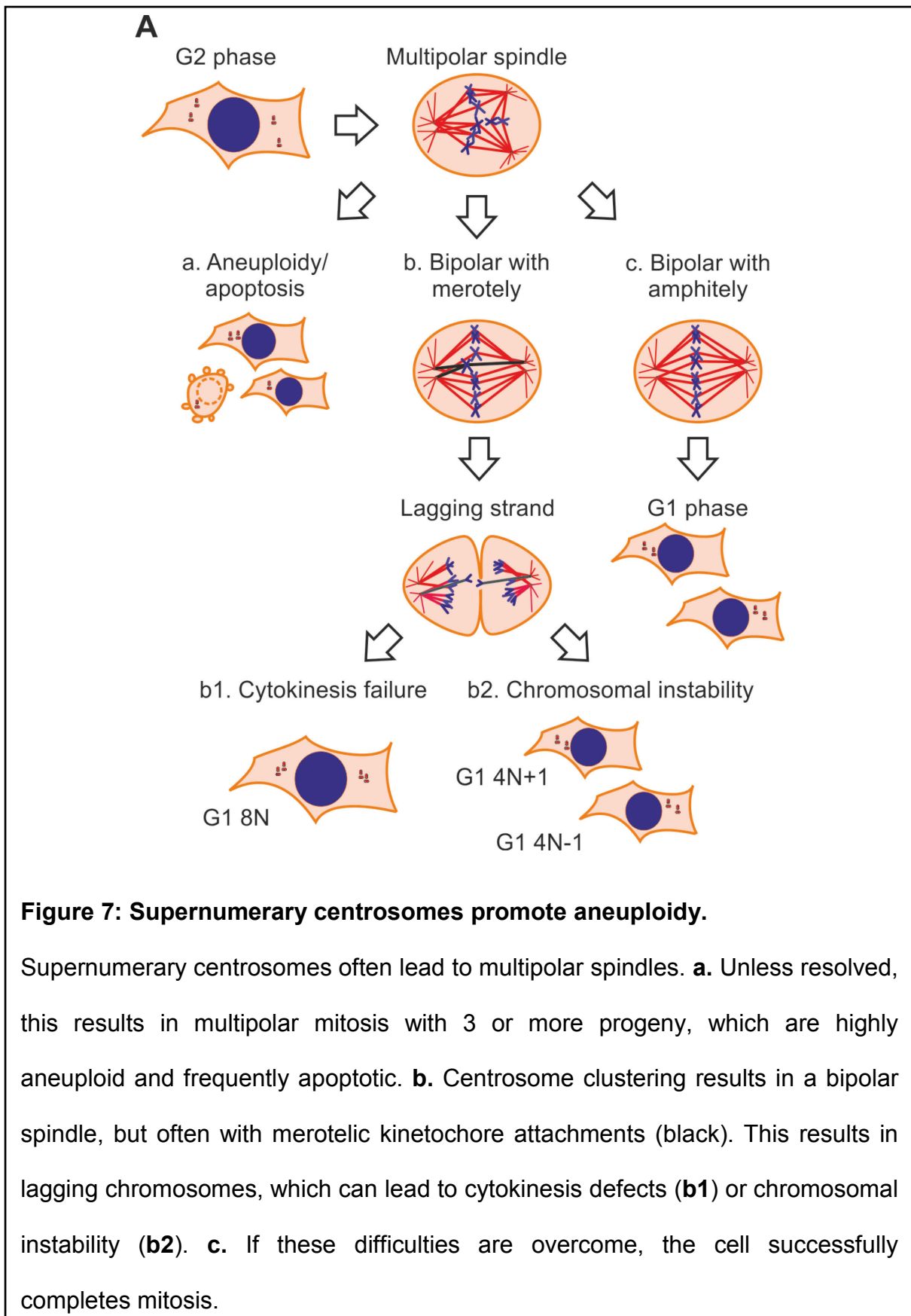


Figure 7: Supernumerary centrosomes promote aneuploidy.

Supernumerary centrosomes often lead to multipolar spindles. **a.** Unless resolved, this results in multipolar mitosis with 3 or more progeny, which are highly aneuploid and frequently apoptotic. **b.** Centrosome clustering results in a bipolar spindle, but often with merotelic kinetochore attachments (black). This results in lagging chromosomes, which can lead to cytokinesis defects (**b1**) or chromosomal instability (**b2**). **c.** If these difficulties are overcome, the cell successfully completes mitosis.

Suppression of tetraploidy/aneuploidy

CIN represents a tremendous mutagenic potential in tetraploid cells and their hyper-diploid progeny, promoting carcinogenesis and driving cancer progression (Schvartzman et al., 2010). It is therefore essential for multi-cellular organisms to suppress propagation of tetraploid/aneuploid cells, e.g. by ensuring cell death or cell cycle arrest.

CIN triggers apoptosis in a p53-dependant manner (Castedo et al., 2006; Zhivotovsky and Kroemer, 2004). Primary cells with induced tetraploidy cannot inoculate tumors *in vivo* or be cultivated, unless the tumor suppressor p53 is deleted (Fujiwara et al., 2005). Also, tetraploidy/aneuploidy in esophageal precancerous lesions coincides with loss of p53 (Maley et al., 2004). However, while the suppressive role of p53 is well established in aneuploid cells (Thompson and Compton, 2010), it is not clear whether p53 suppresses tetraploid cells, or rather their aneuploid progeny. Furthermore, ablation of p53 merely halved the apoptosis rate in dividing tetraploid cells (Castedo et al., 2006), which hints at additional, currently unknown mechanisms contributing to tetraploidy/aneuploidy suppression.

An aneuploidy-specific trigger of p53 activation in cells could be caused by chromosomal imbalances: heteromeric protein complexes are often degraded if they cannot properly form due to gene imbalances, which puts a cell under proteotoxic stress (Torres et al., 2010; Williams and Amon, 2009). Inhibition of autophagy or activation of adenosine-monophosphate(AMP)-activated kinase (AMPK) both selectively induce apoptosis in aneuploid cells, and apoptosis rates correlate with the degree of aneuploidy (Tang et al., 2011). AMPK in turn activates p53 under conditions of proteotoxic stress (Jones et al., 2005), which could induce apoptosis in aneuploid cells.

Tetraploidy per se is apparently not toxic: tetraploid mouse embryos could develop until E14, although they show a high rate of death and their forebrain development was especially defective (Henery et al., 1992). Similarly, tetraploidy/aneuploidy accounts for a sizeable number of human first-trimester miscarriages (Hassold et al., 1980), but case-reports describe tetraploid children surviving for at least two years, albeit with severe growth and developmental retardation (Guc-Scekic et al., 2002; Lafer and Neu, 1988). These findings suggest that wild-type tetraploid cells can be viable. Death observed in tetraploid mouse embryos could be due to CIN occurring during development, whereas longer living embryos could have avoided aneuploidy by chance (Figure 7, p.32). Unfortunately, the p53 status was not established in tetraploid mouse embryos and human children that survived. It could be possible that random inactivation of p53 occurred, allowing them to evade p53-mediated cell death and cell cycle arrest. Lack of p53 does not seriously affect embryonic development (Jacks et al., 1994). Limited embryonic lethality upon p53 deletion is caused by defective brain development (Sah et al., 1995). In contrast, gene defects resulting in increased CIN lead to embryonic lethality (Dobles et al., 2000; Jeganathan et al., 2007).

Tetraploidy induced by defective cytokinesis does not result in G1 phase arrest (Uetake and Sluder, 2004; Wong and Stearns, 2005), refuting earlier claims concerning a putative tetraploidy checkpoint (Andreassen et al., 2001). Rather, for diploid cells it could be shown that G1 arrest results from a prolonged mitotic arrest (Uetake and Sluder, 2010). This arrest was p53- and p38 MAPK-dependent and could only be transiently relieved by inhibition of p38 MAPK. Similar results were observed after mitotic arrest with low doses of taxol: whereas high doses trigger G2/M phase arrest, low doses allowed for cell cycle completion, but induce G1

phase arrest of the daughter cells (Demidenko et al., 2008). Therefore, cell cycle arrest does not appear to specifically suppress tetraploidy/aneuploidy, but rather is a universal outcome of mitotic defects.

Mechanism of p53-mediated repression of tetraploidy/aneuploidy

The molecular mechanism of p53-mediated tetraploidy/aneuploidy suppression is not well understood. Tetraploidy/aneuploidy results in p53-phosphorylation at residues S15 and S46 independently of the canonical DNA damage response mediator ATM, but there are inconclusive reports about the responsible kinase: p53-phosphorylation was BubR1-dependent after mitotic spindle damage, but it was p38 α MAPK-dependent in stable tetraploid cell clones after siRNA-mediated depletion of Chk1 (Ha et al., 2007; Vitale et al., 2008). Further studies support a functional role of both kinases: on the one hand, reduced protein levels of the BubR1-interactor Bub1 resulted in less aneuploidy-dependent apoptosis after chromosomal missegregation (Jeganathan et al., 2007). On the other hand, pharmaceutical inhibition or depletion of p38 suspended the p53-mediated post-mitotic cell cycle arrest (Uetake and Sluder, 2010; Vitale et al., 2008).

Independently of p53 phosphorylation, increased duration of mitosis as observed in cells with supernumerary centrosomes could be sufficient to stabilize p53 protein levels: transcription does not occur during mitosis, and p53 transcript has a longer half-life than the transcripts of its inhibitors (Blagosklonny, 2006). This allows for p53 protein accumulation as soon as its inhibitors are degraded as part of normal turnover. With resumed transcription in the next G1 phase, p53 could induce cell cycle arrest or apoptosis.

5. Aim of the thesis

A number of *in vitro* experiments suggested that migfilin functions in concert with kindlin-2 and possible filamins in mediating cell-matrix and cell-cell adhesion. We initially wanted to test how this interaction contributes to cell adhesion *in vivo* using a reverse genetics approach, i.e. by targeted deletion of the migfilin gene in mice. Mice lacking kindlin-2 were embryonic lethal, prompting us to generate a floxed-allele to enable tissue-restricted ablation of migfilin in case of embryonic lethality upon constitutive deletion of migfilin.

To study the effects of constitutive removal of migfilin, we used female Keratin5-driven Cre recombinase transgenic mice (K5Cre⁺). Germ-line deletion is achieved by oocytic expression of maternal Cre transcript. Tissue-specific deletion can be achieved in parallel with male K5Cre⁺ mice, which express Cre in stratified squamous epithelia.

Unpredictably, constitutive removal of migfilin had no obvious effect, whereas epidermis-specific ablation resulted in post-natal lethality. Therefore, we modified our initial aim of the study thusly:

- I. To test *in vitro* findings on migfilin function *in vivo* in migfilin-null mice (Moik et al., 2011a)
- II. To explain how a tissue restricted gene ablation can cause a lethal phenotype, while constitutive migfilin-null mice were apparently normal (Moik et al., 2011b).

6. Brief summaries of the publications

Summary of Moik et al, 2011a

Migfilin is expressed in adult mice mainly in skin, heart, lung, and in simple epithelia, and in embryos at least from embryonic day 7.5. We generated a constitutive migfilin-null allele in mice using homologous recombination in ES cells. In contrast to previous publications claiming that depletion of migfilin interferes with FA function, homozygous migfilin-null mice had no detectable organ defects in development and homeostasis. Migfilin-null cells had no defects in integrin-mediated functions like integrin activation, adhesion or spreading. A previously described cell migration defect could be confirmed in skin keratinocytes, but excluded in fibroblasts. This overall lack of defects could not be due to long-term compensatory defects, as short-term siRNA-mediated depletion of migfilin in fibroblasts also failed to produce any defect.

Summary of Moik et al, 2011b

Migfilin-null skin epidermis was normal, but Cre recombinase expression in migfilin-null epidermis led to increased tetraploidy and apoptosis. This did not affect epidermal adhesion or barrier function, but led to severe epidermal inflammation and was lethal 7-10 days after birth. Cre expressing wild-type epidermis was normal except for slightly increased apoptosis, indicating that migfilin functioned in suppression of epidermal tetraploidy and apoptosis. Deletion of p53 in Cre-expressing migfilin-null epidermis increased morbidity, suggesting that migfilin suppresses tetraploidy independently of p53. Since tetraploidy drives skin carcinogenesis, we predicted migfilin-null mice to be more sensitive to skin cancer,

6. Brief summaries of the publications

which we tested and confirmed in a DMBA/TPA two-stage skin carcinogenesis model.

7. References

- Akazawa, H., Kudoh, S., Mochizuki, N., Takekoshi, N., Takano, H., Nagai, T. and Komuro, I.** (2004). A novel LIM protein Cal promotes cardiac differentiation by association with CSX/NKX2-5. *J Cell Biol* **164**, 395-405.
- Alberts, B.** (2002). *Molecular biology of the cell*. New York: Garland Science.
- Allavena, P., Garlanda, C., Borrello, M. G., Sica, A. and Mantovani, A.** (2008). Pathways connecting inflammation and cancer. *Curr Opin Genet Dev* **18**, 3-10.
- Andreassen, P. R., Lohez, O. D., Lacroix, F. B. and Margolis, R. L.** (2001). Tetraploid state induces p53-dependent arrest of nontransformed mammalian cells in G1. *Mol Biol Cell* **12**, 1315-28.
- Angel, P., Szabowski, A. and Schorpp-Kistner, M.** (2001). Function and regulation of AP-1 subunits in skin physiology and pathology. *Oncogene* **20**, 2413-23.
- Bartek, J., Lukas, C. and Lukas, J.** (2004). Checking on DNA damage in S phase. *Nat Rev Mol Cell Biol* **5**, 792-804.
- Bignold, L. P., Coghlan, B. L. and Jersmann, H. P.** (2006). Hansemann, Boveri, chromosomes and the gametogenesis-related theories of tumours. *Cell Biol Int* **30**, 640-4.
- Blagosklonny, M. V.** (2006). Prolonged mitosis versus tetraploid checkpoint: how p53 measures the duration of mitosis. *Cell Cycle* **5**, 971-5.
- Boukamp, P.** (2005). Non-melanoma skin cancer: what drives tumor development and progression? *Carcinogenesis* **26**, 1657-67.
- Boveri, T.** (2008). Concerning the origin of malignant tumours by Theodor Boveri. Translated and annotated by Henry Harris. *J Cell Sci* **121 Suppl 1**, 1-84.
- Bowcock, A. M. and Krueger, J. G.** (2005). Getting under the skin: the immunogenetics of psoriasis. *Nat Rev Immunol* **5**, 699-711.
- Box, N. F. and Terzian, T.** (2008). The role of p53 in pigmentation, tanning and melanoma. *Pigment Cell Melanoma Res* **21**, 525-33.
- Brakebusch, C., Grose, R., Quondamatteo, F., Ramirez, A., Jorcano, J. L., Pirro, A., Svensson, M., Herken, R., Sasaki, T., Timpl, R. et al.** (2000). Skin and hair follicle integrity is crucially dependent on beta 1 integrin expression on keratinocytes. *Embo J* **19**, 3990-4003.
- Brandner, J. M., Kief, S., Wladykowski, E., Houdek, P. and Moll, I.** (2006). Tight junction proteins in the skin. *Skin Pharmacol Physiol* **19**, 71-7.
- Brito, D. A. and Rieder, C. L.** (2006). Mitotic checkpoint slippage in humans occurs via cyclin B destruction in the presence of an active checkpoint. *Curr Biol* **16**, 1194-200.
- Bui, J. D. and Schreiber, R. D.** (2007). Cancer immunosurveillance, immunoediting and inflammation: independent or interdependent processes? *Curr Opin Immunol* **19**, 203-8.
- Caldwell, C. M., Green, R. A. and Kaplan, K. B.** (2007). APC mutations lead to cytokinetic failures in vitro and tetraploid genotypes in Min mice. *J Cell Biol* **178**, 1109-20.
- Castedo, M., Coquelle, A., Vivet, S., Vitale, I., Kauffmann, A., Dessen, P., Pequignot, M. O., Casares, N., Valent, A., Mouhamad, S. et al.** (2006). Apoptosis regulation in tetraploid cancer cells. *Embo J* **25**, 2584-95.

- Caswell, P. T., Vadrevu, S. and Norman, J. C.** (2009). Integrins: masters and slaves of endocytic transport. *Nat Rev Mol Cell Biol* **10**, 843-53.
- Chong, H. C., Tan, M. J., Philippe, V., Tan, S. H., Tan, C. K., Ku, C. W., Goh, Y. Y., Wahli, W., Michalik, L. and Tan, N. S.** (2009). Regulation of epithelial-mesenchymal IL-1 signaling by PPARbeta/delta is essential for skin homeostasis and wound healing. *J Cell Biol* **184**, 817-31.
- Clydesdale, G. J., Dandie, G. W. and Muller, H. K.** (2001). Ultraviolet light induced injury: immunological and inflammatory effects. *Immunol Cell Biol* **79**, 547-68.
- Colotta, F., Allavena, P., Sica, A., Garlanda, C. and Mantovani, A.** (2009). Cancer-related inflammation, the seventh hallmark of cancer: links to genetic instability. *Carcinogenesis* **30**, 1073-81.
- Costin, G. E. and Hearing, V. J.** (2007). Human skin pigmentation: melanocytes modulate skin color in response to stress. *Faseb J* **21**, 976-94.
- Cui, R., Widlund, H. R., Feige, E., Lin, J. Y., Wilensky, D. L., Igras, V. E., D'Orazio, J., Fung, C. Y., Schanbacher, C. F., Granter, S. R. et al.** (2007). Central role of p53 in the suntan response and pathologic hyperpigmentation. *Cell* **128**, 853-64.
- Das Thakur, M., Feng, Y., Jagannathan, R., Seppa, M. J., Skeath, J. B. and Longmore, G. D.** (2010). Ajuba LIM proteins are negative regulators of the Hippo signaling pathway. *Curr Biol* **20**, 657-62.
- Davoli, T., Denchi, E. L. and de Lange, T.** (2010). Persistent telomere damage induces bypass of mitosis and tetraploidy. *Cell* **141**, 81-93.
- de Visser, K. E., Eichten, A. and Coussens, L. M.** (2006). Paradoxical roles of the immune system during cancer development. *Nat Rev Cancer* **6**, 24-37.
- Demehri, S., Liu, Z., Lee, J., Lin, M. H., Crosby, S. D., Roberts, C. J., Grigsby, P. W., Miner, J. H., Farr, A. G. and Kopan, R.** (2008). Notch-deficient skin induces a lethal systemic B-lymphoproliferative disorder by secreting TSLP, a sentinel for epidermal integrity. *PLoS Biol* **6**, e123.
- Demidenko, Z. N., Kalurupalle, S., Hanko, C., Lim, C. U., Broude, E. and Blagosklonny, M. V.** (2008). Mechanism of G1-like arrest by low concentrations of paclitaxel: next cell cycle p53-dependent arrest with sub G1 DNA content mediated by prolonged mitosis. *Oncogene* **27**, 4402-10.
- Denecker, G., Hoste, E., Gilbert, B., Hochepped, T., Ovaere, P., Lippens, S., Van den Broecke, C., Van Damme, P., D'Herde, K., Hachem, J. P. et al.** (2007). Caspase-14 protects against epidermal UVB photodamage and water loss. *Nat Cell Biol* **9**, 666-74.
- Descargues, P., Sil, A. K. and Karin, M.** (2008). IKKalpha, a critical regulator of epidermal differentiation and a suppressor of skin cancer. *Embo J* **27**, 2639-47.
- Dobles, M., Liberal, V., Scott, M. L., Benezra, R. and Sorger, P. K.** (2000). Chromosome missegregation and apoptosis in mice lacking the mitotic checkpoint protein Mad2. *Cell* **101**, 635-45.
- Duelli, D. M., Hearn, S., Myers, M. P. and Lazebnik, Y.** (2005). A primate virus generates transformed human cells by fusion. *J Cell Biol* **171**, 493-503.
- Dupasquier, M., Stoitzner, P., van Oudenaren, A., Romani, N. and Leenen, P. J.** (2004). Macrophages and dendritic cells constitute a major subpopulation of cells in the mouse dermis. *J Invest Dermatol* **123**, 876-9.
- Eggert, U. S., Mitchison, T. J. and Field, C. M.** (2006). Animal cytokinesis: from parts list to mechanisms. *Annu Rev Biochem* **75**, 543-66.

- Elias, P. M.** (2005). Stratum corneum defensive functions: an integrated view. *J Invest Dermatol* **125**, 183-200.
- Eming, S. A., Krieg, T. and Davidson, J. M.** (2007). Inflammation in wound repair: molecular and cellular mechanisms. *J Invest Dermatol* **127**, 514-25.
- Epstein, C. J.** (1967). Cell size, nuclear content, and the development of polyploidy in the Mammalian liver. *Proc Natl Acad Sci U S A* **57**, 327-34.
- Fässler, R. and Meyer, M.** (1995). Consequences of lack of beta 1 integrin gene expression in mice. *Genes Dev* **9**, 1896-908.
- Feldmeyer, L., Keller, M., Niklaus, G., Hohl, D., Werner, S. and Beer, H. D.** (2007). The inflammasome mediates UVB-induced activation and secretion of interleukin-1beta by keratinocytes. *Curr Biol* **17**, 1140-5.
- Feng, Y. and Longmore, G. D.** (2005). The LIM protein Ajuba influences interleukin-1-induced NF-kappaB activation by affecting the assembly and activity of the protein kinase Czeta/p62/TRAF6 signaling complex. *Mol Cell Biol* **25**, 4010-22.
- Feng, Y., Zhao, H., Luderer, H. F., Epple, H., Faccio, R., Ross, F. P., Teitelbaum, S. L. and Longmore, G. D.** (2007). The LIM protein, Limd1, regulates AP-1 activation through an interaction with Traf6 to influence osteoclast development. *J Biol Chem* **282**, 39-48.
- Fujiwara, T., Bandi, M., Nitta, M., Ivanova, E. V., Bronson, R. T. and Pellman, D.** (2005). Cytokinesis failure generating tetraploids promotes tumorigenesis in p53-null cells. *Nature* **437**, 1043-7.
- Ganem, N. J., Godinho, S. A. and Pellman, D.** (2009). A mechanism linking extra centrosomes to chromosomal instability. *Nature* **460**, 278-82.
- Ganem, N. J., Storchova, Z. and Pellman, D.** (2007). Tetraploidy, aneuploidy and cancer. *Curr Opin Genet Dev* **17**, 157-62.
- Gareus, R., Huth, M., Breiden, B., Nenci, A., Rosch, N., Haase, I., Bloch, W., Sandhoff, K. and Pasparakis, M.** (2007). Normal epidermal differentiation but impaired skin-barrier formation upon keratinocyte-restricted IKK1 ablation. *Nat Cell Biol* **9**, 461-9.
- Geddis, A. E., Fox, N. E., Tkachenko, E. and Kaushansky, K.** (2007). Endomitotic megakaryocytes that form a bipolar spindle exhibit cleavage furrow ingression followed by furrow regression. *Cell Cycle* **6**, 455-60.
- Gisselsson, D., Hakanson, U., Stoller, P., Marti, D., Jin, Y., Rosengren, A. H., Stewenius, Y., Kahl, F. and Panagopoulos, I.** (2008). When the genome plays dice: circumvention of the spindle assembly checkpoint and near-random chromosome segregation in multipolar cancer cell mitoses. *PLoS One* **3**, e1871.
- Gisselsson, D., Jin, Y., Lindgren, D., Persson, J., Gisselsson, L., Hanks, S., Sehic, D., Mengelbier, L. H., Ora, I., Rahman, N. et al.** (2010). Generation of trisomies in cancer cells by multipolar mitosis and incomplete cytokinesis. *Proc Natl Acad Sci U S A* **107**, 20489-93.
- Gkretsi, V., Zhang, Y., Tu, Y., Chen, K., Stolz, D. B., Yang, Y., Watkins, S. C. and Wu, C.** (2005). Physical and functional association of migfilin with cell-cell adhesions. *J Cell Sci* **118**, 697-710.
- Glotzer, M.** (2009). The 3Ms of central spindle assembly: microtubules, motors and MAPs. *Nat Rev Mol Cell Biol* **10**, 9-20.
- Gray-Schopfer, V., Wellbrock, C. and Marais, R.** (2007). Melanoma biology and new targeted therapy. *Nature* **445**, 851-7.
- Groves, R. W., Mizutani, H., Kieffer, J. D. and Kupper, T. S.** (1995). Inflammatory skin disease in transgenic mice that express high levels of interleukin 1 alpha in basal epidermis. *Proc Natl Acad Sci U S A* **92**, 11874-8.

- Guc-Scekic, M., Milasin, J., Stevanovic, M., Stojanov, L. J. and Djordjevic, M.** (2002). Tetraploidy in a 26-month-old girl (cytogenetic and molecular studies). *Clin Genet* **61**, 62-5.
- Ha, G. H., Baek, K. H., Kim, H. S., Jeong, S. J., Kim, C. M., McKeon, F. and Lee, C. W.** (2007). p53 activation in response to mitotic spindle damage requires signaling via BubR1-mediated phosphorylation. *Cancer Res* **67**, 7155-64.
- Hafner, M., Wenk, J., Nenci, A., Pasparakis, M., Scharffetter-Kochanek, K., Smyth, N., Peters, T., Kess, D., Holtkotter, O., Shephard, P. et al.** (2004). Keratin 14 Cre transgenic mice authenticate keratin 14 as an oocyte-expressed protein. *Genesis* **38**, 176-81.
- Hanada, T. and Yoshimura, A.** (2002). Regulation of cytokine signaling and inflammation. *Cytokine Growth Factor Rev* **13**, 413-21.
- Hanahan, D. and Weinberg, R. A.** (2000). The hallmarks of cancer. *Cell* **100**, 57-70.
- Hanahan, D. and Weinberg, Robert A.** (2011). Hallmarks of Cancer: The Next Generation. *Cell* **144**, 646-674.
- Hass, H. G., Schmidt, A., Nehls, O. and Kaiser, S.** (2008). DNA ploidy, proliferative capacity and intratumoral heterogeneity in primary and recurrent head and neck squamous cell carcinomas (HNSCC)--potential implications for clinical management and treatment decisions. *Oral Oncol* **44**, 78-85.
- Hassold, T., Chen, N., Funkhouser, J., Jooss, T., Manuel, B., Matsuura, J., Matsuyama, A., Wilson, C., Yamane, J. A. and Jacobs, P. A.** (1980). A cytogenetic study of 1000 spontaneous abortions. *Ann Hum Genet* **44**, 151-78.
- Heath, J., Langton, A. K., Hammond, N. L., Overbeek, P. A., Dixon, M. J. and Headon, D. J.** (2009). Hair follicles are required for optimal growth during lateral skin expansion. *J Invest Dermatol* **129**, 2358-64.
- Henery, C. C., Bard, J. B. and Kaufman, M. H.** (1992). Tetraploidy in mice, embryonic cell number, and the grain of the developmental map. *Dev Biol* **152**, 233-41.
- Hennings, H., Glick, A. B., Lowry, D. T., Krsmanovic, L. S., Sly, L. M. and Yuspa, S. H.** (1993). FVB/N mice: an inbred strain sensitive to the chemical induction of squamous cell carcinomas in the skin. *Carcinogenesis* **14**, 2353-8.
- Higashi, A. Y., Ikawa, T., Muramatsu, M., Economides, A. N., Niwa, A., Okuda, T., Murphy, A. J., Rojas, J., Heike, T., Nakahata, T. et al.** (2009). Direct hematological toxicity and illegitimate chromosomal recombination caused by the systemic activation of CreERT2. *J Immunol* **182**, 5633-40.
- Hofbauer, G. F., Bouwes Bavinck, J. N. and Euvrard, S.** (2010). Organ transplantation and skin cancer: basic problems and new perspectives. *Exp Dermatol* **19**, 473-82.
- Hoffman, L. M., Nix, D. A., Benson, B., Boot-Hanford, R., Gustafsson, E., Jamora, C., Menzies, A. S., Goh, K. L., Jensen, C. C., Gertler, F. B. et al.** (2003). Targeted disruption of the murine zyxin gene. *Mol Cell Biol* **23**, 70-9.
- Huber, M. D. and Gerace, L.** (2007). The size-wise nucleus: nuclear volume control in eukaryotes. *J Cell Biol* **179**, 583-4.
- Hynes, R. O.** (2002). Integrins: bidirectional, allosteric signaling machines. *Cell* **110**, 673-87.
- Ithychanda, S. S., Das, M., Ma, Y. Q., Ding, K., Wang, X., Gupta, S., Wu, C., Plow, E. F. and Qin, J.** (2009). Migfilin, a molecular switch in regulation of integrin activation. *J Biol Chem* **284**, 4713-22.

- Jacks, T., Remington, L., Williams, B. O., Schmitt, E. M., Halachmi, S., Bronson, R. T. and Weinberg, R. A.** (1994). Tumor spectrum analysis in p53-mutant mice. *Curr Biol* **4**, 1-7.
- Jeganathan, K., Malureanu, L., Baker, D. J., Abraham, S. C. and van Deursen, J. M.** (2007). Bub1 mediates cell death in response to chromosome missegregation and acts to suppress spontaneous tumorigenesis. *J Cell Biol* **179**, 255-67.
- Jones, R. G., Plas, D. R., Kubek, S., Buzzai, M., Mu, J., Xu, Y., Birnbaum, M. J. and Thompson, C. B.** (2005). AMP-activated protein kinase induces a p53-dependent metabolic checkpoint. *Mol Cell* **18**, 283-93.
- Kadmas, J. L. and Beckerle, M. C.** (2004). The LIM domain: from the cytoskeleton to the nucleus. *Nat Rev Mol Cell Biol* **5**, 920-31.
- Kastan, M. B. and Bartek, J.** (2004). Cell-cycle checkpoints and cancer. *Nature* **432**, 316-23.
- Katalinic, A., Kunze, U. and Schafer, T.** (2003). Epidemiology of cutaneous melanoma and non-melanoma skin cancer in Schleswig-Holstein, Germany: incidence, clinical subtypes, tumour stages and localization (epidemiology of skin cancer). *Br J Dermatol* **149**, 1200-6.
- Kaur, P.** (2006). Interfollicular epidermal stem cells: identification, challenges, potential. *J Invest Dermatol* **126**, 1450-8.
- Kemp, C. J.** (2005). Multistep skin cancer in mice as a model to study the evolution of cancer cells. *Semin Cancer Biol* **15**, 460-73.
- Kiema, T., Lad, Y., Jiang, P., Oxley, C. L., Baldassarre, M., Wegener, K. L., Campbell, I. D., Ylanne, J. and Calderwood, D. A.** (2006). The molecular basis of filamin binding to integrins and competition with talin. *Mol Cell* **21**, 337-47.
- Klement, J. F., Rice, N. R., Car, B. D., Abbondanzo, S. J., Powers, G. D., Bhatt, P. H., Chen, C. H., Rosen, C. A. and Stewart, C. L.** (1996). IkappaBalpha deficiency results in a sustained NF-kappaB response and severe widespread dermatitis in mice. *Mol Cell Biol* **16**, 2341-9.
- Kwon, M., Godinho, S. A., Chandhok, N. S., Ganem, N. J., Azioune, A., Thery, M. and Pellman, D.** (2008). Mechanisms to suppress multipolar divisions in cancer cells with extra centrosomes. *Genes Dev* **22**, 2189-203.
- Lad, Y., Jiang, P., Ruskamo, S., Harburger, D. S., Ylanne, J., Campbell, I. D. and Calderwood, D. A.** (2008). Structural Basis of the Migfilin-Filamin Interaction and Competition with Integrin {beta} Tails. *J Biol Chem* **283**, 35154-63.
- Lafer, C. Z. and Neu, R. L.** (1988). A liveborn infant with tetraploidy. *Am J Med Genet* **31**, 375-8.
- Langton, A. K., Herrick, S. E. and Headon, D. J.** (2008). An extended epidermal response heals cutaneous wounds in the absence of a hair follicle stem cell contribution. *J Invest Dermatol* **128**, 1311-8.
- Lee, J. Y., Ristow, M., Lin, X., White, M. F., Magnuson, M. A. and Hennighausen, L.** (2006). RIP-Cre revisited, evidence for impairments of pancreatic beta-cell function. *J Biol Chem* **281**, 2649-53.
- Legate, K. R., Wickstrom, S. A. and Fassler, R.** (2009). Genetic and cell biological analysis of integrin outside-in signaling. *Genes Dev* **23**, 397-418.
- Lengauer, C., Kinzler, K. W. and Vogelstein, B.** (1998). Genetic instabilities in human cancers. *Nature* **396**, 643-649.
- Levy, V., Lindon, C., Zheng, Y., Harfe, B. D. and Morgan, B. A.** (2007). Epidermal stem cells arise from the hair follicle after wounding. *Faseb J*.

- Lippens, S., Denecker, G., Ovaere, P., Vandenabeele, P. and Declercq, W.** (2005). Death penalty for keratinocytes: apoptosis versus cornification. *Cell Death Differ* **12 Suppl 2**, 1497-508.
- Loonstra, A., Vooijs, M., Beverloo, H. B., Allak, B. A., van Drunen, E., Kanaar, R., Berns, A. and Jonkers, J.** (2001). Growth inhibition and DNA damage induced by Cre recombinase in mammalian cells. *Proc Natl Acad Sci U S A* **98**, 9209-14.
- Lordier, L., Jalil, A., Aurade, F., Larbret, F., Larghero, J., Debili, N., Vainchenker, W. and Chang, Y.** (2008). Megakaryocyte endomitosis is a failure of late cytokinesis related to defects in the contractile ring and Rho/Rock signaling. *Blood* **112**, 3164-74.
- Lorenz, K., Grashoff, C., Torka, R., Sakai, T., Langbein, L., Bloch, W., Aumailley, M. and Fassler, R.** (2007). Integrin-linked kinase is required for epidermal and hair follicle morphogenesis. *J Cell Biol* **177**, 501-13.
- Lowes, M. A., Bowcock, A. M. and Krueger, J. G.** (2007). Pathogenesis and therapy of psoriasis. *Nature* **445**, 866-73.
- Mack, J. A., Anand, S. and Maytin, E. V.** (2005). Proliferation and cornification during development of the mammalian epidermis. *Birth Defects Res C Embryo Today* **75**, 314-29.
- Maley, C. C., Galipeau, P. C., Li, X., Sanchez, C. A., Paulson, T. G., Blount, P. L. and Reid, B. J.** (2004). The combination of genetic instability and clonal expansion predicts progression to esophageal adenocarcinoma. *Cancer Res* **64**, 7629-33.
- Margadant, C., Charafeddine, R. A. and Sonnenberg, A.** (2010). Unique and redundant functions of integrins in the epidermis. *Faseb J* **24**, 4133-52.
- McGowan, K. A., Li, J. Z., Park, C. Y., Beaudry, V., Tabor, H. K., Sabnis, A. J., Zhang, W., Fuchs, H., de Angelis, M. H., Myers, R. M. et al.** (2008). Ribosomal mutations cause p53-mediated dark skin and pleiotropic effects. *Nat Genet* **40**, 963-70.
- McGrath, J. A., Eady, R. A. J. and Pope, F. M.** (2008). *Anatomy and Organization of Human Skin*: Blackwell Publishing, Inc.
- Mitelman, F., Johansson, B. and Mertens, F.** (2011). Mitelman Database of Chromosome Aberrations and Gene Fusions in Cancer. <http://cgap.nci.nih.gov/Chromosomes/Mitelman>.
- Moik, D. V., Janbandhu, V. C. and Fassler, R.** (2011a). Loss of migfilin expression has no overt consequences on murine development and homeostasis. *J Cell Sci* **124**, 414-21.
- Moik, D. V., Janbandhu, V. C. and Fassler, R.** (2011b). Migfilin represses tetraploidy and acts a tumor suppressor in skin. *manuscript in preparation*.
- Montanez, E., Ussar, S., Schifferer, M., Bosl, M., Zent, R., Moser, M. and Fassler, R.** (2008). Kindlin-2 controls bidirectional signaling of integrins. *Genes Dev* **22**, 1325-30.
- Moser, M., Legate, K. R., Zent, R. and Fassler, R.** (2009). The tail of integrins, talin, and kindlins. *Science* **324**, 895-9.
- Moser, M., Nieswandt, B., Ussar, S., Pozgajova, M. and Fassler, R.** (2008). Kindlin-3 is essential for integrin activation and platelet aggregation. *Nat Med* **14**, 325-30.
- Murase, D., Hachiya, A., Amano, Y., Ohuchi, A., Kitahara, T. and Takema, Y.** (2009). The essential role of p53 in hyperpigmentation of the skin via regulation of paracrine melanogenic cytokine receptor signaling. *J Biol Chem* **284**, 4343-53.

- Musacchio, A. and Salmon, E. D.** (2007). The spindle-assembly checkpoint in space and time. *Nat Rev Mol Cell Biol* **8**, 379-93.
- Naiche, L. A. and Papaioannou, V. E.** (2007). Cre activity causes widespread apoptosis and lethal anemia during embryonic development. *Genesis* **45**, 768-75.
- Nenci, A., Huth, M., Funteh, A., Schmidt-Suppran, M., Bloch, W., Metzger, D., Chambon, P., Rajewsky, K., Krieg, T., Haase, I. et al.** (2006). Skin lesion development in a mouse model of incontinentia pigmenti is triggered by NEMO deficiency in epidermal keratinocytes and requires TNF signaling. *Hum Mol Genet* **15**, 531-42.
- Nestle, F. O., Di Meglio, P., Qin, J. Z. and Nickoloff, B. J.** (2009). Skin immune sentinels in health and disease. *Nat Rev Immunol* **9**, 679-91.
- Nickoloff, B. J., Ben-Neriah, Y. and Pikarsky, E.** (2005). Inflammation and cancer: is the link as simple as we think? *J Invest Dermatol* **124**, x-xiv.
- Nickoloff, B. J., Xin, H., Nestle, F. O. and Qin, J. Z.** (2007). The cytokine and chemokine network in psoriasis. *Clin Dermatol* **25**, 568-73.
- Nieswandt, B., Moser, M., Pleines, I., Varga-Szabo, D., Monkley, S., Critchley, D. and Fassler, R.** (2007). Loss of talin1 in platelets abrogates integrin activation, platelet aggregation, and thrombus formation in vitro and in vivo. *J Exp Med* **204**, 3113-8.
- Nindl, I., Gottschling, M. and Stockfleth, E.** (2007). Human papillomaviruses and non-melanoma skin cancer: basic virology and clinical manifestations. *Dis Markers* **23**, 247-59.
- Ogle, B. M., Cascalho, M. and Platt, J. L.** (2005). Biological implications of cell fusion. *Nat Rev Mol Cell Biol* **6**, 567-75.
- Okura, M., Maeda, H., Nishikawa, S. and Mizoguchi, M.** (1995). Effects of monoclonal anti-c-kit antibody (ACK2) on melanocytes in newborn mice. *J Invest Dermatol* **105**, 322-8.
- Olaharski, A. J., Sotelo, R., Solorza-Luna, G., Gonsebatt, M. E., Guzman, P., Mohar, A. and Eastmond, D. A.** (2006). Tetraploidy and chromosomal instability are early events during cervical carcinogenesis. *Carcinogenesis* **27**, 337-43.
- Omori, E., Matsumoto, K., Sanjo, H., Sato, S., Akira, S., Smart, R. C. and Ninomiya-Tsuji, J.** (2006). TAK1 is a master regulator of epidermal homeostasis involving skin inflammation and apoptosis. *J Biol Chem* **281**, 19610-7.
- Pasparakis, M., Courtois, G., Hafner, M., Schmidt-Suppran, M., Nenci, A., Toksoy, A., Krampert, M., Goebeler, M., Gillitzer, R., Israel, A. et al.** (2002). TNF-mediated inflammatory skin disease in mice with epidermis-specific deletion of IKK2. *Nature* **417**, 861-6.
- Pellinen, T., Tuomi, S., Arjonen, A., Wolf, M., Edgren, H., Meyer, H., Grosse, R., Kitzing, T., Rantala, J. K., Kallioniemi, O. et al.** (2008). Integrin trafficking regulated by Rab21 is necessary for cytokinesis. *Dev Cell* **15**, 371-85.
- Pfeifer, A., Brandon, E. P., Kootstra, N., Gage, F. H. and Verma, I. M.** (2001). Delivery of the Cre recombinase by a self-deleting lentiviral vector: efficient gene targeting in vivo. *Proc Natl Acad Sci U S A* **98**, 11450-5.
- Pratt, S. J., Epple, H., Ward, M., Feng, Y., Braga, V. M. and Longmore, G. D.** (2005). The LIM protein Ajuba influences p130Cas localization and Rac1 activity during cell migration. *J Cell Biol* **168**, 813-24.
- Proksch, E., Brandner, J. M. and Jensen, J. M.** (2008). The skin: an indispensable barrier. *Exp Dermatol* **17**, 1063-72.

- Rajewsky, K., Gu, H., Kuhn, R., Betz, U. A., Muller, W., Roes, J. and Schwenk, F.** (1996). Conditional gene targeting. *J Clin Invest* **98**, 600-3.
- Ramirez, A., Page, A., Gandarillas, A., Zanet, J., Pibre, S., Vidal, M., Tusell, L., Genesca, A., Whitaker, D. A., Melton, D. W. et al.** (2004). A keratin K5Cre transgenic line appropriate for tissue-specific or generalized Cre-mediated recombination. *Genesis* **39**, 52-7.
- Robinson, J. K., Rademaker, A. W., Goolsby, C., Traczyk, T. N. and Zoladz, C.** (1996). DNA ploidy in nonmelanoma skin cancer. *Cancer* **77**, 284-91.
- Roumier, T., Valent, A., Perfettini, J. L., Metivier, D., Castedo, M. and Kroemer, G.** (2005). A cellular machine generating apoptosis-prone aneuploid cells. *Cell Death Differ* **12**, 91-3.
- Sah, V. P., Attardi, L. D., Mulligan, G. J., Williams, B. O., Bronson, R. T. and Jacks, T.** (1995). A subset of p53-deficient embryos exhibit exencephaly. *Nat Genet* **10**, 175-80.
- Schafer, M. and Werner, S.** (2008). Cancer as an overhealing wound: an old hypothesis revisited. *Nat Rev Mol Cell Biol* **9**, 628-38.
- Schiller, H. B., Friedel, C. C., Boulegue, C. and Fassler, R.** (2011). Quantitative proteomics of the integrin adhesome show a myosin II-dependent recruitment of LIM domain proteins. *EMBO Rep*.
- Schmidt-Suppran, M., Bloch, W., Courtois, G., Addicks, K., Israel, A., Rajewsky, K. and Pasparakis, M.** (2000). NEMO/IKK gamma-deficient mice model incontinentia pigmenti. *Mol Cell* **5**, 981-92.
- Schmidt-Suppran, M. and Rajewsky, K.** (2007). Vagaries of conditional gene targeting. *Nat Immunol* **8**, 665-8.
- Schmidt, E. E., Taylor, D. S., Prigge, J. R., Barnett, S. and Capecchi, M. R.** (2000). Illegitimate Cre-dependent chromosome rearrangements in transgenic mouse spermatids. *Proc Natl Acad Sci U S A* **97**, 13702-7.
- Schneider, M. R., Schmidt-Ullrich, R. and Paus, R.** (2009). The hair follicle as a dynamic miniorgan. *Curr Biol* **19**, R132-42.
- Schwartzman, J. M., Sotillo, R. and Benezra, R.** (2010). Mitotic chromosomal instability and cancer: mouse modelling of the human disease. *Nat Rev Cancer* **10**, 102-15.
- Segre, J. A.** (2006). Epidermal barrier formation and recovery in skin disorders. *J Clin Invest* **116**, 1150-8.
- Semprini, S., Troup, T. J., Kotelevtseva, N., King, K., Davis, J. R., Mullins, L. J., Chapman, K. E., Dunbar, D. R. and Mullins, J. J.** (2007). Cryptic loxP sites in mammalian genomes: genome-wide distribution and relevance for the efficiency of BAC/PAC recombineering techniques. *Nucleic Acids Res* **35**, 1402-10.
- Serhan, C. N. and Savill, J.** (2005). Resolution of inflammation: the beginning programs the end. *Nat Immunol* **6**, 1191-7.
- Sharp, T. V., Al-Attar, A., Foxler, D. E., Ding, L., de, A. V. T. Q., Zhang, Y., Nijmeh, H. S., Webb, T. M., Nicholson, A. G., Zhang, Q. et al.** (2008). The chromosome 3p21.3-encoded gene, LIMD1, is a critical tumor suppressor involved in human lung cancer development. *Proc Natl Acad Sci U S A* **105**, 19932-7.
- Silver, D. P. and Livingston, D. M.** (2001). Self-excising retroviral vectors encoding the Cre recombinase overcome Cre-mediated cellular toxicity. *Mol Cell* **8**, 233-43.
- Smits, T., Olthuis, D., Blokk, W. A., Kleinpenning, M. M., van de Kerkhof, P. C., van Erp, P. E. and Gerritsen, M. J.** (2007). Aneuploidy and proliferation in keratinocytic intraepidermal neoplasias. *Exp Dermatol* **16**, 81-6.

- Steigemann, P. and Gerlich, D. W.** (2009). Cytokinetic abscission: cellular dynamics at the midbody. *Trends Cell Biol* **19**, 606-16.
- Steigemann, P., Wurzenberger, C., Schmitz, M. H., Held, M., Guizetti, J., Maar, S. and Gerlich, D. W.** (2009). Aurora B-mediated abscission checkpoint protects against tetraploidization. *Cell* **136**, 473-84.
- Stepniak, E., Radice, G. L. and Vasioukhin, V.** (2009). Adhesive and signaling functions of cadherins and catenins in vertebrate development. *Cold Spring Harb Perspect Biol* **1**, a002949.
- Storchova, Z. and Kuffer, C.** (2008). The consequences of tetraploidy and aneuploidy. *J Cell Sci* **121**, 3859-66.
- Sullivan, M. and Morgan, D. O.** (2007). Finishing mitosis, one step at a time. *Nat Rev Mol Cell Biol* **8**, 894-903.
- Takafuta, T., Saeki, M., Fujimoto, T. T., Fujimura, K. and Shapiro, S. S.** (2003). A new member of the LIM protein family binds to filamin B and localizes at stress fibers. *J Biol Chem* **278**, 12175-81.
- Tang, Y. C., Williams, B. R., Siegel, J. J. and Amon, A.** (2011). Identification of Aneuploidy-Selective Antiproliferation Compounds. *Cell*.
- Thompson, S. L. and Compton, D. A.** (2010). Proliferation of aneuploid human cells is limited by a p53-dependent mechanism. *J Cell Biol* **188**, 369-81.
- Thyagarajan, B., Guimaraes, M. J., Groth, A. C. and Calos, M. P.** (2000). Mammalian genomes contain active recombinase recognition sites. *Gene* **244**, 47-54.
- Tinkle, C. L., Lechler, T., Pasolli, H. A. and Fuchs, E.** (2004). Conditional targeting of E-cadherin in skin: insights into hyperproliferative and degenerative responses. *Proc Natl Acad Sci U S A* **101**, 552-7.
- Torres, E. M., Dephoure, N., Panneerselvam, A., Tucker, C. M., Whittaker, C. A., Gygi, S. P., Dunham, M. J. and Amon, A.** (2010). Identification of aneuploidy-tolerating mutations. *Cell* **143**, 71-83.
- Tu, Y., Wu, S., Shi, X., Chen, K. and Wu, C.** (2003). Migfilin and Mig-2 link focal adhesions to filamin and the actin cytoskeleton and function in cell shape modulation. *Cell* **113**, 37-47.
- Uetake, Y. and Sluder, G.** (2004). Cell cycle progression after cleavage failure: mammalian somatic cells do not possess a "tetraploidy checkpoint". *J Cell Biol* **165**, 609-15.
- Uetake, Y. and Sluder, G.** (2010). Prolonged prometaphase blocks daughter cell proliferation despite normal completion of mitosis. *Curr Biol* **20**, 1666-71.
- Ussar, S., Moser, M., Widmaier, M., Rognoni, E., Harrer, C., Genzel-Boroviczeny, O. and Fassler, R.** (2008). Loss of Kindlin-1 causes skin atrophy and lethal neonatal intestinal epithelial dysfunction. *PLoS Genet* **4**, e1000289.
- Vassilopoulos, G., Wang, P. R. and Russell, D. W.** (2003). Transplanted bone marrow regenerates liver by cell fusion. *Nature* **422**, 901-4.
- Vervenne, H. B., Crombez, K. R., Delvaux, E. L., Janssens, V., Van de Ven, W. J. and Petit, M. M.** (2009). Targeted disruption of the mouse Lipoma Preferred Partner gene. *Biochem Biophys Res Commun* **379**, 368-73.
- Vitale, I., Senovilla, L., Galluzzi, L., Criollo, A., Vivet, S., Castedo, M. and Kroemer, G.** (2008). Chk1 inhibition activates p53 through p38 MAPK in tetraploid cancer cells. *Cell Cycle* **7**, 1956-61.
- Vitale, I., Senovilla, L., Jemaa, M., Michaud, M., Galluzzi, L., Kepp, O., Nanty, L., Criollo, A., Rello-Varona, S., Manic, G. et al.** (2010). Multipolar mitosis of tetraploid cells: inhibition by p53 and dependency on Mos. *Embo J* **29**, 1272-84.

- Vousden, K. H.** (2002). Activation of the p53 tumor suppressor protein. *Biochim Biophys Acta* **1602**, 47-59.
- Wagner, E. F., Schonhaler, H. B., Guinea-Viniegra, J. and Tschachler, E.** (2010). Psoriasis: what we have learned from mouse models. *Nat Rev Rheumatol* **6**, 704-14.
- Wakabayashi, Y., Mao, J. H., Brown, K., Girardi, M. and Balmain, A.** (2007). Promotion of Hras-induced squamous carcinomas by a polymorphic variant of the Patched gene in FVB mice. *Nature* **445**, 761-5.
- Wang, X., Willenbring, H., Akkari, Y., Torimaru, Y., Foster, M., Al-Dhalimy, M., Lagasse, E., Finegold, M., Olson, S. and Grompe, M.** (2003). Cell fusion is the principal source of bone-marrow-derived hepatocytes. *Nature* **422**, 897-901.
- Watt, F. M.** (2002). Role of integrins in regulating epidermal adhesion, growth and differentiation. *Embo J* **21**, 3919-26.
- Williams, B. R. and Amon, A.** (2009). Aneuploidy: cancer's fatal flaw? *Cancer Res* **69**, 5289-91.
- Wong, C. and Stearns, T.** (2005). Mammalian cells lack checkpoints for tetraploidy, aberrant centrosome number, and cytokinesis failure. *BMC Cell Biol* **6**, 6.
- Woo, R. A. and Poon, R. Y.** (2003). Cyclin-dependent kinases and S phase control in mammalian cells. *Cell Cycle* **2**, 316-24.
- Yang, J., Meyer, M., Muller, A. K., Bohm, F., Grose, R., Dauwalder, T., Verrey, F., Kopf, M., Partanen, J., Bloch, W. et al.** (2010). Fibroblast growth factor receptors 1 and 2 in keratinocytes control the epidermal barrier and cutaneous homeostasis. *J Cell Biol* **188**, 935-52.
- Yang, Z., Loncarek, J., Khodjakov, A. and Rieder, C. L.** (2008). Extra centrosomes and/or chromosomes prolong mitosis in human cells. *Nat Cell Biol* **10**, 748-51.
- Zhang, Y., Tu, Y., Gkretsi, V. and Wu, C.** (2006). Migfilin interacts with vasodilator-stimulated phosphoprotein (VASP) and regulates VASP localization to cell-matrix adhesions and migration. *J Biol Chem* **281**, 12397-407.
- Zhao, J., Zhang, Y., Ithychanda, S. S., Tu, Y., Chen, K., Qin, J. and Wu, C.** (2009). Migfilin interacts with Src and contributes to cell-matrix adhesion-mediated survival signaling. *J Biol Chem* **284**, 34308-20.
- Zheng, Q. and Zhao, Y.** (2007). The diverse biofunctions of LIM domain proteins: determined by subcellular localization and protein-protein interaction. *Biol Cell* **99**, 489-502.
- Zhivotovsky, B. and Kroemer, G.** (2004). Apoptosis and genomic instability. *Nat Rev Mol Cell Biol* **5**, 752-62.
- Zouboulis, C. C., Baron, J. M., Bohm, M., Kippenberger, S., Kurzen, H., Reichrath, J. and Thielitz, A.** (2008). Frontiers in sebaceous gland biology and pathology. *Exp Dermatol* **17**, 542-51.

8. Acknowledgements

This work would not have been possible without essential contributions by many members of the Department of Molecular Medicine and beyond, and I would like to express my deep-felt feeling of gratitude to them.

First and foremost, I am greatly thankful to my supervisor Prof. Dr. Reinhard Fässler, who helped and supported me in any conceivable manner while exploring the maze inside a labyrinth inside a tangle that turned out to be the analysis of the migfilin-null phenotype.

I would like to thank the members of the thesis committee for reviewing my work: Prof. Dr. Reinhard Fässler as first referee, Prof. Dr. Angelika Vollmar as second referee, and the committee members Prof. Dr. Karl-Peter Hopfner, PD Dr. Manfred Ogris, PD Dr. Stefan Zahler, and Prof. Dr. Klaus Förstemann.

I am indebted in gratitude and friendship to Dr. Vaibhao C. Janbandhu, who joined me in solving the migfilin phenotype conundrum. Without him, we surely would not have elucidated the function of migfilin.

For help with generation of the migfilin-floxed allele, I would like to thank PD Dr. Markus Moser and Dr. Siegrid Ussar. Invaluable introductions to various experimental techniques were thankfully received from Dr. Hao-Ven Wang, Dr. Aurelia Raducanu, Dr. Katrin Lorenz, Dr. Michael Leiss, Dr. Carsten Grashoff and Dr. Attila Aszodi. For helpful discussions and advice, I would like to thank Dr. Sara Wickström and Dr. Marc Schmidt-Supprian. For help with getting to grips with the tetraploidy field, I am deeply thankful to Dr. Zuzana Storchova, Christoph Kuffer and Anastazia Kuznetsova. Raphael Ruppert, Klaus-Dieter Heger and Christoph Vahl offered gratefully received support with cell sorting and flow cytometry. Thanks to Dr.

8. Acknowledgements

Kyle Legate, Christoph Kuffer, Moritz Widmaier and Emanuel Rognoni for critically reading this thesis.

I would also like to thank Dr. Walter Göhring, Dr. Armin Lambacher and Klaus Weber for constant technical and administrative support, Carmen Schmitz for help with administrative work. For ensuring outstanding mouse facilities and help and guidance with animal handling and experimentation, I would like to thank Dr. Heinz Brandstätter and Dr. Eva Hesse. Finally, I would like to express my gratitude to the animal caretakers for excellent animal husbandry, in particular Jens Päßler and Silvana Kaphengst.

All modern scientists are standing on the shoulders of a legion of giants, who drove and expanded science ever further. Thus, deep-felt words of appreciation go towards the countless scientists who devoted their lives to science before us and elevated us to these great heights of scientific knowledge we are privileged to experience today.

Most importantly, I would like to thank my family, especially my wife Stefanie and my daughter Pia Katharina, who gave a deeper purpose to this work and constantly provided support, love, warmth and energy during my doctoral research and writing of this thesis.

9. Curriculum vitae

PERSONAL INFORMATION

Name Daniel V. Moik **Nationality** German

DOCTORAL EDUCATION

10/2005- Ph.D. student with Prof. Dr. Reinhard Fässler,
5/2011 Department of Molecular Medicine, Max-Planck Institute of Biochemistry,
Martinsried, Germany

München, den 15. April 2011

10. Supplements

Reprint of Moik et al, 2011a (including supplementary information).

Manuscript version of Moik et al, 2011b as prepared for submission.

Moik et al, 2011a

Loss of migfilin expression has no overt consequences on murine development and homeostasis

Daniel V. Moik, Vaibhao C. Janbandhu and Reinhard Fässler*

Max-Planck-Institute of Biochemistry, Department of Molecular Medicine, 82152 Martinsried, Germany

*Author for correspondence (faessler@biochem.mpg.de)

Accepted 5 October 2010
Journal of Cell Science 124, 414–421
 © 2011. Published by The Company of Biologists Ltd
 doi:10.1242/jcs.075960

Summary

Migfilin is a LIM-domain-containing protein of the zyxin family of adaptor proteins and is found at cell–matrix and cell–cell adhesion sites and in the nucleus. *In vitro* studies have suggested that migfilin promotes $\beta 1$ integrin activity, regulates cell spreading and migration and induces cardiomyocyte differentiation. To test directly the function of migfilin *in vivo*, we generated a migfilin-null mouse strain. Here, we report that loss of migfilin expression permits normal development and normal postnatal aging. Fibroblasts and keratinocytes from migfilin-null mice display normal spreading and adhesion, and normal integrin expression and activation. The migration velocity and directionality of migfilin-null embryonic fibroblasts were normal, whereas the velocity of migfilin-null keratinocytes in wound scratch assays was slightly but significantly reduced. Our findings indicate that the roles of migfilin are functionally redundant during mouse development and tissue homeostasis.

Key words: Fblim1, Migfilin, Adhesion, Integrin, F-actin, Development, Zyxin family

Introduction

Cell–matrix and cell–cell adhesions are essential for the development and homeostasis of multicellular organisms. During development, cell adhesion to defined substrates or neighboring cells defines spatial identity and can induce cell fate decisions and provide migratory guidance cues. In fully developed organisms, adhesion-mediated signaling provides survival cues and regulates tissue functions. Cell adhesion to extracellular matrix (ECM) proteins is largely mediated through specific transmembrane receptors of the integrin family. Integrins are heterodimeric glycoproteins comprising α and β subunits. Each subunit consists of a large extracellular domain, a transmembrane domain and a short cytoplasmic domain. Integrins function as bidirectional signaling molecules; their affinity for ligands is regulated (integrin activation) by direct interactions of the β -subunit cytoplasmic tails with the cytoskeletal proteins talin and kindlin (inside-out signaling) (Moser et al., 2009). Following ligand binding, integrins transduce signals into cells (outside-in signaling) by forming large signaling hubs called focal adhesions (FAs), which consist of signaling and adaptor proteins that regulate actin dynamics and various intracellular signaling pathways (Hynes, 2002; Legate and Fässler, 2009).

Migfilin [encoded by filamin-binding LIM protein 1 (Fblim1)] is an adaptor protein that is recruited to FAs. It belongs to the zyxin family of LIM-domain-containing proteins (where LIM stands for Lin-11, Isl-1 and Mec-3) and comprises an N-terminal domain, without obvious sequence motifs, followed by a proline-rich region containing a nuclear export signal (NES) and three C-terminal LIM domains. The N-terminal domain of migfilin can bind to filamins, the proline-rich region to VASP (for vasodilator-stimulated phosphoprotein) (Zhang et al., 2006) and the LIM domains to kindlin-2 (FERMT2) and the transcription factor Nkx2.5 (Akazawa et al., 2004; Takafuta et al., 2003; Tu et al., 2003). Migfilin is encoded by a single gene, which can be alternatively spliced to give

rise to two smaller isoforms whose biological relevance is unknown; one splice variant is called migfilin(s), which lacks the NES and the proline-rich region. The other isoform is called filamin-binding LIM protein 1 (Fblp1), which lacks the third LIM domain.

Studies with cultured cell lines have identified migfilin as an important mediator of integrin function. Small interfering RNA (siRNA)-mediated depletion of migfilin in different cell lines results in reduced integrin-mediated adhesion, spreading and migration (Tu et al., 2003; Zhang et al., 2006). Talin and the kindlins activate integrins (Montanez et al., 2008; Moser et al., 2009), whereas filamins compete with talin for binding to the cytoplasmic tails of integrins and thereby attenuate integrin activation (Kiema et al., 2006). On the basis of findings showing that migfilin can compete with β -integrin cytoplasmic tails for binding to filamins, it has been proposed that migfilin conveys its stimulating role on integrins by promoting talin binding to integrin tails, resulting in integrin activation (Ithychanda et al., 2009; Lad et al., 2008). Interestingly, overexpression of migfilin can also diminish cell migration, which was shown to depend on the proline-rich motif (Zhang et al., 2006). Furthermore, the proline-rich motif seems to be required for recruiting VASP to FAs. It is not entirely clear, however, whether recruitment of VASP plays a regulative role for modulating cell migration.

Besides its role in cell–matrix adhesions, migfilin has been shown to have several additional functions. Migfilin is found at cell–cell junctions together with β -catenin; formation of cell–cell contacts was impaired after siRNA-mediated knockdown of migfilin, as shown in a time course with keratinocytes after addition of Ca^{2+} (Gkretsi et al., 2005). Furthermore, migfilin is also present in the nucleus, where it might co-activate transcription factors including Nkx2.5 (Akazawa et al., 2004), whose activity is essential for heart morphogenesis. Finally, migfilin has also been shown to bind to c-Src, which promotes cell survival (Zhao et al., 2009).

To test directly the role of migfilin function *in vivo*, we used homologous recombination in embryonic stem (ES) cells to generate null alleles for the gene encoding migfilin. Surprisingly, migfilin-null mice develop and age normally. These results suggest that the role of migfilin in adhesion signaling and developmental pathways overlaps with functions of other LIM-domain-containing proteins.

Results

Migfilin-null mice have no apparent phenotype

We generated a conditional floxed (fl) allele of the gene encoding migfilin by flanking exons 2 and 3 with loxP sites (supplementary material Fig. S1A,B). Intercrossing of floxed migfilin mice with a deleter flippase removed the neomycin selection cassette and resulted in migfilin floxed mice, which expressed comparable migfilin levels in all tissues tested including heart (supplementary material Fig. S1C and data not shown). Mating migfilin floxed mice with a deleter-Cre strain removed the loxP-flanked exons, which contain the start codon of migfilin. Given that downstream ATG codons would not be in the correct reading frame, we expected to observe loss of migfilin expression. To confirm this, we performed western blotting of lung and heart lysates using an antibody raised against a peptide from the first LIM domain of migfilin. In control lysates the antibody recognized a single band at an apparent molecular mass of 50 kDa (Fig. 1A). This was larger than the predicted size calculated from the primary sequence but comparable with the reported molecular mass of human migfilin (Tu et al., 2003). We did not detect bands at molecular masses below 50 kDa, suggesting that Fblp1 or migfilin(s) was not expressed in heart and lung (Fig. 1A). As expected, migfilin protein was absent from homozygous mutant migfilin ($-/-$) mice and

reduced in migfilin heterozygous ($+/-$) mice (Fig. 1A). Cre-mediated deletion of exons 2 and 3 did not significantly affect the level of the transcript encoding migfilin, as measured by quantitative RT-PCR (supplementary material Fig. S1D). Offspring from migfilin heterozygous intercrosses yielded normal numbers of migfilin-null mice, which presented no apparent defects (Fig. 1B), gained weight in the same manner as wild-type and heterozygous littermates (Fig. 1C) and were fertile.

To test whether other zyxin family members were upregulated, thereby compensating for the loss of migfilin, we performed quantitative RT-PCR and western blotting in heart and lung. We did not observe significant changes of their transcript or protein levels upon migfilin deletion (Fig. 1D,E; supplementary material Fig. S1E,F), indicating that compensatory upregulation did not occur.

Expression profile of migfilin

As migfilin-null mice did not have an obvious phenotype, we decided to analyze migfilin expression in various mouse tissues. Western blotting detected migfilin protein in heart, lung, skin, spleen, uterus and in the entire intestinal tract (Fig. 2A). In line with a previous report (Takafuta et al., 2003), migfilin levels were not detectable in platelets (supplementary material Fig. S2A). Furthermore, we could not detect migfilin in B cells and mast cells and found only very low amounts in macrophages (supplementary material Fig. S2A). Northern blotting showed a major transcript encoding migfilin of 3.2 kb in heart, lung, skin, intestinal tract, spleen and uterus (Fig. 2B). As previously reported (Akazawa et al., 2004), lung contained a second transcript with a size of approximately 6 kb (Fig. 2B). Brain, kidney, liver, skeletal muscle and thymus lacked detectable migfilin mRNAs (Fig. 2B). RT-PCR confirmed the absence of migfilin expression in brain, liver and

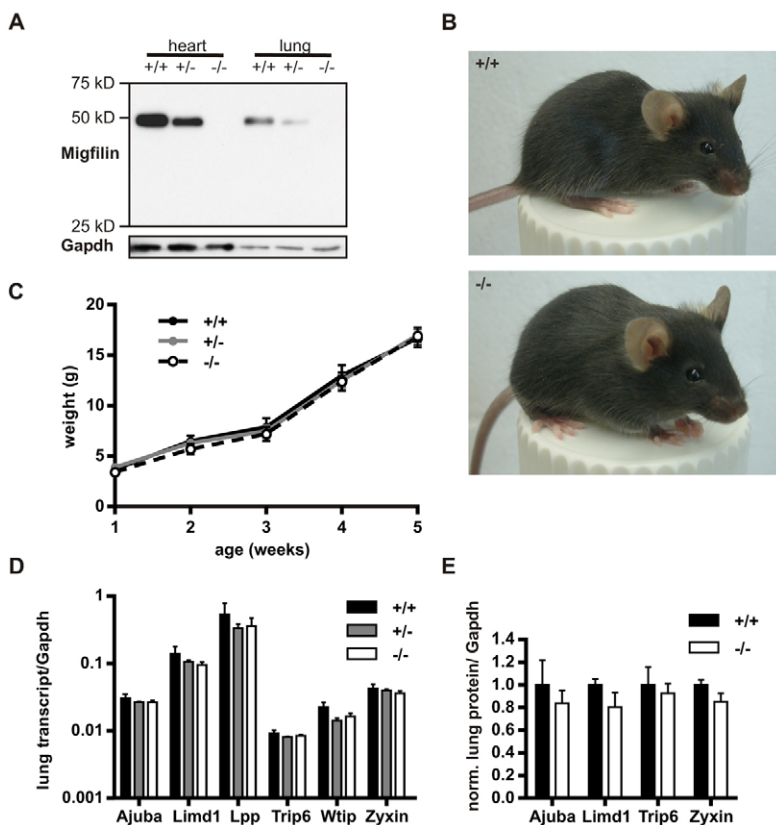


Fig. 1. Migfilin-null mice are viable and without obvious phenotype. (A) Western blot of migfilin expression in heart and lung from migfilin wild-type, heterozygous and null ($+/+$, $+/-$ and $-/-$, respectively) littermates. Gapdh served as the loading control. (B) Wild-type and migfilin-null littermates at 4 weeks of age. (C) Weight-gain curve of migfilin wild-type ($n=7$), heterozygous ($n=15$) and null ($n=7$) littermates. (D) Quantitative RT-PCR analysis of the zyxin family members using total RNA isolated from migfilin wild-type, heterozygous and null lung. Transcript levels were normalized to the levels of Gapdh. Results are means + s.d. (E) Expression levels of the indicated proteins in wild-type and migfilin-null lungs (three animals per genotype). Band intensities of western blots were first normalized to that of Gapdh, then normalized to the wild-type expression levels. Results are means + s.d.

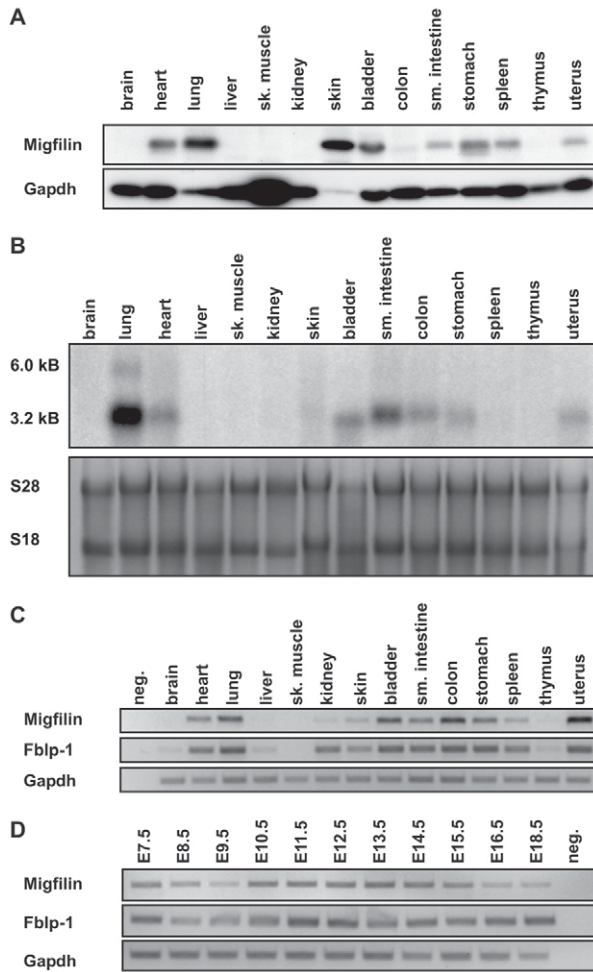


Fig. 2. Expression profile of murine migfilin. (A) Western blot of migfilin in different organs. Gapdh served as the loading control. (B) Northern blot analysis of migfilin from indicated tissues. The 28S and 18S ribosomal RNAs are shown as a loading control. (C) Semi-quantitative RT-PCR from the indicated tissues. The migfilin-specific primers span exons 5 and 8 and the *Fblp1*-specific primers span exons 6 and 7b (results are after 36 cycles for the latter) (see supplementary material Fig. S2C for a schematic of the primer positions). neg. represents a no-template control. (D) Semi-quantitative RT-PCR from whole embryos at the indicated embryonic age (E).

skeletal muscle and revealed only minute amounts in kidney and thymus (Fig. 2C).

The *FBLP1* transcript in humans is generated by a read-through of exon 7 into the following intron (supplementary material Fig. S2B) and thus lacks exons 8 and 9 coding for the third LIM domain. Primers specific for the equivalent murine *Fblp1* transcript (supplementary material Fig. S2C) detected very low *Fblp1* mRNA levels, as we required 36 amplification cycles to detect *Fblp1* mRNA in brain and liver (Fig. 2C). Expression of the migfilin(s) transcript could not be detected with primers flanking exons 3 and 6 (data not shown). Semi-quantitative RT-PCR with total RNA isolated from embryos of embryonic day (E) 7.5 to 18.5 (Fig. 2D) detected mRNAs encoding migfilin and *Fblp1* in all stages analyzed.

Migfilin-null mice have no apparent organ abnormalities

Next we carried out hematoxylin and eosin (HE) and immunofluorescence stainings of sections from various tissues.

HE staining revealed no abnormalities in hearts from migfilin-null mice (Fig. 3A). Migfilin colocalized with vinculin at the intercalated discs in the wild-type heart (Fig. 3A; see also supplementary material Fig. S3A for single-color channels). Previous data implicated a nuclear localization of migfilin in cardiomyocytes (Akazawa et al., 2004), which we could not confirm (Fig. 3A). As expected, migfilin expression was lost in hearts from migfilin-null mice. Although migfilin expression was lost, we found a normal distribution of vinculin (Fig. 3A; supplementary material Fig. S3A).

Despite the high expression of migfilin in the lung, we did not detect abnormalities in lungs from migfilin-null mice (Fig. 3B). Migfilin levels were high in lung epithelial cells (Fig. 3B), in mural cells of the lung vasculature (supplementary material Fig. S3B) and in residential macrophages (Fig. 3B, arrowheads; supplementary material Fig. S3C). Lung endothelial cells, visualized by endomucin co-staining, did not express detectable levels of migfilin (Fig. 3B).

The morphology of colon and kidney was unaltered in migfilin-null mice, as determined by HE staining (Fig. 3C,D), and immunofluorescence stains revealed low expression of migfilin in cryptal enterocytes and high expression in upward moving and differentiated enterocytes (Fig. 3C). Although we did not detect migfilin protein in lysates of whole kidney (Fig. 2A), migfilin levels were high in glomeruli (Fig. 3D).

Finally, apoptosis was normal in all the organs we tested (data not shown). We also could not detect changes in the levels of total Src and Src phosphorylated at Tyr416 in lung tissue lysates from migfilin-null mice (supplementary material Fig. S3D).

Migfilin-null cells display normal F-actin distribution and $\beta 1$ integrin activation

Next, we isolated primary migfilin-null keratinocytes, cultured them in the presence of low levels of Ca^{2+} , to prevent differentiation, and analyzed integrin- and actin-mediated functions. Migfilin was present in FAs of wild-type keratinocytes, where it colocalized with vinculin (Fig. 4A). Migfilin-null cells developed normal FAs, in terms of number and size, which were connected to F-actin stress fibers in a manner similar to that in wild-type cells (Fig. 4B). In contrast with a previous report (Zhang et al., 2006), we found robust recruitment of VASP to vinculin-containing FAs both in migfilin-null keratinocytes (Fig. 4C,D) and in migfilin-null fibroblasts (data not shown). Addition of Ca^{2+} induced migfilin translocation to cell-cell adhesion sites, where it colocalized with vinculin (Fig. 4E). Upon Ca^{2+} treatment migfilin-null cells were also able to form cell-cell adhesions with a fine, but prominent, lining of vinculin (Fig. 4F).

We next tested whether migfilin-null cells have a normal integrin profile. The levels of integrin $\beta 1$, $\beta 4$, $\alpha 2$, $\alpha 5$ and αv were similar on wild-type and migfilin-null keratinocytes (Fig. 4G; supplementary material Fig. S4B). We also found normal 9EG7 binding on migfilin-null keratinocytes (Fig. 4H; supplementary material Fig. S4B) and a similar increase in 9EG7 binding on wild-type and migfilin-null keratinocytes after treatment with Mn^{2+} (Fig. 4H). These findings suggest that migfilin is required neither for maintaining the basal $\beta 1$ integrin activity nor for inducing $\beta 1$ integrin activation by Mn^{2+} .

Migfilin promotes the migration speed of keratinocytes

siRNA-mediated depletion of migfilin has been shown to impair integrin-mediated adhesion and spreading of human cells (Tu et

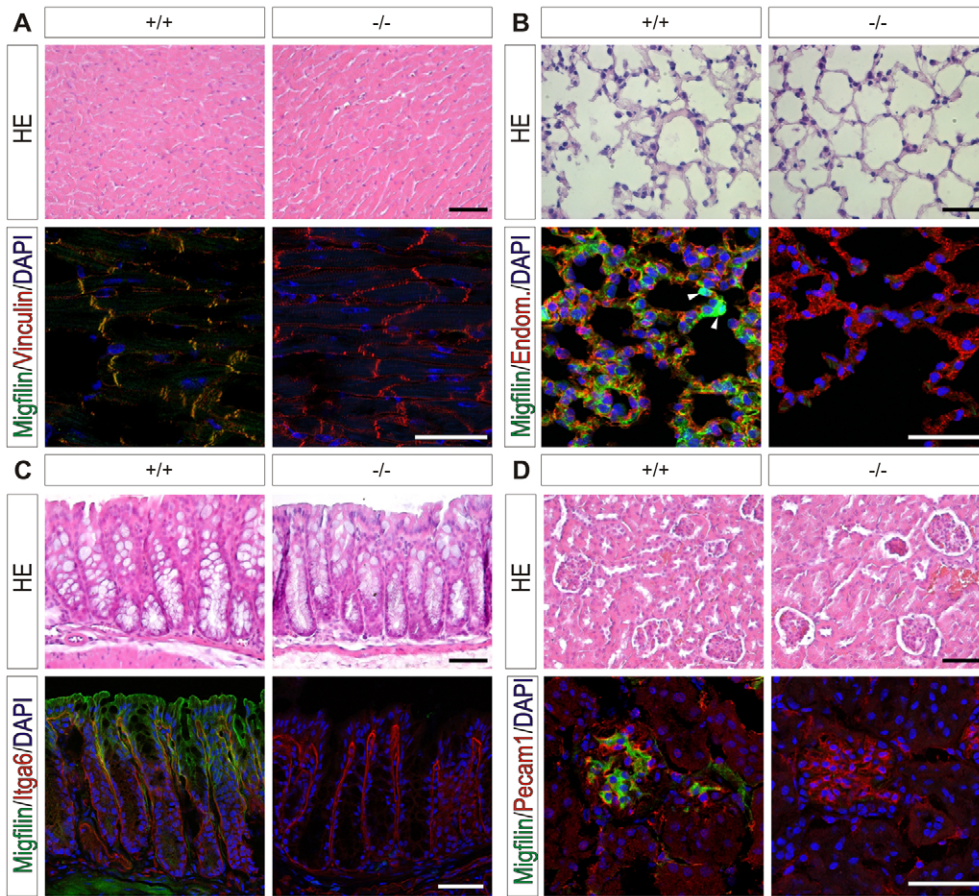


Fig. 3. Migfilin is not required for tissue homeostasis. Hematoxylin and eosin (HE) and immunofluorescence staining of migfilin wild-type (+/+) and null (-/-) heart (A), lung (B), colon (C) and kidney (D) with the indicated antibodies. Endom., endomucin. The arrowheads in B indicate residual macrophages. Scale bars: 50 μ m.

al., 2003; Zhang et al., 2006). To test whether genetic ablation led to similar defects, we plated wild-type and migfilin-null keratinocytes on different substrates to compare their adhesive and spreading properties. Loss of migfilin expression did not affect adhesion to collagen I, collagen IV, fibronectin or laminin-322 (Fig. 4I). Furthermore, spreading of migfilin-null keratinocytes on a mixture of collagen I and fibronectin was also indistinguishable from that displayed in wild-type cells (Fig. 4J).

It is possible that abrupt migfilin depletion by specific siRNAs results in phenotypic changes that are not visible in the 'compensation prone' genetic model used in the present study. To test this possibility, we performed siRNA-mediated depletion of migfilin in immortalized migfilin floxed (fl/fl) mouse embryonic fibroblasts (MEFs). This resulted in an efficient knockdown of migfilin, whereas cells transfected with a scrambled control siRNA expressed normal levels of migfilin (supplementary material Fig. S5A and data not shown). To control off-target effects, we also transfected migfilin-null MEFs derived from fl/fl MEF clones with these siRNAs. Vinculin localized to FAs in both migfilin fl/fl and null MEFs transfected with either migfilin-specific or scrambled siRNAs (supplementary material Fig. S5B). Furthermore, the size and the number of FAs were similar in cells transfected with either siRNA (supplementary material Fig. S5B). Moreover, we did not find defects in cell adhesion or in spreading kinetics (supplementary material Fig. S5C,D).

Given that it has also been reported that siRNA-mediated migfilin depletion impairs cell migration (Zhang et al., 2006), we analyzed cell migration in a scratch wound assay. Whereas migfilin-null MEFs showed a migration behavior similar to that of wild-

type cells (Fig. 5A; supplementary material Fig. S5E), migration velocity was reduced by 28% in migfilin-null keratinocytes when compared with that of wild-type keratinocytes ($P < 0.001$; Fig. 5B; supplementary material Fig. S5F). The directionality of migration was unchanged in migfilin-null keratinocytes (Fig. 5B).

To ensure that the migration defect of migfilin-null keratinocytes was specific to migfilin loss, we retrovirally transduced migfilin-null keratinocytes with expression constructs encoding either the wild-type migfilin-GFP (green fluorescent protein) fusion protein or for the filamin-binding-deficient (D11A13 mutated) migfilin-GFP fusion protein (Ithychanda et al., 2009). The transduced cells were sorted by FACS for equal GFP levels (Fig. 5C) and the subcellular localization of the fusion proteins was analyzed. Both migfilin-GFP and migfilin(D11A13)-GFP localized to FAs (Fig. 5D). Similar to endogenous migfilin in wild-type keratinocytes (Fig. 4A), the re-expressed wild-type protein also weakly localized to F-actin stress fibers (Fig. 5E). This stress fiber localization depended on interaction with filamins as it could not be observed in cells expressing migfilin(D11A13)-GFP (Fig. 5E). Both constructs were able to rescue the defect in the migration velocity of migfilin-null keratinocytes ($P < 0.001$; Fig. 5F). These findings suggest that the migfilin-filamin interaction is not required for controlling the migration speed in keratinocytes.

Discussion

Cell-ECM adhesion is important for cell shape, motility and signaling. Migfilin is an integrin-proximal adaptor localized to FAs and provides a link between integrins and the actin cytoskeleton (Takafuta et al., 2003; Tu et al., 2003). Here, we tested the role of

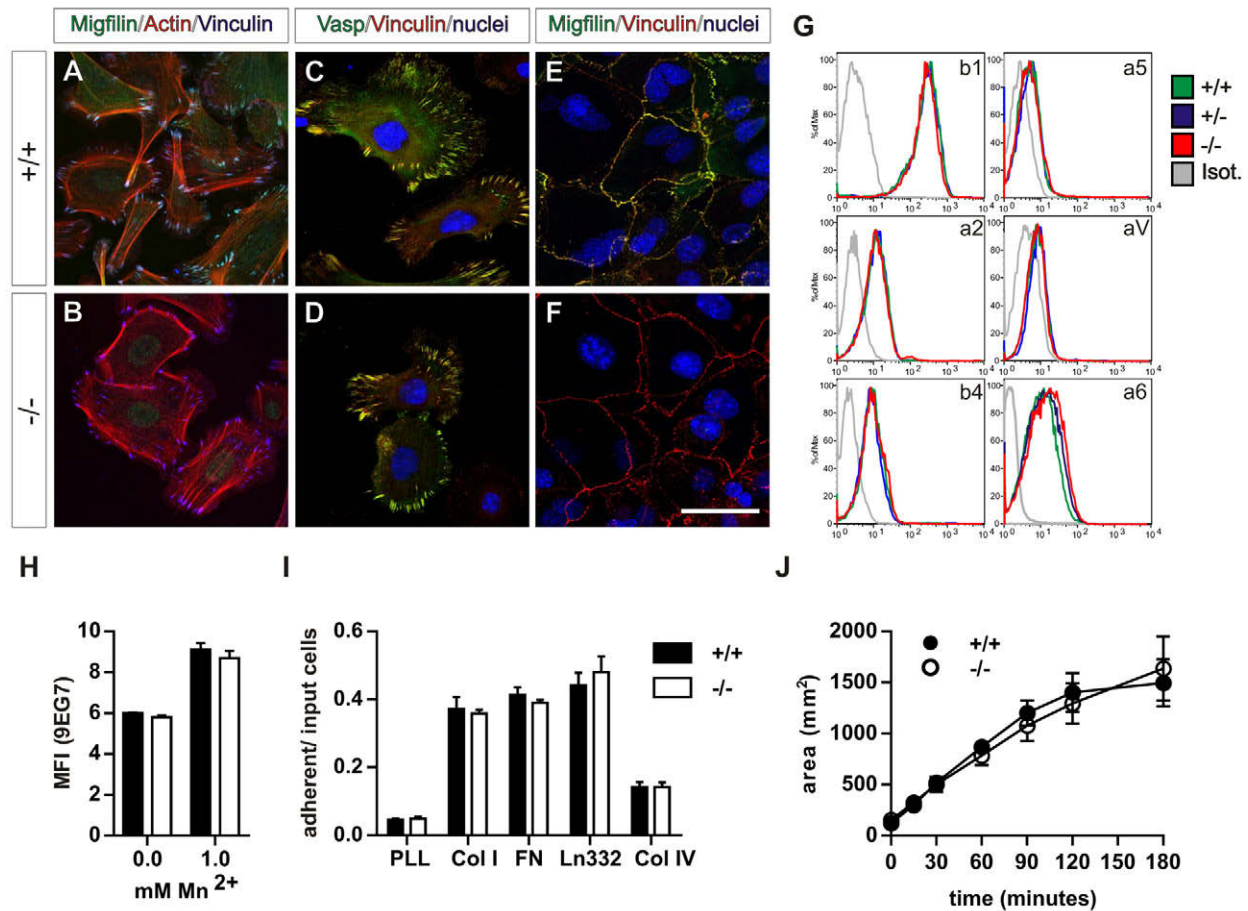


Fig. 4. Migfilin-null keratinocytes have normal integrin function. Immunofluorescence staining of primary migfilin wild-type (+/+; A,C,E) and null (-/-; B,D,F) keratinocytes for migfilin (green), F-actin (red) and vinculin (blue) (panels A and B); for VASP (green), vinculin (red) and nuclei (blue) (panels C and D); and for migfilin (green), vinculin (red) and nuclei (blue) after Ca²⁺ treatment for 24 hours (panels E and F). Scale bar: 20 μ m. (G) Primary keratinocytes from migfilin wild-type, heterozygous (+/-) and null mice were stained with antibodies against the indicated integrin subunits and analyzed by flow cytometry. Isot., isotype control. (H) Flow cytometry of primary keratinocytes stained with the monoclonal antibody 9EG7 before and after treatment with 1 mM Mn²⁺. Normalized mean fluorescence intensity (MFI) values are shown. Data are measurements from a single representative experiment repeated three times and are means + s.d. (I) Cell adhesion assay with primary migfilin wild-type and null keratinocytes on poly-L-lysine (PLL), collagen I (Col I), fibronectin (FN), laminin 322 (Ln322) and collagen IV (Col IV). Results are the means + s.e.m. for four replicates. (J) Spreading kinetics of primary keratinocytes on FN+Col I when visualized by time-lapse microscopy. A total of ten cells per genotype were analyzed; the cell area was measured using ImageJ. Results are means \pm s.e.m.

migfilin *in vivo* by genetically ablating the gene encoding migfilin. Unexpectedly, we found that migfilin is dispensable for development and tissue maintenance.

The wide expression pattern of migfilin suggested a role for this FA protein in several organs. Although high levels were found at the intercalated discs of cardiomyocytes and in smooth muscle cells, migfilin was not detected in skeletal muscle. Similarly, some epithelia, such as epidermis, lung and intestine, expressed high levels of migfilin, whereas in others, such as in the epithelium of the esophagus, tongue or mammary gland, it could not be detected (data not shown). However, regardless of the migfilin expression level in the different tissues, we were unable to detect abnormalities in migfilin-null organs, including changes in cell survival.

It has been suggested that migfilin promotes activation of integrin β 1 *in vitro* (Ithychanda et al., 2009); however, we observed no change in activation of integrin β 1 upon eliminating migfilin expression *in vivo*. This also holds true for all previously published *in vitro* findings regarding cell–matrix adhesion and cell spreading. In line with a previous observation (Zhang et al., 2006), we noticed

a reduction in the migration speed of migfilin-null keratinocytes in scratch assays. Migfilin-null fibroblasts, however, did not display this defect. Previous cell culture studies demonstrated that both siRNA-mediated depletion, as well as overexpression, of migfilin reduce migration speed (Zhang et al., 2006). It has been proposed that a diminished localization of VASP to FAs might cause the diminished migration speed. Clearly, this observation cannot explain the defect in primary cells as we did not observe defects in VASP localization after genetic ablation of migfilin in keratinocytes.

We do not know why migration velocity is reduced in migfilin-null keratinocytes. Neither polarity nor directionality of migration was affected, which excludes a requirement for migfilin in initiating or maintaining a polarized lamellipodium (Harms et al., 2005). Integrin activation and keratinocyte adhesion were also unchanged, precluding increased integrin activity as a cause for the reduced migration speed. We can also exclude abnormal distribution or reduced levels of p130Cas (Bcar1) in nascent FAs as cause for the reduced migration speed (data not shown). Such a reduced p130Cas level leading to diminished Rac1 activity was shown to be causative

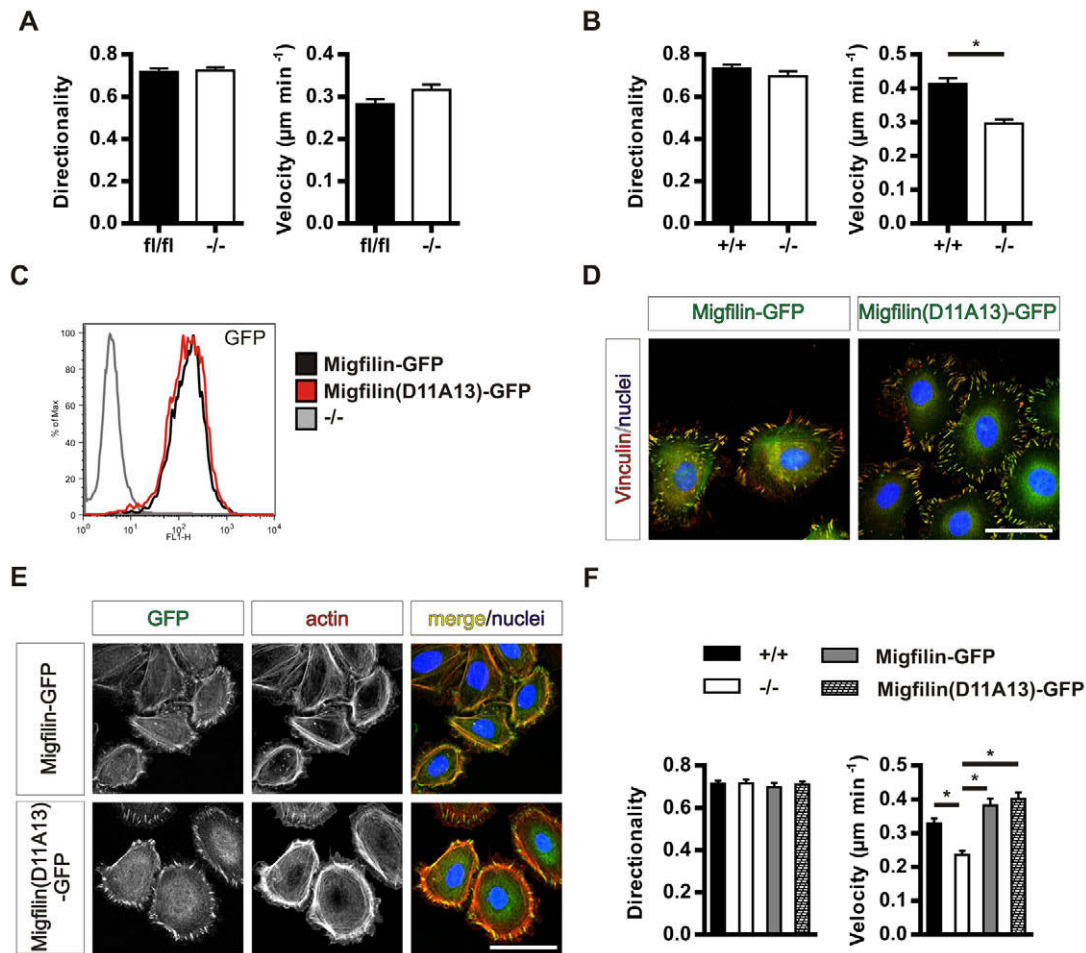


Fig. 5. Migfilin-null keratinocytes have a reduced migration velocity. (A) Monolayers of migfilin (fl/fl) and null (-/-) MEFs were scratch wounded and scratch closure was visualized by time-lapse microscopy. Migration was analyzed by tracking single cells using ImageJ. Data shown are measurements from three experiments and are mean + s.e.m. for 30 tracks. (B) Migfilin wild-type (+/+) and null primary keratinocytes were grown to confluence, wounded and analyzed as in A. Data shown are measurements from three experiments and are means + s.e.m. for 40 keratinocyte tracks. * $P < 0.001$. (C) Representative FACS plot of migfilin-null immortalized keratinocytes expressing migfilin-GFP or migfilin(D11A13)-GFP. (D) Immunofluorescence staining for vinculin (red) and nuclei (blue) of migfilin-null keratinocytes re-expressing migfilin-GFP or migfilin(D11A13)-GFP. The GFP signal is shown in green. Scale bar: 20 μm . (E) Immunofluorescence staining for F-actin (red) and nuclei (blue) of migfilin-null keratinocytes re-expressing migfilin-GFP or migfilin(D11A13)-GFP. The GFP signal is green in the 'merge' image. The single channels for the GFP and actin signal are also shown. Scale bar: 20 μm . (F) Monolayers of immortalized migfilin wild-type and null, and migfilin-null keratinocytes rescued with either migfilin-GFP or migfilin(D11A13)-GFP, were scratch wounded and analyzed as in A. Data shown are measurements from three experiments and are means + s.e.m. for 40 keratinocyte tracks. * $P < 0.001$.

for the migration defect in Ajuba-deficient cells (Pratt et al. 2005). The migration defect was specific to the loss of migfilin as re-expression of migfilin in migfilin-null keratinocytes restored the wild-type migration speed. Interestingly, re-expression of a filamin-binding-deficient migfilin mutant was also able to rescue the migration speed. Clearly, future studies are required to unravel how migfilin affects migration.

Several zyxin family members can translocate to the nucleus, where they influence gene expression (Hervy et al., 2006). Migfilin has also been shown to be present in nuclei and, furthermore, has an NES for exiting the nuclear compartment (Akazawa et al., 2004). These findings, together with the observation that migfilin can interact with the transcription factor Nkx2.5, led to the proposal that migfilin might be required for heart development (Akazawa et al., 2004). However, genetic ablation of migfilin resulted neither in abnormal heart development nor in structural heart defects or heart

failure. As we never observed nuclear accumulation of migfilin in heart or any other tissue, as analyzed by immunofluorescence staining, nuclear translocation of migfilin is either a transient event or it occurs only under specific conditions such as tissue stress.

The zyxin gene family consists of seven members in mammals. Although we could demonstrate that none of these members was upregulated in the absence of migfilin expression, functional redundancy could serve as the explanation for the lack of phenotype. Flies have two zyxin family members and thus less possibility for redundancy. This might explain why depletion of one of the two zyxin family members in flies induces pharate lethality (Das Thakur et al., 2010). Genetic studies on different zyxin family members in mice have so far revealed that single genetic ablations allow normal development and tissue homeostasis; ablations of migfilin (the present study), ajuba (Pratt et al., 2005), limd1 (Feng et al., 2007) and zyxin allow mice to develop normally

(Hoffman et al., 2003), although *Lpp*-null mice show slightly reduced female viability and fertility (Vervenne et al., 2009). The functions of *ajuba* and *limd1* have been further elucidated by challenging the mutant mice in disease models or by drug treatment. These studies have revealed that *ajuba* promotes activation of nuclear factor κ B (NF- κ B) after stimulation with interleukin-1 (Feng and Longmore, 2005) and that *limd1* can act as a tumor suppressor (*limd1*-null mice are more prone to the development of lung cancer) (Sharp et al., 2008). It is therefore possible that zyxin family members have specialized roles in dealing with cellular or physiological stress. The presence of such potential non-compensatable functions must be addressed in the future by subjecting *migfilin*-null mice to different pathological situations.

Materials and Methods

Mouse generation

Migfilin cDNA was obtained from IMAGE clone no. 3257486. A single-nucleotide polymorphism resulting in the mutation I159R was reversed by site-directed mutagenesis (Stratagene). The cDNA was cloned into pBluescript II SK (Stratagene). Final constructs were confirmed by DNA sequencing. Details of the cloning of the targeting construct and mouse generation are available from the corresponding authors on request. In brief, full-length *migfilin* cDNA was used to generate a radiolabeled probe. This was then used to isolate a *SpeI* fragment, including exons 1 to 3 of the gene encoding *migfilin* and the flanking arms of the targeting construct, from a 129/SvRPC1 mouse PAC library 21 clone. A loxP site was inserted 5' of exon 2, and a loxP site together with an *frt*-flanked neomycin selection cassette was inserted 3' of exon 3. The linearized targeting vector was electroporated into R1 mouse ES cells, which were selected with G418. Surviving clones were analyzed for homologous recombination by Southern blotting using an external probe (Fässler and Meyer, 1995). Three clones showing successful homologous recombination were injected into blastocysts, which were then transplanted into foster mice. Chimeras derived from two clones gave germline transmission. Mice were kept at the MPI of Biochemistry animal facilities in accordance with Bavarian animal welfare laws.

Southern and northern blotting

For Southern blotting (SB), 15 μ g of DNA was separated on an agarose gel and transferred onto Hybond N+ membranes (GE Healthcare). For northern blotting (NB), 10 μ g of total RNA extracted with TRIzol (Invitrogen) was separated on a denaturing agarose gel and transferred onto Hybond N+ membranes (GE Healthcare). Full-length *migfilin* cDNA was excised from the pBS-*Migfilin*(SK) vector and radiolabeled with [α - 32 P]CTP using a RediPrime II DNA labeling kit (GE Healthcare). Membranes were hybridized overnight at 65°C in Church buffer [250 mM Na₂HPO₄, 0.34% (v/v) H₃PO₄, pH 7.4, 7.0% (w/v) SDS, 1.0% (w/v) BSA and 0.1 g of sheared salmon sperm/l], and were then washed and exposed to Kodak Biomax MS screens for 1–8 days at –80°C.

RT-PCR

TRIzol-extracted total RNA (2 μ g) was used for first-strand cDNA synthesis, using SuperScript III reverse transcriptase according to the manufacturer's protocol (Invitrogen), with random hexamer primers. Specific cDNA fragments were amplified using the following primers: *migfilin* forward (fwd), 5'-CAGAGAGAGAAGTG-TCCACG-3' and reverse (rev), 5'-GATTCTCGCAGATGCTGCAC-3'; *Fblp* fwd, 5'-GTTGGCTGGACAGAGATTCTA-3' and rev, 5'-CATTCCCGAAGCCCCAGTC-3'; glyceraldehyde-3-phosphate dehydrogenase (*Gapdh*) fwd, 5'-GGTGTGAA-CCACGAGAAATAG-3' and rev, 5'-CAGTGAGCTTCCCGTTTACAG-3'; *migfilin*(s) fwd, 5'-GATGTAGCCGTGAGTGAGG-3' and rev, 5'-CAGGCTTGACAGAAACCAC-3'. *Migfilin*(s) primers produce two amplicons, one specific for *migfilin*(s) with a size of a 207 nt and a second one specific for *migfilin* and *Fblp* with a size of 505 nt. The latter amplicons are suppressed by shortening the amplification cycle during PCR. Primers used to amplify zyxin family transcripts were: *ajuba*-exon1 fwd, 5'-GAGTCTCTGGTCCCTTCG-3' and *ajuba*-exon3 rev, 5'-CTTCTCACAGTAGACAGAGC-3'; *Limd1*-exon1 fwd, 5'-CCTCACCCAGCGTCTGG-3' and *Limd1*-exon4 rev, 5'-GTCCATGATCAGGTGTCCAC-3'; *Lpp*-exon5 fwd, 5'-CCAGTTGTTGCTCCGAAACC-3' and *Lpp*-exon7 rev, 5'-CCAAGATGC-TGGTCAAGGAG-3'; *Trip6*-exon3 fwd, 5'-TGGCAGTCTGGATGCTGAG-3' and *Trip6*-exon4 rev, 5'-GCCACCTTCACTTGATACAGG-3'; *Wtip*-exon2 fwd, 5'-GGCATCTACGGAGCGAGG-3' and *Wtip*-exon5 rev, 5'-GCAGCGGAAGCAG-CCTGG-3'; and zyxin-exon3 fwd, 5'-CCATTCCCCCTGCTCT-3' and zyxin-exon5 rev, 5'-GGCAACTGGTGGGGGTAC-3'.

Antibody generation

A *migfilin*-specific peptide sequence (CVSPRELAVEAMKRQY; residues 192–206) located within LIM domain 1 was coupled to Injunct Maleimide Activated mKLLH

(Pierce Biotechnology) and used to immunize rabbits. The resulting serum was subsequently affinity-purified using a SulfoLink Kit (Pierce Biotechnology). Affinity purified antibodies were eluted using 100 mM glycine buffer, pH 2.7, and dialyzed against PBS.

Western blotting

Cells or tissues from adult C57BL/6 mice were homogenized in RIPA buffer, pH 7.6 [150 mM NaCl, 50 mM Tris-HCl, pH 7.6, 5 mM EDTA, pH 8.0, 0.1% SDS, 1.0% (w/v) sodium deoxycholate, 1.0% (v/v) Triton X-100 and phosphatase inhibitor cocktails P1 and P2; all purchased from Sigma] with Complete protease inhibitors (Roche). A total of 20 to 50 μ g of protein per lane was separated on a polyacrylamide gel and transferred onto a PVDF membrane (Millipore). Membrane blocking and antibody dilution were performed with Tris-buffered saline (TBS), pH 7.6, supplemented with 5% (w/v) skimmed milk powder (Fluka) and 0.1% Tween 20 (Serva). Subsequently, membranes were incubated for 1 hour at room temperature or overnight at 4°C with antibodies against *migfilin* (self-made), actin (Sigma), Src (Invitrogen), Src phosphorylated at Tyr419 (Cell Signaling), zyxin (Abcam) or *Gapdh* (Chemicon). Anti-Trip6 antiserum was provided by Mary Beckerle (University of Utah, Salt Lake City, UT), and anti-*Ajuba* and anti-*Limd1* antisera were provided by Gregory Longmore (Washington University, St Louis, MO). Appropriate HRP-coupled secondary antibodies (BioRad) were applied for 1 hour at room temperature followed by enhanced chemiluminescence (ECL) detection (Western Lightning, PerkinElmer).

Cell culture

Primary keratinocytes were isolated from mice at the telogen phase of the hair cycle. Mice were killed, shaved and skinned. Then the muscle and fatty layer were scraped off, and the skin was incubated for 1 hour in Dulbecco's phosphate-buffered saline (PBS) supplemented with 0.8% trypsin (Gibco) at 37°C. Afterwards the epidermis was peeled off the underlying dermis and manually dissociated. The resulting suspension was filtered through a 45- μ m nylon mesh. Cells were seeded and maintained at 37°C under a 5% CO₂ atmosphere in growth medium [Spinner's MEM supplemented with 5 mg of insulin/l, 10 mg of EGF/l (Roche), 10 mg of transferrin/l, 10 μ M phosphoethanolamine, 10 μ M ethanolamine, 0.36 mg of hydrocortisone/l (Calbiochem), 0.3 g of glutamine/l, 100 units penicillin/ml, 100 mg of streptomycin/l, 45 μ M CaCl₂ and 8% (v/v) chelated fetal calf serum (FCS)]. For differentiation, keratinocytes were cultured in growth medium containing 1 mM CaCl₂. For spontaneous immortalization, keratinocytes were maintained as above, at high confluency, for 2 months. When colonies of immortalized keratinocytes appeared, they were pooled and expanded.

For generation of the *migfilin*(D11A13)-GFP expression construct, *migfilin* cDNA was mutated with the Quickchange kit (Stratagene) using primers 5'-GAGAAA-AGGGTGGCCGACTCTGCTTTCATCACCTTGGCA-3' and 5'-TGCCAGGG-TGATGAAAGCAGAGTCGGCCACCTTTTCTC-3'. Successful mutagenesis was confirmed by sequencing. Both wild-type and mutant *migfilin* cDNA were cloned into pEGFP-N1 (Clontech) and subsequently into pCLMFG-MCS for generating the viral supernatants used to infect the immortalized *migfilin*-null keratinocytes. Cells expressing *migfilin*-GFP or *migfilin*(D11A13)-GFP were sorted using a FACS method for equal GFP levels.

Mouse embryonic fibroblasts (MEFs) were isolated from E13.5 embryos by standard methods. Immortalization was achieved by retroviral transduction of SV40 large T antigen and immortalized MEFs were subsequently cloned. *Migfilin*-null MEFs were derived from *migfilin* fl/fl MEFs by adenoviral Cre transduction followed by cloning. MEFs were maintained at 37°C under a 5% CO₂ atmosphere in Dulbecco's modified Eagle's medium (DMEM) with 4 mM glutamax, 100 units/ml penicillin and 100 mg of streptomycin/l and supplemented with 10% v/v FCS.

In some experiments, culture dishes were coated with ECM molecules as indicated. The ECM molecules used were collagen I, collagen IV, fibronectin or laminin-322 (kindly provided by Monique Aumailley, University of Cologne, Cologne, Germany). Unless noted otherwise, all cell culture reagents were purchased from Invitrogen or Sigma.

Adhesion assays

Adhesion assays were conducted in 96-well plates. Quadruplet wells were coated with the substrate overnight at 4°C. Nonspecific adhesion was assayed in wells coated with 1% BSA in PBS. Before the assay, the coating substrate was washed out and the wells were blocked with 1% BSA in PBS. A total of 40,000 cells per well were added in Spinner's MEM supplemented with 40 μ M CaCl₂ and 2 mM glutamine. After 30 minutes at 37°C under a 5% CO₂ atmosphere, the wells were washed three times with PBS and substrate solution (3.8 mM 4-nitrophenyl *N*-acetyl- β -D-glucosaminide, 0.25% Triton X-100 and 50 mM sodium citrate, pH 5.0) was added. After an overnight incubation at 37°C, 1.5 volumes of stop solution (50 mM glycine and 5 mM EDTA, pH 10.4) was added and absorption was measured at 405 nm.

Spreading and scratch wound healing assays

Cell spreading and migration were assayed with a live-cell imaging setup consisting of a microscope (Axiovert; Carl Zeiss MicroImaging) equipped with a \times 10 0.3NA objective, motorized scanning table (Märzhäuser) and a stage incubator (EMBL Precision Engineering) at 37°C and under 5% CO₂ atmosphere. Images were captured

with a cooled charge-coupled-device camera (MicroMAX; Roper Scientific) using the MetaMorph software (Universal Imaging) for microscope control and data acquisition.

For spreading analysis, cells were added to pre-equilibrated culture dishes and image acquisition was started immediately. Images were collected every 5 minutes. Cell area over time was measured using ImageJ software (National Institutes of Health). The data shown were generated by randomly choosing ten cells per genotype from a representative experiment, which was repeated three times.

For migration analysis, cells were treated with 4 mg of mitomycin C/I (Sigma), to abolish proliferation, and were seeded and allowed to achieve confluency overnight. The resulting monolayer was scratched using a 1-ml plastic pipette tip. Image acquisition was started after 1 hour and images were collected every 10 minutes for up to 30 hours. Cells at the wound edge were chosen randomly and tracked with the manual tracking plug-in from ImageJ. The resulting tracks were analyzed for directionality and velocity using the 'cell migration and chemotaxis' tool (Ibidi). The data shown were generated from experiments that were repeated three times.

siRNA-mediated knockdown

Migfilin fl/fl and the derived migfilin-null MEFs were plated to ~60–70% confluency and cultured as described above. After 24 hours, MEFs were transfected with scrambled control siRNA (siScr, 5'-GAUGAAACGCGUACAGAU-3') or with siRNA targeting migfilin (siMig, 5'-GAAGGAAUUCACGGAA-3', Sigma) using Lipofectamine 2000 in Opti-MEM 1 (both by Invitrogen) according to the manufacturer's protocol. After 6 hours, the medium was changed to normal growth medium and MEFs were cultured for an additional 48 hours before further assays were conducted.

Flow cytometry

Freshly isolated primary keratinocytes were stained directly with primary antibodies for 10 minutes on ice, and after washing were then stained with secondary antibody for 10 minutes on ice. After washing, cells were resuspended in PBS containing BSA and propidium iodide. Immortalized keratinocytes were trypsinized and treated as described above. Flow cytometry was conducted on a FACSCalibur or FACSAria flow cytometer (BD). Antibodies were purchased from BD (clone 9EG7, which detects active integrin β 1, and against integrins β 1, α 2, α 5, α 6 or α V) or Serotec (against integrin β 4).

Immunofluorescence

Cryosections from frozen adult and embryonic tissues were prepared and embedded according to standard protocols. All tissues sections, except heart, were fixed for 10 minutes in 3.7% paraformaldehyde (PFA) in PBS, then permeabilized for 3 minutes with 0.1% Triton X-100 in PBS and blocked for 1 hour in 5% BSA in PBS. Heart sections were fixed for 10 minutes in acetone at -20°C and blocked as described above. Cells were grown on glass coverslips coated with fibronectin (5 mg/l, Calbiochem) and then fixed with PFA and blocked as described above. Antibodies were used against vinculin (Sigma), migfilin (self-made), endomucin (Santa Cruz Biotechnology), integrin α 6, Mac1, Pecam1 (all by BD Pharmingen) and VASP (Cell Signaling). Appropriate fluorophore-labeled secondary antibodies were used to detect primary antibodies. Alexa-Fluoro-546-labelled phalloidin (Invitrogen) was used to visualize F-actin. Slides were mounted in Elvanol. Pictures were taken with a TCS SP2 AOBs confocal laser-scanning microscope (Leica).

Statistics

All data are given as a mean value with the standard error of the mean (s.e.m.) or standard deviation (s.d.) as indicated. Statistical significance was tested with a non-paired two-tailed Student's *t*-test.

We thank Monique Aumailley for providing laminin-332, Mary Beckerle for Trip6 antiserum and Greg Longmore for antisera against Ajuba and Limd1. We are grateful to Markus Moser and Siegfried Ussar for help with design of the migfilin floxed allele. This work was supported by the Max-Planck Society.

Supplementary material available online at <http://jcs.biologists.org/cgi/content/full/124/3/414/DC1>

References

- Akazawa, H., Kudoh, S., Mochizuki, N., Takekoshi, N., Takano, H., Nagai, T. and Komuro, I. (2004). A novel LIM protein Cal promotes cardiac differentiation by association with CSX/NKX2-5. *J. Cell Biol.* **164**, 395–405.
- Das Thakur, M., Feng, Y., Jagannathan, R., Seppa, M. J., Skeath, J. B. and Longmore, G. D. (2010). Ajuba LIM proteins are negative regulators of the hippo signaling pathway. *Curr. Biol.* **20**, 657–662.
- Fässler, R. and Meyer, M. (1995). Consequences of lack of beta 1 integrin gene expression in mice. *Genes Dev.* **9**, 1896–1908.
- Feng, Y. and Longmore, G. D. (2005). The LIM protein Ajuba influences interleukin-1-induced NF-kappaB activation by affecting the assembly and activity of the protein kinase C ζ /TRAF6 signaling complex. *Mol. Cell Biol.* **25**, 4010–4022.
- Feng, Y., Zhao, H., Luderer, H. F., Epple, H., Faccio, R., Ross, F. P., Teitelbaum, S. L. and Longmore, G. D. (2007). The LIM protein, Limd1, regulates AP-1 activation through an interaction with Traf6 to influence osteoclast development. *J. Biol. Chem.* **282**, 39–48.
- Gkretsi, V., Zhang, Y., Tu, Y., Chen, K., Stolz, D. B., Yang, Y., Watkins, S. C. and Wu, C. (2005). Physical and functional association of migfilin with cell-cell adhesions. *J. Cell Sci.* **118**, 697–710.
- Harms, B. D., Bassi, G. M., Horwitz, A. R. and Lauffenburger, D. A. (2005). Directional persistence of EGF-induced cell migration is associated with stabilization of lamellipodial protrusions. *Biophys. J.* **88**, 1479–1488.
- Hervy, M., Hoffman, L. and Beckerle, M. C. (2006). From the membrane to the nucleus and back again: bifunctional focal adhesion proteins. *Curr. Opin. Cell Biol.* **18**, 524–532.
- Hoffman, L. M., Nix, D. A., Benson, B., Boot-Hanford, R., Gustafsson, E., Jamora, C., Menzies, A. S., Goh, K. L., Jensen, C. C., Gertler, F. B. et al. (2003). Targeted disruption of the murine zyxin gene. *Mol. Cell Biol.* **23**, 70–79.
- Hynes, R. O. (2002). Integrins: bidirectional, allosteric signaling machines. *Cell* **110**, 673–687.
- Ithychanda, S. S., Das, M., Ma, Y. Q., Ding, K., Wang, X., Gupta, S., Wu, C., Plow, E. F. and Qin, J. (2009). Migfilin, a molecular switch in regulation of integrin activation. *J. Biol. Chem.* **284**, 4713–4722.
- Kiema, T., Lad, Y., Jiang, P., Oxley, C. L., Baldassarre, M., Wegener, K. L., Campbell, I. D., Ylanne, J. and Calderwood, D. A. (2006). The molecular basis of filamin binding to integrins and competition with talin. *Mol. Cell* **21**, 337–347.
- Lad, Y., Jiang, P., Ruskamo, S., Harburger, D. S., Ylanne, J., Campbell, I. D. and Calderwood, D. A. (2008). Structural basis of the migfilin-filamin interaction and competition with integrin β tails. *J. Biol. Chem.* **283**, 35154–35163.
- Legate, K. R. and Fässler, R. (2009). Mechanisms that regulate adaptor binding to beta-integrin cytoplasmic tails. *J. Cell Sci.* **122**, 187–198.
- Montanez, E., Ussar, S., Schifferer, M., Bosl, M., Zent, R., Moser, M. and Fassler, R. (2008). Kindlin-2 controls bidirectional signaling of integrins. *Genes Dev.* **22**, 1325–1330.
- Moser, M., Legate, K. R., Zent, R. and Fassler, R. (2009). The tail of integrins, talin, and kindlins. *Science* **324**, 895–899.
- Pratt, S. J., Epple, H., Ward, M., Feng, Y., Braga, V. M. and Longmore, G. D. (2005). The LIM protein Ajuba influences p130Cas localization and Rac1 activity during cell migration. *J. Cell Biol.* **168**, 813–824.
- Sharp, T. V., Al-Attar, A., Foxler, D. E., Ding, L., de A Vallim, T. Q., Zhang, Y., Nijmeh, H. S., Webb, T. M., Nicholson, A. G., Zhang, Q. et al. (2008). The chromosome 3p21.3-encoded gene, LIMD1, is a critical tumor suppressor involved in human lung cancer development. *Proc. Natl. Acad. Sci. USA* **105**, 19932–19937.
- Takafuta, T., Sacki, M., Fujimoto, T. T., Fujimura, K. and Shapiro, S. S. (2003). A new member of the LIM protein family binds to filamin B and localizes at stress fibers. *J. Biol. Chem.* **278**, 12175–12181.
- Tu, Y., Wu, S., Shi, X., Chen, K. and Wu, C. (2003). Migfilin and Mig-2 link focal adhesions to filamin and the actin cytoskeleton and function in cell shape modulation. *Cell* **113**, 37–47.
- Vervenne, H. B., Crombez, K. R., Delvaux, E. L., Janssens, V., Van de Ven, W. J. and Petit, M. M. (2009). Targeted disruption of the mouse Lipoma Preferred Partner gene. *Biochem. Biophys. Res. Commun.* **379**, 368–373.
- Zhang, Y., Tu, Y., Gkretsi, V. and Wu, C. (2006). Migfilin interacts with vasodilator-stimulated phosphoprotein (VASP) and regulates VASP localization to cell-matrix adhesions and migration. *J. Biol. Chem.* **281**, 12397–12407.
- Zhao, J., Zhang, Y., Ithychanda, S. S., Tu, Y., Chen, K., Qin, J. and Wu, C. (2009). Migfilin interacts with Src and contributes to cell-matrix adhesion-mediated survival signaling. *J. Biol. Chem.* **284**, 34308–34320.

Supplementary Figure Legends – Moik et al. 2011a

Figure S1. Migfilin gene ablation.

(A) Targeting strategy to generate migfilin floxed (fl) and null (-) alleles. Depicted is a part of the wt migfilin gene locus containing exons 1-4 (numbered white boxes). SpeI and EcoRI restriction sites are designated with S and E, respectively. The targeting vector contains exons 1-3. The Start codon is located in exon 2. Exons 2-3 are flanked by loxP1 sites (white triangles) and a neo cassette (grey box) in intron 3 is flanked by frt sites (black ovals). The external 5' and 3' probes used in Southern blot (SB) are indicated with red and green bars, respectively. The sizes of EcoRI fragments detected in wt and recombinant locus are indicated below the respective loci. The migfilin floxed allele is obtained after Flp-mediated excision of the neo cassette. The migfilin null allele is obtained after Cre-mediated excision of exons 2-3.

(B) Southern blot of migfilin +/+ and +/- genomic DNA using the external 3' and 5' Probes. (C) Western blot of migfilin in heart isolated from migfilin +/+, +/- and fl/fl littermates. (D) Quantitative RT-PCR from heart and lung with primers spanning migfilin exons 5-8. Transcript levels of migfilin were normalized against Gapdh levels. Error bars indicate mean \pm s.d. (E) Quantitative RT-PCR analysis of the zyxin family members using total RNA isolated from heart. Transcript levels of migfilin were normalized against Gapdh levels. Error bars indicate mean \pm s.d. (F) Expression levels of indicated proteins in migfilin+/+, +/-, and -/- heart. Gapdh served as loading control.

Figure S2. Migfilin expression in hematopoietic cells and migfilin gene structure.

(A) Western blot of migfilin in hematopoietic cell types. Keratinocyte lysates served as positive control and Gapdh served as loading control. (B) Exon structure of the murine *migfilin* gene. (C) Exon composition of the murine migfilin and Fblp-1 and indications of the primers used to amplify specific transcripts in Fig. S1D, Fig. 2C,D.

Figure S3. Expression of migfilin in heart and lung.

(A) Single color channels of migfilin +/+ and -/- heart IF stainings shown in Fig. 3A. Size bars represent 50 μ m. (B-C) Staining of wild-type lung tissues with indicated antibodies. Size bar represents 50 μ m. (D) Western blot of lung lysate from three migfilin +/+ and three -/- littermates using antibodies against src pY416 (pY419 in human, indicated with asterisk), total src and migfilin.

Figure S4. Integrin expression profiles on primary keratinocytes.

(A) Normalized MFI values of the FACS experiment shown in Fig. 4G. Results for +/- and -/- keratinocytes were normalized to +/+ MFI values for each experiment. Cells of three animals per genotype were used except for Itga6 where n=5. Error bars indicate mean \pm s.d. (B) Representative 9EG7 FACS plot used to generate Fig. 4H.

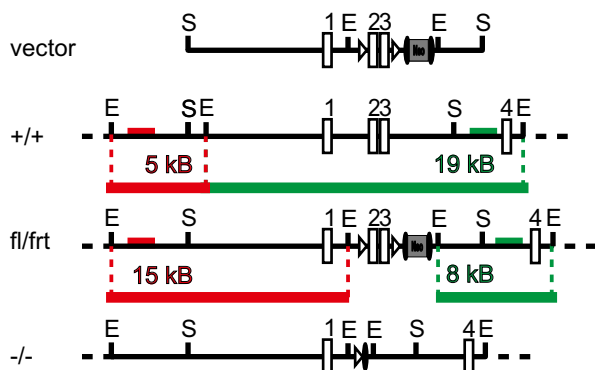
Figure S5. siRNA-mediated depletion of migfilin neither affects spreading nor adhesion of immortalized MEFs.

(A) Western blot of migfilin in immortalized fl/fl and Adeno-Cre derived -/- MEFs transfected either with scrambled (siScr) or migfilin-specific siRNAs (siMig). (B) IF

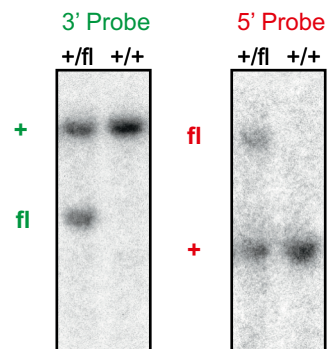
stainings for migfilin (green), vinculin (red) and nuclei (blue) of immortalized migfilin fl/fl and Adeno-Cre derived -/- MEFs transfected with either scrambled (siScr) or migfilin-specific siRNAs (siMig). Size bar represents 50 μ m. **(C)** Cell adhesion assay with migfilin fl/fl and -/- MEFs on Coll/FN. Error bars indicate mean \pm s.e.m. of 3 replicates. **(D)** Spreading assay of migfilin fl/fl and -/- MEFs on Coll/FN. 10 cells per genotype were analyzed. Error bars indicate the mean \pm s.e.m. **(E)** Tracks of migrating migfilin fl/fl and -/- MEFs analyzed in Fig. 5A. **(F)** Tracks of migrating migfilin +/+ and -/- keratinocytes analyzed in Fig. 5B.

Fig. S1 - Moik et al. 2011a

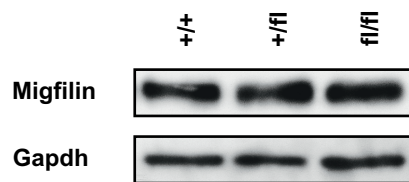
A



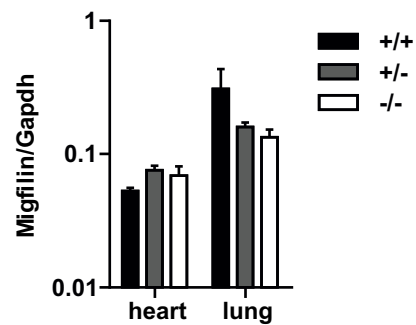
B



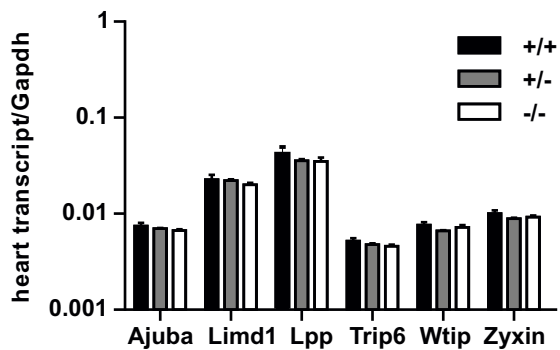
C



D



E



F

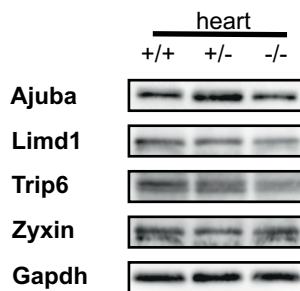
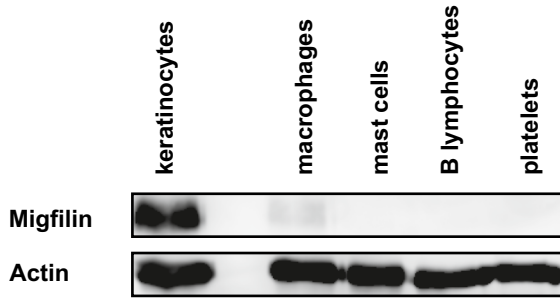
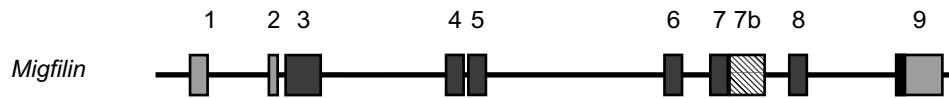


Fig. S2 - Moik et al. 2011a

A



B



C

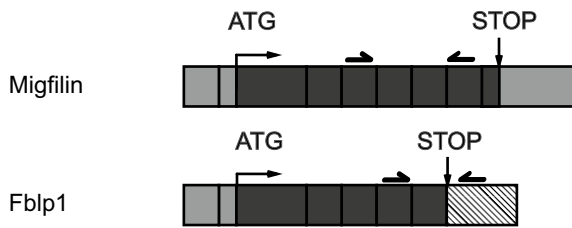


Fig. S3 - Moik et al. 2011a

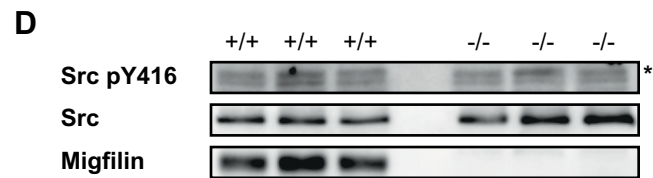
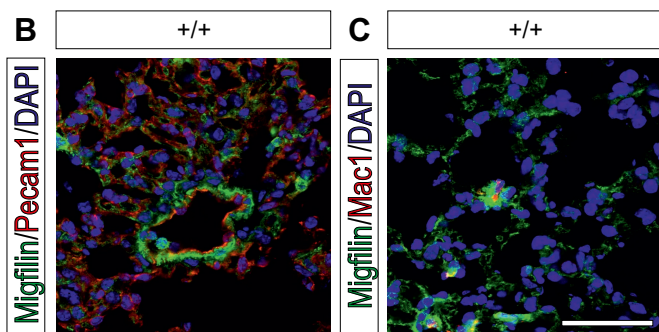
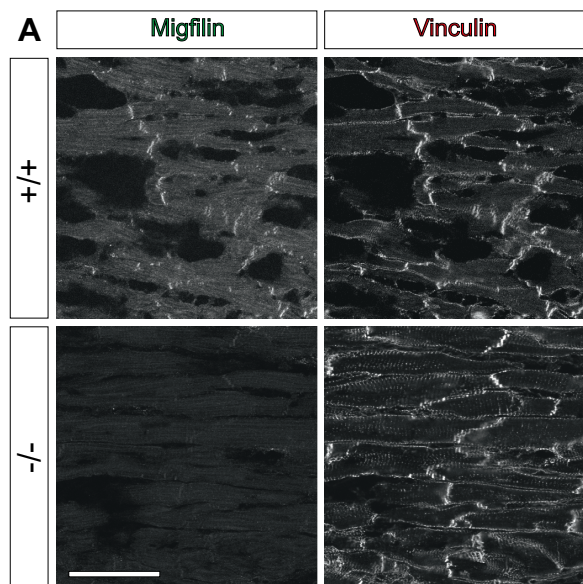
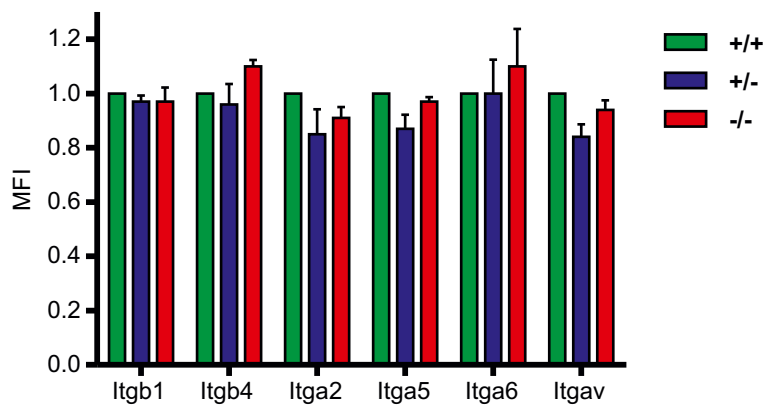


Fig. S4 - Moik et al. 2011a

A



B

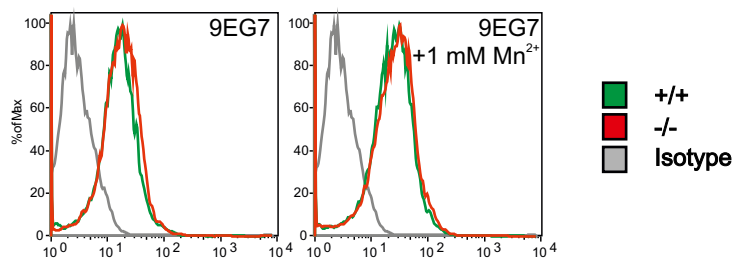
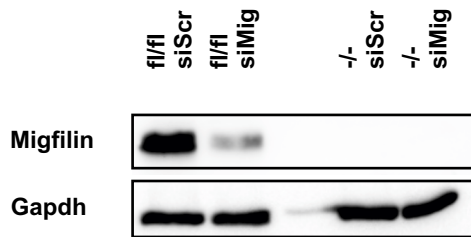
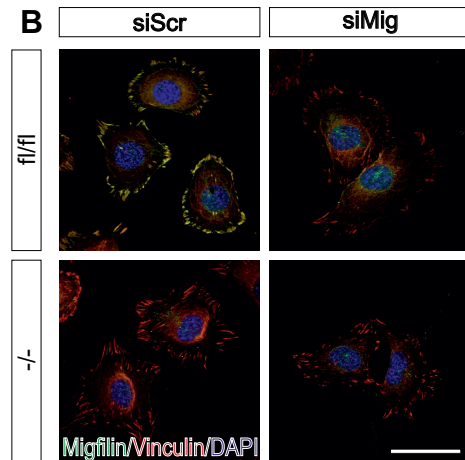


Fig. S5 - Moik et al. 2011a

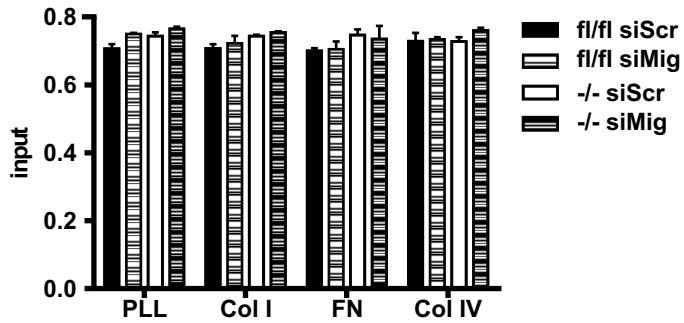
A



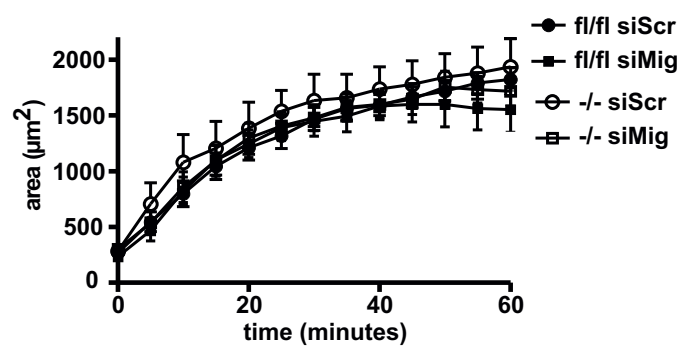
B



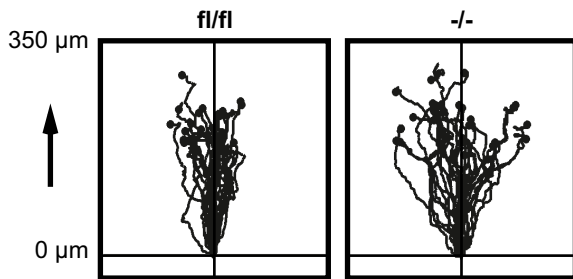
C



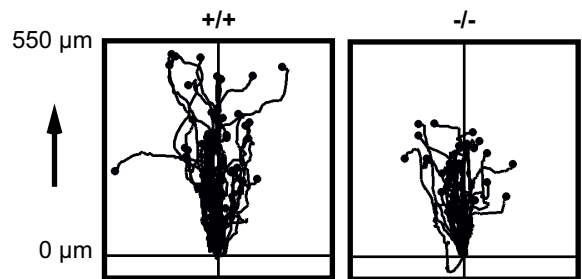
D



E



F



Moik et al, 2011b

Migfilin suppresses tetraploidy and tumorigenesis in stressed skin

Daniel V. Moik, Vaibhao C. Janbandhu, Christian Kuffer, Zuzana Storchova, and Reinhard Fässler*

Max-Planck-Institute of Biochemistry, 82152 Martinsried, Germany.

Running title: Migfilin suppresses tetraploidy and skin cancer

Keywords: Migfilin, Fblim1, p53, mouse, skin, epidermis, Cre recombinase, tetraploidy, DMBA/TPA, cancer, non-melanoma skin cancer, tumor suppressor

*Corresponding author: faessler@biochem.mpg.de

SUMMARY

Mice lacking the zyxin-family LIM protein migfilin (encoded by *Fblim1*) have no obvious developmental or physiological defects. Here we report that the expression of Cre recombinase in *Migfilin*^{-/-} epidermis triggered a lethal hyperinflammatory skin phenotype characterized by increased occurrence of tetraploid cells and apoptosis. The tumor and tetraploidy suppressor p53 was activated in Cre-expressing *Migfilin*^{-/-} epidermis, but was unable to suppress tetraploidy and morbidity. Furthermore, deletion of p53 and migfilin further increased epidermal apoptosis and morbidity, indicating that both proteins contribute to suppression of tetraploidy. Tetraploidy is an early event in skin carcinogenesis, and loss of migfilin made mice more susceptible to chemically induced skin cancer. Our findings indicate that migfilin diminishes carcinogenesis by suppressing tetraploidy.

INTRODUCTION

The zyxin gene family consists of seven members in mammals. They function as adaptor proteins and are composed of a variable N-terminus, a proline-rich domain with a nuclear export signal (NES), and three C-terminal Lin-11/Is1-1/Mec-3 (LIM) domains. LIM domains are protein-binding tandem zinc fingers that target the zyxin family proteins to cell-matrix (focal adhesions, FAs) and cell-cell adhesions (adherens junctions, AJ) and to the nucleus (Kadmas and Beckerle, 2004; Zheng and Zhao, 2007). Although their function at cell adhesion sites is not fully clear (Kadmas and Beckerle, 2004; Zheng and Zhao, 2007) recent proteomics studies suggested that they control mechano-transduction (Schiller et al., 2011). Nuclear accumulation of zyxin family proteins is prevented by the NES, but can be transiently induced by specific stimuli such as UV irradiation (Hervy et al., 2006), resulting in the transcription of specific genes (Hervy et al., 2010; Zheng and Zhao, 2007).

The most recently discovered member of the zyxin family is migfilin/Fblim1 (filamin-binding LIM protein 1). Migfilin interacts with kindlin-2 and filamin A to C at focal adhesions and actin stress fibers (Takafuta et al., 2003; Tu et al., 2003), and with the transcription factor Nkx2.5 in the nucleus (Akazawa et al., 2004). Overexpression as well as siRNA-mediated depletion associate migfilin with integrin activation (Lad et al., 2008), cell adhesion (Gkretsi et al., 2005; Tu et al., 2003), migration (Zhang et al., 2006), transcriptional activation (Akazawa et al., 2004), and cell survival (Zhao et al., 2009). Gene ablation studies have shown that Migfilin^{-/-} mice develop and age normally (Moik et al., 2011) suggesting that the loss of migfilin is compensated by other members of the zyxin family.

Four other members of the zyxin gene family have also been ablated in mouse: *ajuba* (Pratt et al., 2005), *limd1* (Feng et al., 2007), *lpp* (Vervenne et al., 2009) and

zyxin (Hoffman et al., 2003). Similar to migfilin, their pre- and postnatal development proceeded normally despite ample *in vitro* data pointing to important roles e.g. in cell adhesion, actin dynamics, and cell migration (Hoffman et al., 2006; Pratt et al., 2005; Yi et al., 2002). Interestingly, specific stressors revealed an important role of *ajuba* in inflammation (Feng and Longmore, 2005) and of *limd1* in tumour suppression (Sharp et al., 2008), pointing to the possibility that migfilin may also exert essential functions during certain stress situations.

The protected breeding of laboratory mice ensures that they do not encounter certain stressors such as microbial infections or DNA damage induced by UV light or ionizing irradiation. Another form of genotoxic stress is caused by the viral Cre recombinase, which is routinely used to specifically excise genomic sequences that are flanked by *loxP* sites ("flox", fl) (Schmidt-Supprian and Rajewsky, 2007). It has been shown that Cre can also bind to *loxP*-like sequences present in the mammalian genome (Semprini et al., 2007; Thyagarajan et al., 2000). Such an unspecific Cre activity can result in inhibition of cell proliferation, increased cell size, increased DNA content/ploidy, chromosomal instability (CIN) *in vitro* (Loonstra et al., 2001; Pfeifer et al., 2001; Schmidt et al., 2000; Silver and Livingston, 2001) and apoptosis *in vivo* (Naiche and Papaioannou, 2007; Pfeifer et al., 2001). Although the underlying cause for these defects is unclear, it has been speculated that Cre recombinase induces DNA damage, which in turn triggers mitotic checkpoint activation and finally apoptosis (Loonstra et al., 2001). Tetraploidy and CIN caused by unspecific Cre activity could contribute to cancer development (Ganem et al., 2007), as the majority of human cancers have been shown to employ CIN to acquire the mutations necessary for promotion and progression (Hanahan and Weinberg, 2000; Hanahan and Weinberg, 2011; Lengauer et al., 1998).

The mammalian tissue that is most exposed to environmental stressors is the epidermis, as it constitutes the barrier preventing any harm from the outside as well as loss of water from the inside (Proksch et al., 2008). To maintain this protective role, it is constantly renewed by programmed differentiation of basal keratinocytes (Mack et al., 2005), which are replenished from a pool of epidermal stem cells (Kaur, 2006). Breaches in the epidermal barrier (Segre, 2006) or stressors like increased cell death (Omori et al., 2006) trigger an inflammatory hyperproliferative wound healing response in skin.

When we generated a constitutive deletion of the migfilin gene (Moik et al., 2011), we also bred Migfilin^{fl/fl} mice with a transgenic line expressing Cre recombinase under control of the Keratin 5(K5) promoter (K5Cre) to specifically delete the migfilin gene in keratinocytes (K5Cre; Brakebusch et al., 2000; Ramirez et al., 2004). We initially assumed that Migfilin^{-/-} mice develop defects, which, however, turned out not to be the case (Moik et al., 2011). To our surprise we found that K5Cre-mediated deletion of migfilin resulted in a lethal reactive hyperplastic skin phenotype characterized by tetraploidy and apoptosis of keratinocytes. Furthermore, migfilin-null mice were more sensitive to chemically induced skin carcinogenesis. Our findings assign a novel role to migfilin in suppressing tetraploidy and cancer.

RESULTS

Loss of migfilin affects neither skin nor hair follicles

We previously reported that Migfilin^{-/-} mice develop no overt phenotype during development or adult life (Moik et al., 2011). When examining Migfilin^{-/-} skin, we found that the interfollicular epidermis and HF number and morphogenesis were indistinguishable from littermate controls (Figure 1A). We confirmed expression of migfilin in skin lysates (Moik et al., 2011), but did not detect migfilin in other stratified epithelia including cervix, esophagus, tongue, nor in composite (simple and stratified) epithelia like mammary and salivary glands (Figure 1B). While our migfilin anti-serum did not work in staining tissue sections, it readily detected migfilin in primary keratinocytes at focal adhesions (FAs) and at cell-cell contacts after Ca²⁺ treatment (Figure 1C). We observed no nuclear migfilin staining in undifferentiated or differentiated keratinocytes (Figure 1C).

Cre-mediated deletion of the migfilin gene in keratinocytes leads to postnatal lethality

In parallel to the study of Migfilin^{-/-} mice, we crossed migfilin floxed mice (Migfilin^{fl/fl}) with K5Cre transgenic mice to induce a keratinocyte-specific deletion of migfilin (Brakebusch et al., 2000). The resulting Migfilin^{fl/fl;K5Cre+} offspring were slightly smaller than their littermate controls (Migfilin^{fl/fl}, Migfilin^{+fl}) at birth, failed to thrive, became cachectic and lethargic (Figure 1D,E) and usually died within 7-10 days after birth. The skin of Migfilin^{fl/fl;K5Cre+} mice became increasingly scaly and hairless (Figure 1D). Furthermore, Migfilin^{fl/fl;K5Cre+} mice developed epidermal hyperpigmentation at ears, paws and tail, which gradually expanded to the whole skin. Heterozygous floxed mice expressing K5Cre (Migfilin^{+fl;K5Cre+}) had a decreased pelagic hair density

and displayed a weak epidermal hyperpigmentation, but gained weight normally (Figure 1D,E). The severe skin defects and lethality were faithfully reproduced in Migfilin^{fl/fl;K5Cre+} mice derived from a second embryonic stem cell clone.

Migfilin^{fl/fl;K5Cre+} mice develop epidermal hyperplasia and skin inflammation

Hematoxylin-eosin (H/E) stainings of back skin from 8 day old (P8) Migfilin^{fl/fl;K5Cre+} mice showed inflammatory infiltrations in the dermis and a hyperthickening of the epidermis, but neither blisters nor epidermolysis (Figure 1F). In P8 control mice the HFs have reached the subcutis, while in Migfilin^{fl/fl;K5Cre+} mice the majority of HFs were misaligned and malformed (Figure 1F).

Inflammatory infiltrations were further characterized by immunofluorescence (IF); whereas activated Mac-1-positive macrophages were rare in control skin, they were abundant in P8 Migfilin^{fl/fl;K5Cre+} dermis and occasionally also seen in the epidermis (Figure 1G,H). T-cells and neutrophils were largely unchanged when compared to controls (data not shown). Inflammatory stress was also indicated by the expression of keratin 6 (K6) in P8 Migfilin^{fl/fl;K5Cre+} epidermis, whereas K6 expression was absent in control skin and weak in HFs (Figure 1I,J). Masson-Fontana staining revealed an increased number of melanocytes in the epidermis of Migfilin^{fl/fl;K5Cre+}, which are absent in wild-type epidermis at this stage of development (Figure 1K and Okura et al., 1995). The increased melanocyte numbers caused the hyperpigmentation of Migfilin^{-/-;K5Cre+} mice (Figure 1D).

Migfilin and Cre gene dosages influence phenotype severity

Since Migfilin^{-/-} mice were normal, we suspected a synthetic lethality upon disruption of the migfilin gene together with expression of the Cre transgene. To test

this, we intercrossed Migfilin^{-/-} mice with the K5Cre transgenic strain to generate Migfilin^{-/-};K5Cre⁺ offspring. Migfilin^{-/-};K5Cre⁺ mice were born at sub-Mendelian ratios (Table 1) and fully phenocopied the skin defects of Migfilin^{fl/fl};K5Cre⁺ mice and also died around 7-10 days after birth.

The insertion of the K5Cre transgene could have disrupted a genomic locus that together with migfilin loss causes the defects. To examine such a possibility, we intercrossed Migfilin^{-/-} mice with a transgenic mouse line expressing the Cre recombinase under the control of the keratin 14 (K14) promoter (K14Cre ;Hafner et al., 2004). All Migfilin^{-/-};K14Cre⁺ mice analyzed (n=71) died before or shortly after birth. Since the K14Cre and K5Cre transgenes have inserted into different loci, we exclude an insertional mutation by the transgene as cause for the defects of Migfilin^{-/-} mice expressing Cre in the epidermis.

Since Cre protein levels were higher in K14Cre than in K5Cre mice (Figure 2A), we suspected that a Cre gene dosage effect might underlie the early death of Migfilin^{-/-};K14Cre⁺ mice. To test whether Cre dosage can indeed modulate the severity of the phenotype, we generated heterozygous mice (Migfilin^{+/-}) with none, either one (K5Cre or K14Cre) or both (K5Cre;K14Cre) Cre transgenes. As expected, Cre protein levels were higher in K14Cre than in K5Cre skin, and even higher in mice expressing both transgenes (Figure 2A). Migfilin^{+/-};K5Cre⁺ and Migfilin^{+/-};K14Cre⁺ offspring developed a similar mild skin hyperpigmentation and sparse fur (Figure 2B). Migfilin^{+/-};K5Cre⁺;K14Cre⁺ carrying both Cre transgenes died around 10 days after birth and displayed a similar phenotype as Migfilin^{-/-};K5Cre⁺ mice (Figure 2B). Similar to Migfilin^{-/-};K5Cre⁺ epidermis, their epidermis was hyperthickened and contained numerous epidermal melanocytes (Figure 2C).

Altogether the data show that germ-line deletion of migfilin or expression of keratin-driven Cre alone produced normal mice, while the combination of migfilin loss and epidermal expression of Cre resulted in synthetic lethality. Furthermore, migfilin and Cre gene dosages correlate with phenotype severity.

Migfilin^{fl/fl;K5Cre+} epidermis does not display adhesion or terminal differentiation defects

Loss of migfilin affected cell-matrix adhesion neither *in vivo* nor *in vitro* (Moik et al., 2011). To test whether Cre expression in Migfilin^{-/-} epidermis altered integrin expression or localization, we stained skin sections with specific antibodies and determined integrin levels on primary keratinocytes by flow cytometry. Immunostaining revealed that basal keratinocytes of control and Migfilin^{fl/fl;K5Cre+} epidermis had a similar distribution of integrins, with β 1 integrin around the entire plasma membrane (Figure 3A,B), and α 6 and β 4 integrins at the basal side (Figure 3E-J,M-P and data not shown). Flow cytometry showed that β 1 and α 6 integrin levels and the activation of β 1 integrin were also normal at P3 (Figure 3Q). In line with the normal integrin expression, the assembly of Laminin-511 and Laminin-322 into a dermal-epidermal basement membrane was unaffected in Migfilin^{fl/fl;K5Cre+} skin (LM-322, Figure 3A-D,K,L).

The immunostaining also demonstrated that in Migfilin^{fl/fl;K5Cre+} epidermis β 1 and α 6 integrins were present on suprabasal keratinocytes. Concordant with the ectopic expression of integrin subunits, we also found K5 in suprabasal layers of Migfilin^{-/-;K5Cre+} epidermis, while in controls it was only found in basal cells (Figure 3E,F). Keratin 10 (K10) expression is turned on when basal cells move to the suprabasal layer in both Migfilin^{fl/fl;K5Cre+} and control epidermis, but it appeared less

intense and patchy in Migfilin^{fl/fl;K5Cre+} epidermis (Figure 3G,H). Loricrin, which is upregulated during terminal keratinocytes differentiation, was similarly expressed in control and Migfilin^{fl/fl;K5Cre+} epidermis (Figure 3I,J).

Migfilin is also present at cell-cell adhesions (Gkretsi et al., 2005). Adhesion molecules such as E-cadherin (Cadh1, Figure 3K,L), desmoplakin (Dsp, Figure 3M,N), and kindlin-2 (Kind2, Figure 3O,P) were similarly distributed in control and Migfilin^{fl/fl;K5Cre+} epidermis. To exclude potential dysfunction of the cell-cell adhesion sites in Migfilin^{fl/fl;K5Cre+} epidermis, we compared their skin barrier function with controls. Trans-epidermal water loss (TEWL) measurements of P3 skin were similar regardless of genotype (Figure 3R). Furthermore, outside-in dye exclusion assays confirmed a normal skin barrier function in Migfilin^{fl/fl;K5Cre+} skin (Figure 3S), indicating that such defects could be excluded as cause for the lethality.

Migfilin-null^{K5Cre+} epidermis contains enlarged and multi-/binucleated keratinocytes

H/E and immune staining of skin sections revealed that the cells and their nuclei were markedly enlarged in Migfilin^{-/-;K5Cre+} epidermis at embryonic day (E) 18.5, P3, and P6 (Figure 4A). Furthermore, we found a large number of bi- and multinucleated cells in P3 Migfilin^{-/-;K5Cre+} epidermis (176 ± 16 per mm^2 epidermis, mean \pm SEM) (Figure 4A arrowheads), while binucleated cells were very rare in P3 Migfilin^{-/-} or Migfilin^{+/+} epidermis (both 4 ± 5 per mm^2 epidermis) and more frequent in Migfilin^{+/+;K5Cre+} (40 ± 3 per mm^2 epidermis).

The epidermal thickness and the number of cell layers were similar at E18.5 and P3 for Migfilin^{-/-;K5Cre+} and control mice (Migfilin^{+/+}, Migfilin^{-/-}, Migfilin^{+/+;K5Cre+}, Figure 4B,C), but increased in Migfilin^{-/-;K5Cre+} mice when hyperthickening became apparent

by P6 (Figure 4B,C). The number of basal keratinocytes per mm epidermis was slightly reduced in Migfilin^{-/-;K5Cre+} epidermis at E18.5 and stagnated (Figure 4D), whereas in control mice their numbers increased as part of normal post-natal development (Figure 4D). These data indicate that the reduced cell number at E18.5 and P3 is associated with an increase in cell size, which preserved epidermal thickness.

To test whether decreased survival and/or proliferation were responsible for the reduced cellularity, we determined the rates of proliferation and apoptosis in Migfilin^{-/-;K5Cre+} and control epidermis. The absolute number of Ki67-positive keratinocytes per mm epidermis was similar in control and Migfilin^{-/-;K5Cre+} epidermis at E18.5 and P3 (Figure 4E), but increased significantly in Migfilin^{-/-;K5Cre+} epidermis at P6 (Figure 4E,F). The proliferative index of basal keratinocytes (Ki67+ cells/basal cells) was significantly increased at P3 and P6 (Figure 4G), indicating that a diminished proliferation rate cannot account for the reduced cell number in the basal keratinocyte layer.

Apoptosis is a rare event in unstressed epidermis, as damaged cells are usually discarded by terminal differentiation (Lippens et al., 2005). Indeed, the epidermis of Migfilin^{+/+} and Migfilin^{-/-} mice contained rarely cleaved caspase3-positive cells at all time points analyzed (Figure 4H). We found a slightly increased apoptosis rate in Migfilin^{+/+;K5Cre+} epidermis (Figure 4H), which did not affect epidermal thickness, cell or layer numbers (Figure 4B-E). In Migfilin^{-/-;K5Cre+} epidermis, the number of apoptotic cells was highly increased at all time points tested (Figure 4H,I), indicating that increased apoptosis is likely causing hypo-cellularity in the basal layer of Migfilin^{-/-;K5Cre+} epidermis.

Migfilin^{-/-};K5Cre⁺ keratinocytes become tetra- and hyperploid

We observed binucleated keratinocytes in Migfilin^{-/-};K5Cre⁺ epidermis (Figure 4A, arrowheads). Binucleated cells are tetraploid and can occur after defective mitoses (Storchova and Kuffer, 2008). Since Cre can induce tetraploidy and/or a G2/M cell cycle arrest (Loonstra et al., 2001; Silver and Livingston, 2001), we next examined the DNA content of freshly isolated P3 keratinocytes by flow cytometry to identify the percentage of tetraploid G2 and/or polyploid G1 cells with >4C DNA content, diploid G2 cells and/or tetraploid G1 cells with 4C DNA content, diploid S phase cells with DNA content between 2C and 4C, and diploid G0/G1 cells with 2C DNA content. The relative cell numbers of these fractions were unchanged in control keratinocytes (Migfilin^{+/+}, Migfilin^{-/-}, Migfilin^{+/+};K5Cre⁺, Figure 5A,B). In sharp contrast, the numbers of Migfilin^{-/-};K5Cre⁺ cells with 4C and >4C DNA contents were significantly increased, the number of cells with 2C to 4C content was unchanged, and the number of cells with 2C content was decreased. The increased ratio of S phase to diploid G0/G1 cells points to an increased proliferative index and is in line with the increased Ki67 staining (Figure 4G). The increased number of cells with >4C DNA content is due to increased ploidy, whereas the increase in the 4C cell number is either due to tetraploidy or G2/M cell cycle arrest.

Altogether these results indicate that Cre-expression in Migfilin^{-/-} epidermis causes increased ploidy levels. Since defective mitoses do not increase cell numbers, increased ploidy together with an increased apoptosis rate results in reduced number of basal Migfilin^{-/-};K5Cre⁺ keratinocyte.

Cell cycle progression and DNA-damage response are normal in Migfilin^{-/-};K5Cre⁺ keratinocytes

Cre activity can cause tetraploidy and/or induce DNA damage followed by G2/M cell cycle arrest and apoptosis (Loonstra et al., 2001; Silver and Livingston, 2001). To clarify if the increase in 4C DNA content was due to tetraploidy or cell cycle arrest, we examined the DNA damage response and cell cycle progression in control and Migfilin^{-/-};K5Cre⁺ keratinocytes. Migfilin^{-/-} keratinocytes adhered normally to different extra-cellular matrix substrates and could readily be cultivated (Moik et al., 2011). In contrast, Migfilin^{-/-};K5Cre⁺ keratinocytes underwent collective apoptosis after isolation and thus could not be cultured, excluding further *in vitro* studies. To test if the loss of migfilin alone or in conjunction with DNA damage affected mitosis, we compared the duration of mitosis (defined by breakdown and reformation of the nuclear membrane) in Migfilin^{+/+} and Migfilin^{-/-} cells before and after γ -irradiation. The duration of mitosis of Migfilin^{+/+} and Migfilin^{-/-} cells was identical under basal conditions and increased to a similar extent after γ -irradiation with a dose of 5 Gy (Figure 5C). Furthermore, the localization of essential mediators of cytokinesis like aurora kinase B was unchanged during mitosis in Migfilin^{-/-} keratinocytes with or without γ -irradiation when compared to Migfilin^{+/+} controls (Figure 5D). Collectively, these results argue against migfilin-dependent changes of mitotic progression under basal conditions or after DNA damage.

To test if migfilin has a critical function in DNA repair, we γ -irradiated primary Migfilin^{+/+} and Migfilin^{-/-} keratinocytes and examined the number of nuclear serine139 phosphorylated (pS139) H2ax foci, which mark sites of DNA damage (Bonner et al., 2008). We used a dose of 5 Gy, which caused a >10 fold increase in foci number *in vitro* (Figure 5E), but does not cause skin damage *in vivo* (Iwakawa et al., 2003).

Since H2ax is also strongly phosphorylated in apoptotic cells due to DNA laddering (Lu et al., 2006; Rogakou et al., 2000), we excluded apoptotic cells identifiable by abnormal nuclear shape from our analysis. After irradiation we observed similar increase of pS139-H2ax foci numbers in Migfilin^{+/+} and Migfilin^{-/-} keratinocytes, which reverted to background levels after 36 hours (Figure 5E). These findings indicate that loss of migfilin does not affect recognition and repair of DNA breaks.

To assess whether the extent of DNA damage is also normal *in vivo*, we examined the pS139-H2ax levels in keratinocytes freshly isolated from control and Migfilin^{-/-};K5Cre⁺ mice using flow cytometry. Mean fluorescence intensities (MFIs) of pS139-H2ax were 1.6-fold increased in Migfilin^{-/-};K5Cre⁺ keratinocytes when compared with control cells (Figure 5F,G). This increase correlated with increased DNA content (Figure 5A) and side scatter (ssc) MFIs (Figure 5F), both of which correspond to increased nuclear size (Grove and Ghosh, 2006; Roumier et al., 2005). Activation of the DNA damage response markers Ataxia telangiectasia mutated protein (Atm) as indicated by its phosphorylation at S1981 and Chk1 indicated by phosphorylation at S345 were normal in Migfilin^{-/-};K5Cre⁺ epidermis (Figure 5H). Altogether these data indicate that Cre expression in Migfilin^{-/-};K5Cre⁺ epidermis does not trigger an abnormal DNA damage response.

Cell cycle arrest is associated with changes in the expression of cyclins (Samuel et al., 2002; Sullivan and Morgan, 2007). Specifically, an increase in cyclin B levels indicates a G2/M arrest, leading to an increase in the 4C DNA content cell fraction. To test whether Migfilin^{-/-};K5Cre⁺ keratinocytes display a G2/M arrest, we determined the expression levels of cyclins D1/2, E1, A1, and B1 in epidermal lysates. We found that cyclin E1, A1 and B1 levels were unchanged (Figure 5I), while the cyclins D1/2 levels were increased in Migfilin^{-/-};K5Cre⁺ epidermis (Figure 5I). Elevated cyclin D1/2

indicate a heightened rate of cell cycle entry and normal levels of cyclins E1, A1, and B1 indicate normal cell cycle progression in Migfilin^{-/-;K5Cre+} epidermis and exclude G2/M arrest as an explanation for the increases in 4C DNA content. We therefore, conclude that the increased numbers of 4C and >4C DNA content cells in Migfilin^{-/-;K5Cre+} epidermis were solely due to an increased ploidy.

Loss of p53 in Migfilin^{-/-;K5Cre+} epidermis increases morbidity

After induction of tetraploidy, the tumor suppressor p53 (encoded by Trp53) is phosphorylated at S18 (pS18) and stabilized, leading to increased p53 protein levels and suppression of tetraploid cells (Castedo et al., 2006; Vitale et al., 2010a). Loss of p53 expression combined with cytochalasin D-mediated induction of tetraploidy can make primary cells tumorigenic (Fujiwara et al., 2005). To assess whether the accumulation of tetraploid cells in the Migfilin^{-/-;K5Cre+} epidermis is due to impaired activation of p53, we compared the levels of total and pS18-p53 in Migfilin^{+/+;K5Cre+} and Migfilin^{-/-;K5Cre+} epidermis. The increase of tetraploidy in Migfilin^{-/-;K5Cre+} epidermis correlated with increased total p53 and pS18-p53 levels (Figure 6A). Thus, activation of p53 by tetraploidy was not impaired, but did not suffice to efficiently repress tetraploidy in Migfilin^{-/-;K5Cre+} epidermis.

If migfilin was a down-stream target of p53 in tetraploidy suppression, additional deletion of p53 should not further affect the phenotype of Migfilin^{-/-;K5Cre+} mice. To this end we intercrossed a Trp53-floxed allele (Jonkers et al., 2001) to obtain Migfilin^{-/-;K5Cre+} mice with either Trp53^{fl/+} or Trp53^{fl/fl} alleles in their epidermis. The loss of a single Trp53 allele did not decrease p53 protein levels, while ablation of both alleles resulted in the loss of p53 expression (Figure 6B). Migfilin^{-/-;Trp53^{fl/fl}} epidermis was normal (Figure 6C). Ablation of both p53 alleles increased morbidity of Migfilin^{-/-;K5Cre+}

offspring, which rarely survived until P6. Their epidermis lacked the hyperpigmentation observed in Migfilin^{-/-};K5Cre⁺ epidermis (Figure 6C,D) and appeared dysplastic with keratinocytes of abnormal size, shape and layering (Figure 6C). The epidermal thickness and the absolute number of proliferating cells were comparable to both Migfilin^{-/-};K5Cre⁺;Trp53^{+/+} and Migfilin^{-/-};Trp53^{fl/fl} mice (Figure 6E,F), whereas the number of basal keratinocytes was decreased compared to Migfilin^{-/-};Trp53^{fl/fl} controls and similar to Migfilin^{-/-};K5Cre⁺ mice with wild-type p53 (Figure 6G). The increased morbidity of Migfilin^{-/-};K5Cre⁺;Trp53^{fl/fl} mice correlated with a further 3fold increase in the number of apoptotic cells compared to Migfilin^{-/-};K5Cre⁺ mice with Trp53^{+/+} or Trp53^{fl/+} alleles (Figure 6H). This indicates that both migfilin and p53 function in suppression of tetraploidy.

Migfilin is a novel tumor suppressor

Tetraploidy can give rise to aneuploidy by CIN and thus promotes carcinogenesis (Ganem et al., 2007; Storchova and Kuffer, 2008). To test whether migfilin loss modulates tumor development, we made use of the two-stage carcinogenesis model involving DMBA and TPA (Kemp, 2005) to directly compare the effects of Migfilin loss on tumor development. We found that DMBA/TPA treatment increased tumor incidence ($p < 0.005$) and tumor burden (mean tumor number per mouse) ($p < 0.05$) of Migfilin^{-/-} mice compared to Migfilin^{+/+} controls (Figure 7A,B). Tumor growth was evaluated by grouping papillomas into 4 size categories. The relative abundances of those groups did not reveal a significant difference between Migfilin^{-/-} and Migfilin^{+/+} tumors (Figure 7C), indicating that the overall growth rate of tumors was unchanged. Histological examination revealed that tumors from Migfilin^{+/+} mice were well-differentiated, even after acquiring endophytic

growth characteristics (Figure 7D,E). The majority of tumors from Migfilin^{-/-} mice were also well-differentiated (Figure 7F,G). A few endophytic tumors from Migfilin^{-/-} mice featured a high degree of inflammatory infiltration and showed signs of progression characterized by loss of layering, de-differentiation and disintegration of basal membranes (Figure 7H,I). Treatment of control and Migfilin^{-/-} mice every other day with TPA resulted in comparable dermal inflammation and epidermal hyperthickening (Figure 7J). However, a prolonged TPA treatment for 16 weeks did not induce tumor development in control or Migfilin^{-/-} mice, indicating that the loss of migfilin does not change the outcome of the TPA-induced reactive epidermal hyperplasia or modulate the rate of spontaneous cancer development in skin. Altogether these findings point to a tumor suppressor role of migfilin in skin.

DISCUSSION

The *in vivo* function of migfilin is obscure, as migfilin expression is dispensable for mouse development and postnatal life (Moik et al., 2011). Here we report the surprising observation that the combination of migfilin loss and the expression of Cre in the epidermis led to a hyperthickened epidermis with massively enlarged and significantly fewer cells in the basal keratinocyte layer, cutaneous inflammation and lethality at around 10 days after birth. The basal keratinocytes showed increased binucleation, tetraploidy, and apoptosis. The tumor and tetraploidy suppressor p53 was induced and activated in the mutant epidermis, and deletion of p53 further increased epidermal apoptosis rates and accelerated lethality, indicating that migfilin is a novel and p53-independent suppressor of tetraploidy in keratinocytes. A defect in tetraploidy suppression was further corroborated by the observation showing that loss of migfilin enhanced chemically induced skin carcinogenesis.

Keratinocyte binucleation, tetraploidy and apoptosis were evident already *in utero*, where embryonic skin is protected from environmental stressors like microbial infections, irradiation or defects in skin barrier function. Interestingly, other defects such as epidermal blistering due to impaired integrin function or barrier defects due to compromised cell-cell adhesion were not apparent in mutant skin. We therefore conclude that tetraploidy and/or apoptosis represent the trigger for the lethal inflammatory hyperplasia in Migfilin^{-/-;K5Cre+} and Migfilin^{fl/fl;K5Cre+} epidermis.

It is well known that Cre recombinase activity can cause apoptosis *in vivo* (Naiche and Papaioannou, 2007) and inhibit cell proliferation *in vitro* due to an increase in >4C and 4C DNA content, and increased CIN (Loonstra et al., 2001). Pfeiffer et al. (2001) reported similar defects induced by Cre activity, and furthermore showed they were associated with a dramatic enlargement of cells. The cytotoxicity

of Cre depended on its recombinase activity (Pfeifer et al., 2001; Schmidt et al., 2000; Silver and Livingston, 2001). Furthermore, it was also shown that Cre can bind and process cryptic loxP sites present in mammalian genomes, albeit with low efficacy, and induce DNA breaks (Semprini et al., 2007; Thyagarajan et al., 2000). These Cre-induced DNA breaks represent a DNA damage that can lead to G2/M cell cycle arrest and apoptosis (Loonstra et al., 2001). Although this course of events provides a plausible explanation for the increased cellular 4C DNA content, apoptosis and CIN, it fails to explain the increased cell size and >4C DNA content (Loonstra et al., 2001).

Could failure of an ongoing DNA damage response cause the defects in the Migfilin^{-/-;K5Cre+} and Migfilin^{fl/fl;K5Cre+} epidermis? We made several observations that argue against such a possibility. First, the extent of DNA damage determined by the levels of pS139-H2ax was slightly increased in Migfilin^{-/-;K5Cre+} keratinocytes, which associate to their increased nuclear size and DNA content and thus to a higher probability of spontaneous DNA damage. Second, we excluded an abnormal response to DNA damage by measuring the activation of Atm, which was similar in Migfilin^{-/-;K5Cre+} and control epidermis. Third, we also found normal cyclin B1 levels and thus no signs of a DNA damage-induced G2/M cell cycle arrest in Migfilin^{-/-;K5Cre+} keratinocytes. Finally, activation of the DNA damage response should also repress cell cycle entry and thus induce senescence in Migfilin^{-/-;K5Cre+} keratinocytes (Campisi and d'Adda di Fagagna, 2007), but we observed an increase in the number of cycling keratinocytes when examining Ki67- and cyclin D1/2-levels, arguing against induced senescence. Thus, an abnormal activation of the DNA damage response does clearly not explain the defects observed in Cre-expressing migfilin-null epidermis.

Tetraploidy can arise from endomitosis (a failure to segregate the replicated DNA), from defective cytokinesis (a failure to separate the two daughter cells) or from cell fusion (Storchova and Kuffer, 2008). Since endomitosis increases ploidy levels without producing binucleated cells we can exclude this possibility as cause for the tetraploidy in Migfilin^{-/-;K5Cre+} and Migfilin^{fl/fl;K5Cre+} epidermis. Cell fusion and cytokinesis defects can give rise to binucleation and have not been excluded as cause for the tetraploidy in our mouse model. However, since Cre activity is inducing cell fusion to the same extent as in non-Cre expressing cells (Pfannkuche et al., 2010) we consider cell fusion an unlikely cause for the Cre-induced binucleation in migfilin-null keratinocytes. A cytokinesis defect is more likely, as Cre activity causes low level DNA damage which is believed to be not sufficient to trigger a cell cycle arrest in mammalian cells (Deckbar et al., 2007) but sufficient to induce cytokinesis defects. Such cytokinesis failure occurs when the DNA damage persists into mitosis and leads to the formation of cytokinetic DNA bridges (Ichijima et al., 2010; Steigemann and Gerlich, 2009). Thus, the increased incidence in binucleation combined with the dependence on Cre recombinase activity makes a strong case for a cytokinesis failure in the Migfilin^{-/-;K5Cre+} and Migfilin^{fl/fl;K5Cre+} epidermis. Clearly, the possibility of cell fusion, however, must also be experimentally excluded in future studies.

Since the DNA damage response was not activated, it is unclear how Cre expression can account for the increased rate in apoptosis in the Cre-expressing migfilin-null epidermis. There are no indications that tetraploidy per se is recognized by cells (Uetake and Sluder, 2004; Wong and Stearns, 2005) and triggers apoptosis. Tetraploid cells, however, are prone to CIN and aneuploidy through multipolar mitoses or lagging chromosomes (Ganem et al., 2009; Kwon et al., 2008; Vitale et

al., 2010b), which in turn can result in lethal nullisomy, i.e. the lack of a chromosome (Gisselsson et al., 2008), or in senescence or apoptosis in a p53-dependent (Ganem et al., 2009; Kwon et al., 2008; Thompson and Compton, 2010; Vitale et al., 2010a; Vitale et al., 2010b; Zhivotovsky and Kroemer, 2004) as well as -independent manner (Castedo et al., 2006).

In line with a role of p53 in repression of tetraploidy/aneuploidy, we observed a pronounced pS18 phosphorylation and thus activation of p53 in Migfilin^{-/-};K5Cre⁺ epidermis. The mechanism underlying p53-mediated suppression of tetraploidy and aneuploidy is not well-understood. Several candidate kinases for S18-p53 phosphorylation in the context of tetraploidy/aneuploidy have been proposed including p38 mitogen-activated kinase (MAPK), ATM and AMP-activated protein kinase (AMPK). p38 is necessary for p53-mediated senescence (Uetake and Sluder, 2010). AMPK has been implicated in p53-mediated aneuploidy-suppression caused by proteotoxic stress due to chromosome imbalance (Jones et al., 2005; Tang et al., 2011). The role of ATM is more complex: spontaneously arising, radiation-, and aneuploidy-induced thymic lymphoma are repressed by p53 and ATM in a cooperative manner (Bailey et al., 2008; Li et al., 2010), while loss of ATM has no impact on the outcome of DMBA/TPA-induced skin cancer (Bailey et al., 2008).

The tissue-dependent differences of p53-activation reflect the tumor spectrum of p53-null mice, which develop mainly lymphomas and sarcomas at a median age of 4.5 months, but seldom carcinomas (Jacks et al., 1994). Epidermal ablation of p53 with a K14Cre transgene does not lead to obvious skin abnormalities, and spontaneous skin tumor development occurs at a median age of 8.3 months (Martinez-Cruz et al., 2008). The limited impact of p53-deletion on skin tumorigenesis could be due to the fact that the central role of p53 in the skin is to

regulate tanning response after exposure to UV light, which leads to p53-mediated secretion of melanogenic cytokines by keratinocytes, stimulating proliferation of and pigment production of melanocytes (Cui et al., 2007). Thus, this skin-specific function of p53 might be incompatible with its role in suppressing tetraploidy, which has likely been taken over by other genes including migfilin. Indeed, in a ribosomal stress model where p53 is constitutively activated, p53 induced hyperpigmentation but not apoptosis in the skin, while it strongly increased apoptosis in lymphocytes (McGowan et al., 2008). We found a strong activation of p53 in Migfilin^{-/-};K5Cre⁺ epidermis suggesting that the mechanisms recognizing aneuploidy may still be functioning. The activated p53, however, did not efficiently suppress tetraploidy/aneuploidy to prevent morbidity. Furthermore, deletion of p53 in Migfilin^{-/-};K5Cre⁺ epidermis rescued the epidermal hyperpigmentation, but increased rather than decreased epidermal apoptosis, resulting in a slightly accelerated morbidity.

How could migfilin suppress tetraploidy and/or aneuploidy? Similar to p53, migfilin could induce apoptosis and/or block proliferation (Figure 7K). In the presence of migfilin, epidermal Cre-expression induced a minor increase of binucleation and apoptosis, but did not affect cell cycle progression or the DNA content profile. The increased apoptosis in Cre-expressing wild-type epidermis could result from an efficient repression of tetraploidy. In the case of migfilin loss, tetraploid cells accumulate and become apoptotic, e.g. due to nullisomy.

The link between cancer and tetraploidy/aneuploidy has been subject to intensive analysis for more than a century (Boveri, 1914). It is now accepted that tetraploidy represents an intermediate to aneuploidy and thus promotes progression to cancer (Schvartzman et al., 2010; Thompson and Compton, 2010). In line with this

dogma, tetraploidy or aneuploidy is found in the majority of cancers (Mitelman et al., 2011; Schwartzman et al., 2010). In epithelial tissues such as skin, esophagus and cervix tetraploidy and aneuploidy are major predictors for cancer progression (Conti et al., 1986; Maley et al., 2004; Olaharski et al., 2006; Robinson et al., 1996). Loss of a suppressor of tetraploidy like migfilin therefore sensitizes skin to carcinogenesis, which we indeed observed in the DMBA/TPA skin cancer model.

Since Cre is such a widely used tool in mouse genetics, it is surprising that there are so few reports of Cre mediated cytotoxicity. The K5Cre transgene used in this study is widely used without reports of inducing apparent skin defects. The lack of such observations is likely due to the mildness of the defects. Interestingly, a Cre transgene driven by the human K5 promotor produced normal hemizygous mice (Tarutani et al., 1997), but at homozygosity the mice suffered from a wavy-hair phenotype and an accelerated skin cancer progression (Chan et al., 2007). Notably, also in this study the authors did not report an increased DNA damage response as measured by ATM activation (Chan et al., 2007).

An interesting observation is that all Migfilin^{fl/fl;K5Cre+} and Migfilin^{-/-;K5Cre+} mice died around 10 days after birth. The cause for this early lethality is not clear. Inflammatory hyperplasia followed by a cytokine storm can lead to lethality. A similar inflammation can be induced by a diverse range of keratinocytes dysfunctions including defective cell-matrix adhesion (Brakebusch et al., 2000; Lorenz et al., 2007), tight junction formation (Yang et al., 2010), or a precocious sensitivity to apoptosis (Omori et al., 2006). These defects trigger a wound healing reaction that is not intrinsically lethal, but can become lethal in conjunction with additional defects, as seen after K5Cre-mediated integrin β 1 ablation, where esophageal defects interfere with feeding (Brakebusch et al., 2000). The lethal epidermal inflammatory hyperplasia of

Migfilin^{-/-;K5Cre+} mice is reminiscent of the phenotype resulting from epidermal deletion of Transforming growth factor β -activated kinase 1 (TAK1) (Omori et al., 2006). TAK1-null keratinocytes are driven into apoptosis by endogenous TNF, which induces the inflammatory hyperplasia and further upregulates TNF expression, and thereby escalates the lethal phenotype. A similar vulnerability to inflammation-mediated apoptosis after loss of migfilin can be excluded, since loss of migfilin did not modulate the TPA-induced hyperplastic skin inflammation. We rather postulate that the inflammation promotes proliferation, which results in apoptosis of aneuploid Migfilin^{-/-;K5Cre+} keratinocytes, a dramatic aggravation of the phenotype and finally death at P10.

EXPERIMENTAL PROCEDURES

Mouse strains

Generation and characterization of Migfilin^{fl/fl} and Migfilin^{-/-} strains was described (Moik et al., 2011). K5Cre⁺ and K14Cre⁺ mice were described previously (Hafner et al., 2004; Ramirez et al., 2004). Trp53 floxed mice (Trp53^{tm1Brn}) (Jonkers et al., 2001) were obtained from Dr. Anton Berns, University of Amsterdam, NL. All mouse strains were backcrossed at least 5 times to the C57BL/6 mouse strain.

Animal husbandry and tumor experiments

C57BL/6 mice were kept and bred according to German animal welfare laws at the MPI of Biochemistry animal facilities. Animal experiments were approved by the State Government of Bavaria. For the two-stage skin carcinogenesis experiments, mice were shaved at the back at 6-7 weeks of age and 2 days later treated with 7,12-Dimethylbenz(a)anthracene (DMBA) (2 mM in acetone, 100 μ L per treatment, Supelco). Two weeks later, a bi-weekly treatment with 12-O-Tetradecanoylphorbol-13-acetate (TPA) (0.2 mM in acetone, 100 μ L per treatment, Sigma) was started. Papillomas were counted when their diameter reached 1 mm and they were present at least for 2 consecutive weeks.

Antibodies

The source and working dilution used for immunoblotting (IB), immunofluorescence (IF) or flow cytometry (flow.) of primary antibodies are listed in Table 2. Appropriate horse radish peroxidase(HRP)- or fluorophor-conjugated secondary antibodies were obtained from Biorad or Jackson Laboratories.

Cell culture and live cell imaging

Primary keratinocytes were isolated at P3 or in telogen phase of the hair cycle. Mice were killed, shaved and skinned. Muscle and fatty layer were scraped off and the skin was incubated for 1 hour in Dulbecco's phosphate-buffered saline (PBS) supplemented with 0.8% Trypsin (Gibco) at 37°C. Afterwards the epidermis was peeled off from the underlying dermis and manually dissociated. The resulting suspension was filtered through a 45 µm nylon mesh. Cells were seeded onto bovine Collagen I (AdvancedBiomatrix) coated culture dishes and maintained at 37°C and 5% CO₂ in growth medium (Spinner's MEM supplemented with 5 mg/L Insulin, 10 mg/L EGF (Roche), 10 mg/L transferrin, 10 µM phosphoethanolamine, 10 µM ethanolamine, 0.36 mg/L hydrocortisone (Calbiochem), 0.3 g/L glutamine, 100 units/mL Penicillin, 100 mg/L Streptomycin, 45 µM CaCl₂ and 8% chelated FCS). Unless otherwise noted, all cell culture reagents were reagent grade purchased from Invitrogen or Sigma.

Live cell imaging was performed as described (Moik et al., 2011) with one picture taken every 3 minutes. Phase contrast was sufficient to visualize nuclear membrane breakdown and reformation.

Flow cytometry

Freshly isolated primary keratinocytes were stained with primary antibodies for 10-30 minutes on ice, washed, and stained with secondary antibody for 10-30 minutes on ice. After washing, cells were resuspended in PBS containing BSA and propidium iodide. Immortalized keratinocytes were trypsinized and treated as above. Flow cytometry was performed on a FACSCalibur flow cytometer (Becton &

Dickinson). For measuring nuclear antigens, primary antibody staining was performed overnight on ice after PFA fixation.

Histology, epidermal morphometry and proliferation/cell death analysis

Skin and tumor samples were prepared by standard methods for paraffin or cryo embedding (Montanez et al., 2007) and stained according to Mayer's hematoxylin and eosin (H/E) or the Masson-Fontana protocol. For generation of epidermal whole mounts, P3 mice were killed and skinned. Muscle and fatty layer were scraped off, followed by careful mechanical separation of dermis and epidermis. Epidermis was fixed for 10 Minutes in 4% PFA/PBS and kept in PBS with 0.05% NaN_3 at 4°C until use.

For morphometric measurements, 2-5 animals were used for each genotype and time point. To measure the epidermal thickness and number of nucleated layers, back skin sections were immunostained for β -Catenin and $\alpha 6$ integrin. Images randomly chosen along the whole length of the skin section were obtained with a TCS SP5 AOBS Confocal Laser Scanning Microscope (Leica) and a 63x/1.4NA objective. Epidermal thickness was measured from the $\alpha 6$ integrin-stained basement membrane to the top of the upmost cell expressing β -Catenin using the Leica microscope operating software. Infundibula, i.e. the egress funnels for hair shafts, were avoided. Layer numbers were counted similarly.

For measurements of proliferation and basal cell number, back skin sections were immunostained for Ki67, Laminin-322 and nuclei. 5 images per mouse were obtained as above using a 40x/1.25NA objective. For each image, the Laminin-322 stained basement membrane was aligned with one border of the field-of-view. Ki67-positive cells and total number of nuclei were counted. Cell number was estimated at

infundibula. Cell numbers were divided by the length of the field-of-view of 0.385 mm to obtain the cell numbers per mm epidermis.

Apoptosis was measured by staining 10 back skin sections per animal for cleaved Caspase 3 (clCasp3) and integrin $\alpha 6$. clCasp3+ apoptotic epidermal keratinocytes were counted by eye under microscopic epifluorescence illumination (ImagerZ1, Zeiss) with a 40x/1.25NA objective. Follicular keratinocytes were excluded. Section lengths were measured with a ruler, the derived quotient of cell number and section length gave the number of clCasp3-positive cells per mm epidermis.

For determination of bi- or multinucleation, epidermal whole mount preparations were immunostained for integrin $\alpha 6$ and counterstained with DAPI. After image acquisition of z-stacks, adjacent nuclei that were surrounded by integrin staining and deformed each other were counted as belonging to the same cell.

Skin barrier assays

Inside-out skin barrier function was assayed by measuring trans-epidermal water loss (TEWL) using a Tewameter TM300 (Courage+Khazaka electronic GmbH) with a probe equilibrated to 37°C. Outside-in barrier function was tested by euthanizing pups and immersing the back skin for 30 minutes at 37°C in 1 mM LuciferYellow (Sigma)/PBS before isolation of skin and subsequent embedding for cryo sectioning. Outside-in barrier function is intact when the LuciferYellow signal is restricted to the outermost epidermal cornified layer.

Western blotting

Cells or tissues were homogenized in RIPA buffer (150 mM NaCl, 50 mM Tris-HCl, 5 mM EDTA, 0.1% w/v SDS, 1.0% w/v sodium deoxycholate, 1.0% v/v Triton X-100, Phosphatase inhibitor cocktails P1 and P2 [pH 7.6]; all by Sigma), with Complete protease inhibitors (Roche). 20 to 50 µg of total protein per lane were separated on a polyacrylamide gel and transferred to PVDF membranes (Millipore). Membrane blocking and antibody dilution was performed with Tris-buffered saline (TBS) pH 7.6 supplemented with 0.1% Tween20 (Serva) and 5% skim milk (Fluka) or 5% bovine serum albumin (BSA) (PAA Laboratories). Subsequently membranes were incubated for 1 hour at room temperature (RT) or overnight at 4°C with primary antibody. After washing with TBS, appropriate HRP-coupled secondary antibodies (BioRad) were applied for 1 hour at RT. After washing, ECL detection (Immobilon, Millipore) was performed at a LAS4000 (Fujifilm).

Immunofluorescence

Cryo sections from frozen adult and embryonic tissues were prepared and embedded according to standard protocols. Cells were grown on glass cover slips coated with bovine Collagen I (5 mg/L, Advanced Biomatrix). Samples were fixed 10 minutes in 3.7% PFA/ PBS, permeabilized 3 minutes with 0.1% Triton X-100/ PBS and blocked for 1 hour in 5% BSA/ PBS. Primary antibodies were diluted in blocking solution and applied overnight at 4°C. After washing with PBS, appropriate secondary antibodies were diluted in blocking solution and applied for 1 hour at RT. After washing and DAPI staining (1:10.000 in PBS), slides were mounted in Elvanol. Pictures were taken with a TCS SP5 AOBS or TCS SP2 AOBS Confocal Laser Scanning Microscope (Leica).

DNA damage repair kinetics

Cells were seeded on glass cover slips pre-coated with Collagen I (5 mg/L, Advanced Biomatrix). After 24 h of growth, cells were irradiated with 5 Gy ionizing radiation (IR). At defined time points, the cells were immunostained for pS139-H2ax. DNA was stained with DAPI. Confocal pictures focused on the maximal diameter of the nucleus were acquired from randomly chosen fields-of-view with a TCS SP5 AOBS Confocal Laser Scanning Microscope (Leica) using a 100x/1.4NA objective. The number of foci and the nuclear area were analysed with ImageJ (Rasband, 1997-2009) using the watershed algorithm and analyze particles functions.

Statistics

All numerical data are given as a mean value with the standard error of the mean (SEM). Statistical significance was tested as indicated in the figure legends.

ACKNOWLEDGEMENTS

We thank Drs. Marc Schmidt-Supprian for helpful discussions and suggestions, Monique Aumailley for the LM-322 antibody and Anton Berns for the Trp53^{tm1Bm} mice. The work was supported by the Max Planck Society.

REFERENCES

- Akazawa, H., Kudoh, S., Mochizuki, N., Takekoshi, N., Takano, H., Nagai, T. and Komuro, I.** (2004). A novel LIM protein Cal promotes cardiac differentiation by association with CSX/NKX2-5. *J Cell Biol* **164**, 395-405.
- Bailey, S. L., Gurley, K. E., Hoon-Kim, K., Kelly-Spratt, K. S. and Kemp, C. J.** (2008). Tumor suppression by p53 in the absence of Atm. *Mol Cancer Res* **6**, 1185-92.
- Bonner, W. M., Redon, C. E., Dickey, J. S., Nakamura, A. J., Sedelnikova, O. A., Solier, S. and Pommier, Y.** (2008). GammaH2AX and cancer. *Nat Rev Cancer* **8**, 957-67.
- Boveri, T.** (1914). Zur Frage der Entstehung maligner Tumoren. Jena, Germany: G. Fischer Verlag.
- Brakebusch, C., Grose, R., Quondamatteo, F., Ramirez, A., Jorcano, J. L., Pirro, A., Svensson, M., Herken, R., Sasaki, T., Timpl, R. et al.** (2000). Skin and hair follicle integrity is crucially dependent on beta 1 integrin expression on keratinocytes. *Embo J* **19**, 3990-4003.
- Campisi, J. and d'Adda di Fagagna, F.** (2007). Cellular senescence: when bad things happen to good cells. *Nature reviews. Molecular cell biology* **8**, 729-40.
- Castedo, M., Coquelle, A., Vivet, S., Vitale, I., Kauffmann, A., Dessen, P., Pequignot, M. O., Casares, N., Valent, A., Mouhamad, S. et al.** (2006). Apoptosis regulation in tetraploid cancer cells. *Embo J* **25**, 2584-95.
- Chan, E. L., Peace, B. E., Toney, K., Kader, S. A., Pathrose, P., Collins, M. H. and Waltz, S. E.** (2007). Homozygous K5Cre transgenic mice have wavy hair and accelerated malignant progression in a murine model of skin carcinogenesis. *Mol Carcinog* **46**, 49-59.
- Conti, C. J., Aldaz, C. M., O'Connell, J., Klein-Szanto, A. J. and Slaga, T. J.** (1986). Aneuploidy, an early event in mouse skin tumor development. *Carcinogenesis* **7**, 1845-8.
- Cui, R., Widlund, H. R., Feige, E., Lin, J. Y., Wilensky, D. L., Igras, V. E., D'Orazio, J., Fung, C. Y., Schanbacher, C. F., Granter, S. R. et al.** (2007). Central role of p53 in the suntan response and pathologic hyperpigmentation. *Cell* **128**, 853-64.
- Deckbar, D., Birraux, J., Krempler, A., Tchouandong, L., Beucher, A., Walker, S., Stiff, T., Jeggo, P. and Lobrich, M.** (2007). Chromosome breakage after G2 checkpoint release. *J Cell Biol* **176**, 749-55.
- Feng, Y. and Longmore, G. D.** (2005). The LIM protein Ajuba influences interleukin-1-induced NF-kappaB activation by affecting the assembly and activity of the protein kinase Czeta/p62/TRAF6 signaling complex. *Mol Cell Biol* **25**, 4010-22.
- Feng, Y., Zhao, H., Luderer, H. F., Epple, H., Faccio, R., Ross, F. P., Teitelbaum, S. L. and Longmore, G. D.** (2007). The LIM protein, Limd1, regulates AP-1 activation through an interaction with Traf6 to influence osteoclast development. *J Biol Chem* **282**, 39-48.
- Fujiwara, T., Bandi, M., Nitta, M., Ivanova, E. V., Bronson, R. T. and Pellman, D.** (2005). Cytokinesis failure generating tetraploids promotes tumorigenesis in p53-null cells. *Nature* **437**, 1043-7.
- Ganem, N. J., Godinho, S. A. and Pellman, D.** (2009). A mechanism linking extra centrosomes to chromosomal instability. *Nature* **460**, 278-82.
- Ganem, N. J., Storchova, Z. and Pellman, D.** (2007). Tetraploidy, aneuploidy and cancer. *Curr Opin Genet Dev* **17**, 157-62.

Gisselsson, D., Hakanson, U., Stoller, P., Marti, D., Jin, Y., Rosengren, A. H., Stewenius, Y., Kahl, F. and Panagopoulos, I. (2008). When the genome plays dice: circumvention of the spindle assembly checkpoint and near-random chromosome segregation in multipolar cancer cell mitoses. *PLoS One* **3**, e1871.

Gkretsi, V., Zhang, Y., Tu, Y., Chen, K., Stolz, D. B., Yang, Y., Watkins, S. C. and Wu, C. (2005). Physical and functional association of migfilin with cell-cell adhesions. *J Cell Sci* **118**, 697-710.

Grove, L. E. and Ghosh, R. N. (2006). Quantitative characterization of mitosis-blocked tetraploid cells using high content analysis. *Assay Drug Dev Technol* **4**, 421-42.

Hafner, M., Wenk, J., Nenci, A., Pasparakis, M., Scharffetter-Kochanek, K., Smyth, N., Peters, T., Kess, D., Holtkotter, O., Shephard, P. et al. (2004). Keratin 14 Cre transgenic mice authenticate keratin 14 as an oocyte-expressed protein. *Genesis* **38**, 176-81.

Hanahan, D. and Weinberg, R. A. (2000). The hallmarks of cancer. *Cell* **100**, 57-70.

Hanahan, D. and Weinberg, R. A. (2011). Hallmarks of cancer: the next generation. *Cell* **144**, 646-74.

Hervy, M., Hoffman, L. and Beckerle, M. C. (2006). From the membrane to the nucleus and back again: bifunctional focal adhesion proteins. *Curr Opin Cell Biol* **18**, 524-32.

Hervy, M., Hoffman, L. M., Jensen, C. C., Smith, M. and Beckerle, M. C. (2010). The LIM Protein Zyxin Binds CARP-1 and Promotes Apoptosis. *Genes Cancer* **1**, 506-515.

Hoffman, L. M., Jensen, C. C., Kloeker, S., Wang, C. L., Yoshigi, M. and Beckerle, M. C. (2006). Genetic ablation of zyxin causes Mena/VASP mislocalization, increased motility, and deficits in actin remodeling. *J Cell Biol* **172**, 771-82.

Hoffman, L. M., Nix, D. A., Benson, B., Boot-Hanford, R., Gustafsson, E., Jamora, C., Menzies, A. S., Goh, K. L., Jensen, C. C., Gertler, F. B. et al. (2003). Targeted disruption of the murine zyxin gene. *Mol Cell Biol* **23**, 70-9.

Ichijima, Y., Yoshioka, K., Yoshioka, Y., Shinohe, K., Fujimori, H., Unno, J., Takagi, M., Goto, H., Inagaki, M., Mizutani, S. et al. (2010). DNA lesions induced by replication stress trigger mitotic aberration and tetraploidy development. *PLoS One* **5**, e8821.

Jacks, T., Remington, L., Williams, B. O., Schmitt, E. M., Halachmi, S., Bronson, R. T. and Weinberg, R. A. (1994). Tumor spectrum analysis in p53-mutant mice. *Curr Biol* **4**, 1-7.

Jones, R. G., Plas, D. R., Kubek, S., Buzzai, M., Mu, J., Xu, Y., Birnbaum, M. J. and Thompson, C. B. (2005). AMP-activated protein kinase induces a p53-dependent metabolic checkpoint. *Mol Cell* **18**, 283-93.

Jonkers, J., Meuwissen, R., van der Gulden, H., Peterse, H., van der Valk, M. and Berns, A. (2001). Synergistic tumor suppressor activity of BRCA2 and p53 in a conditional mouse model for breast cancer. *Nat Genet* **29**, 418-25.

Kadmas, J. L. and Beckerle, M. C. (2004). The LIM domain: from the cytoskeleton to the nucleus. *Nat Rev Mol Cell Biol* **5**, 920-31.

Kaur, P. (2006). Interfollicular epidermal stem cells: identification, challenges, potential. *J Invest Dermatol* **126**, 1450-8.

Kemp, C. J. (2005). Multistep skin cancer in mice as a model to study the evolution of cancer cells. *Semin Cancer Biol* **15**, 460-73.

Kwon, M., Godinho, S. A., Chandhok, N. S., Ganem, N. J., Azioune, A., They, M. and Pellman, D. (2008). Mechanisms to suppress multipolar divisions in cancer cells with extra centrosomes. *Genes Dev* **22**, 2189-203.

Lad, Y., Jiang, P., Ruskamo, S., Harburger, D. S., Ylanne, J., Campbell, I. D. and Calderwood, D. A. (2008). Structural Basis of the Migfilin-Filamin Interaction and Competition with Integrin {beta} Tails. *J Biol Chem* **283**, 35154-63.

Lengauer, C., Kinzler, K. W. and Vogelstein, B. (1998). Genetic instabilities in human cancers. *Nature* **396**, 643-9.

Li, M., Fang, X., Baker, D. J., Guo, L., Gao, X., Wei, Z., Han, S., van Deursen, J. M. and Zhang, P. (2010). The ATM-p53 pathway suppresses aneuploidy-induced tumorigenesis. *Proc Natl Acad Sci U S A* **107**, 14188-93.

Lippens, S., Denecker, G., Ovaere, P., Vandenabeele, P. and Declercq, W. (2005). Death penalty for keratinocytes: apoptosis versus cornification. *Cell Death Differ* **12 Suppl 2**, 1497-508.

Loonstra, A., Vooijs, M., Beverloo, H. B., Allak, B. A., van Drunen, E., Kanaar, R., Berns, A. and Jonkers, J. (2001). Growth inhibition and DNA damage induced by Cre recombinase in mammalian cells. *Proc Natl Acad Sci U S A* **98**, 9209-14.

Lorenz, K., Grashoff, C., Torka, R., Sakai, T., Langbein, L., Bloch, W., Aumailley, M. and Fassler, R. (2007). Integrin-linked kinase is required for epidermal and hair follicle morphogenesis. *J Cell Biol* **177**, 501-13.

Lu, C., Zhu, F., Cho, Y. Y., Tang, F., Zykova, T., Ma, W. Y., Bode, A. M. and Dong, Z. (2006). Cell apoptosis: requirement of H2AX in DNA ladder formation, but not for the activation of caspase-3. *Mol Cell* **23**, 121-32.

Mack, J. A., Anand, S. and Maytin, E. V. (2005). Proliferation and cornification during development of the mammalian epidermis. *Birth Defects Res C Embryo Today* **75**, 314-29.

Maley, C. C., Galipeau, P. C., Li, X., Sanchez, C. A., Paulson, T. G., Blount, P. L. and Reid, B. J. (2004). The combination of genetic instability and clonal expansion predicts progression to esophageal adenocarcinoma. *Cancer Res* **64**, 7629-33.

Martinez-Cruz, A. B., Santos, M., Lara, M. F., Segrelles, C., Ruiz, S., Moral, M., Lorz, C., Garcia-Escudero, R. and Paramio, J. M. (2008). Spontaneous squamous cell carcinoma induced by the somatic inactivation of retinoblastoma and Trp53 tumor suppressors. *Cancer Res* **68**, 683-92.

McGowan, K. A., Li, J. Z., Park, C. Y., Beaudry, V., Tabor, H. K., Sabnis, A. J., Zhang, W., Fuchs, H., de Angelis, M. H., Myers, R. M. et al. (2008). Ribosomal mutations cause p53-mediated dark skin and pleiotropic effects. *Nat Genet* **40**, 963-70.

Mitelman, F., Johansson, B. and Mertens, F. (2011). Mitelman Database of Chromosome Aberrations and Gene Fusions in Cancer. <http://cgap.nci.nih.gov/Chromosomes/Mitelman>.

Moik, D. V., Janbandhu, V. C. and Fassler, R. (2011). Loss of migfilin expression has no overt consequences on murine development and homeostasis. *J Cell Sci* **124**, 414-21.

Montanez, E., Piwko-Czuchra, A., Bauer, M., Li, S., Yurchenco, P. and Fassler, R. (2007). Analysis of integrin functions in peri-implantation embryos, hematopoietic system, and skin. *Methods Enzymol* **426**, 239-89.

Montanez, E., Ussar, S., Schifferer, M., Bosl, M., Zent, R., Moser, M. and Fassler, R. (2008). Kindlin-2 controls bidirectional signaling of integrins. *Genes Dev* **22**, 1325-30.

Naiche, L. A. and Papaioannou, V. E. (2007). Cre activity causes widespread apoptosis and lethal anemia during embryonic development. *Genesis* **45**, 768-75.

Okura, M., Maeda, H., Nishikawa, S. and Mizoguchi, M. (1995). Effects of monoclonal anti-c-kit antibody (ACK2) on melanocytes in newborn mice. *J Invest Dermatol* **105**, 322-8.

Olaharski, A. J., Sotelo, R., Solorza-Luna, G., Gonsebatt, M. E., Guzman, P., Mohar, A. and Eastmond, D. A. (2006). Tetraploidy and chromosomal instability are early events during cervical carcinogenesis. *Carcinogenesis* **27**, 337-43.

Omori, E., Matsumoto, K., Sanjo, H., Sato, S., Akira, S., Smart, R. C. and Ninomiya-Tsuji, J. (2006). TAK1 is a master regulator of epidermal homeostasis involving skin inflammation and apoptosis. *J Biol Chem* **281**, 19610-7.

Pfeifer, A., Brandon, E. P., Kootstra, N., Gage, F. H. and Verma, I. M. (2001). Delivery of the Cre recombinase by a self-deleting lentiviral vector: efficient gene targeting in vivo. *Proc Natl Acad Sci U S A* **98**, 11450-5.

Pratt, S. J., Epple, H., Ward, M., Feng, Y., Braga, V. M. and Longmore, G. D. (2005). The LIM protein Ajuba influences p130Cas localization and Rac1 activity during cell migration. *J Cell Biol* **168**, 813-24.

Proksch, E., Brandner, J. M. and Jensen, J. M. (2008). The skin: an indispensable barrier. *Exp Dermatol* **17**, 1063-72.

Ramirez, A., Page, A., Gandarillas, A., Zanet, J., Pibre, S., Vidal, M., Tusell, L., Genesca, A., Whitaker, D. A., Melton, D. W. et al. (2004). A keratin K5Cre transgenic line appropriate for tissue-specific or generalized Cre-mediated recombination. *Genesis* **39**, 52-7.

Rasband, W. S. (1997-2009). ImageJ: U. S. National Institutes of Health, Bethesda, Maryland, USA.

Robinson, J. K., Rademaker, A. W., Goolsby, C., Traczyk, T. N. and Zoladz, C. (1996). DNA ploidy in nonmelanoma skin cancer. *Cancer* **77**, 284-91.

Rogakou, E. P., Nieves-Neira, W., Boon, C., Pommier, Y. and Bonner, W. M. (2000). Initiation of DNA fragmentation during apoptosis induces phosphorylation of H2AX histone at serine 139. *J Biol Chem* **275**, 9390-5.

Roumier, T., Valent, A., Perfettini, J. L., Metivier, D., Castedo, M. and Kroemer, G. (2005). A cellular machine generating apoptosis-prone aneuploid cells. *Cell Death Differ* **12**, 91-3.

Samuel, T., Weber, H. O. and Funk, J. O. (2002). Linking DNA damage to cell cycle checkpoints. *Cell Cycle* **1**, 162-8.

Schiller, H. B., Friedel, C. C., Boulegue, C. and Fassler, R. (2011). Quantitative proteomics of the integrin adhesome show a myosin II-dependent recruitment of LIM domain proteins. *EMBO Rep*.

Schmidt-Suppran, M. and Rajewsky, K. (2007). Vagaries of conditional gene targeting. *Nat Immunol* **8**, 665-8.

Schmidt, E. E., Taylor, D. S., Prigge, J. R., Barnett, S. and Capecchi, M. R. (2000). Illegitimate Cre-dependent chromosome rearrangements in transgenic mouse spermatids. *Proc Natl Acad Sci U S A* **97**, 13702-7.

Schwartzman, J. M., Sotillo, R. and Benezra, R. (2010). Mitotic chromosomal instability and cancer: mouse modelling of the human disease. *Nat Rev Cancer* **10**, 102-15.

Segre, J. A. (2006). Epidermal barrier formation and recovery in skin disorders. *J Clin Invest* **116**, 1150-8.

Semprini, S., Troup, T. J., Kotelevtseva, N., King, K., Davis, J. R., Mullins, L. J., Chapman, K. E., Dunbar, D. R. and Mullins, J. J. (2007). Cryptic loxP sites in mammalian genomes: genome-wide distribution and relevance for the efficiency of BAC/PAC recombineering techniques. *Nucleic Acids Res* **35**, 1402-10.

Sharp, T. V., Al-Attar, A., Foxler, D. E., Ding, L., de, A. V. T. Q., Zhang, Y., Nijmeh, H. S., Webb, T. M., Nicholson, A. G., Zhang, Q. et al. (2008). The chromosome 3p21.3-encoded gene, LIMD1, is a critical tumor suppressor involved in human lung cancer development. *Proc Natl Acad Sci U S A* **105**, 19932-7.

Silver, D. P. and Livingston, D. M. (2001). Self-excising retroviral vectors encoding the Cre recombinase overcome Cre-mediated cellular toxicity. *Mol Cell* **8**, 233-43.

Steigemann, P. and Gerlich, D. W. (2009). An evolutionary conserved checkpoint controls abscission timing. *Cell Cycle* **8**, 1814-5.

Storchova, Z. and Kuffer, C. (2008). The consequences of tetraploidy and aneuploidy. *J Cell Sci* **121**, 3859-66.

Sullivan, M. and Morgan, D. O. (2007). Finishing mitosis, one step at a time. *Nat Rev Mol Cell Biol* **8**, 894-903.

Takafuta, T., Saeki, M., Fujimoto, T. T., Fujimura, K. and Shapiro, S. S. (2003). A new member of the LIM protein family binds to filamin B and localizes at stress fibers. *J Biol Chem* **278**, 12175-81.

Tang, Y. C., Williams, B. R., Siegel, J. J. and Amon, A. (2011). Identification of Aneuploidy-Selective Antiproliferation Compounds. *Cell*.

Tarutani, M., Itami, S., Okabe, M., Ikawa, M., Tezuka, T., Yoshikawa, K., Kinoshita, T. and Takeda, J. (1997). Tissue-specific knockout of the mouse Pig-a gene reveals important roles for GPI-anchored proteins in skin development. *Proc Natl Acad Sci U S A* **94**, 7400-5.

Thompson, S. L. and Compton, D. A. (2010). Proliferation of aneuploid human cells is limited by a p53-dependent mechanism. *J Cell Biol* **188**, 369-81.

Thyagarajan, B., Guimaraes, M. J., Groth, A. C. and Calos, M. P. (2000). Mammalian genomes contain active recombinase recognition sites. *Gene* **244**, 47-54.

Tu, Y., Wu, S., Shi, X., Chen, K. and Wu, C. (2003). Migfilin and Mig-2 link focal adhesions to filamin and the actin cytoskeleton and function in cell shape modulation. *Cell* **113**, 37-47.

Uetake, Y. and Sluder, G. (2004). Cell cycle progression after cleavage failure: mammalian somatic cells do not possess a "tetraploidy checkpoint". *J Cell Biol* **165**, 609-15.

Uetake, Y. and Sluder, G. (2010). Prolonged prometaphase blocks daughter cell proliferation despite normal completion of mitosis. *Curr Biol* **20**, 1666-71.

Vervenne, H. B., Crombez, K. R., Delvaux, E. L., Janssens, V., Van de Ven, W. J. and Petit, M. M. (2009). Targeted disruption of the mouse Lipoma Preferred Partner gene. *Biochem Biophys Res Commun* **379**, 368-73.

Vitale, I., Galluzzi, L., Senovilla, L., Criollo, A., Jemaa, M., Castedo, M. and Kroemer, G. (2010a). Illicit survival of cancer cells during polyploidization and depolyploidization. *Cell Death Differ*.

Vitale, I., Senovilla, L., Jemaa, M., Michaud, M., Galluzzi, L., Kepp, O., Nanty, L., Criollo, A., Rello-Varona, S., Manic, G. et al. (2010b). Multipolar mitosis of tetraploid cells: inhibition by p53 and dependency on Mos. *Embo J* **29**, 1272-84.

Wong, C. and Stearns, T. (2005). Mammalian cells lack checkpoints for tetraploidy, aberrant centrosome number, and cytokinesis failure. *BMC Cell Biol* **6**, 6.

Yang, J., Meyer, M., Muller, A. K., Bohm, F., Grose, R., Dauwalder, T., Verrey, F., Kopf, M., Partanen, J., Bloch, W. et al. (2010). Fibroblast growth factor receptors 1 and 2 in keratinocytes control the epidermal barrier and cutaneous homeostasis. *J Cell Biol* **188**, 935-52.

Yi, J., Kloeker, S., Jensen, C. C., Bockholt, S., Honda, H., Hirai, H. and Beckerle, M. C. (2002). Members of the Zyxin family of LIM proteins interact with members of the p130Cas family of signal transducers. *J Biol Chem* **277**, 9580-9.

Zhang, Y., Tu, Y., Gkretsi, V. and Wu, C. (2006). Migfilin interacts with vasodilator-stimulated phosphoprotein (VASP) and regulates VASP localization to cell-matrix adhesions and migration. *J Biol Chem* **281**, 12397-407.

Zhao, J., Zhang, Y., Ithychanda, S. S., Tu, Y., Chen, K., Qin, J. and Wu, C. (2009). Migfilin interacts with Src and contributes to cell-matrix adhesion-mediated survival signaling. *J Biol Chem* **284**, 34308-20.

Zheng, Q. and Zhao, Y. (2007). The diverse biofunctions of LIM domain proteins: determined by subcellular localization and protein-protein interaction. *Biol Cell* **99**, 489-502.

Zhivotovsky, B. and Kroemer, G. (2004). Apoptosis and genomic instability. *Nat Rev Mol Cell Biol* **5**, 752-62.

Abbreviations

+, wild-type allele; -, null allele; Atm, Ataxia telangiectasia mutated protein; BSA, bovine serum albumin; C, number of chromosomal complements; CIN, chromosomal instability; DAPI, 4',6-Diamidino-2-phenylindole; DMBA, 7,12-Dimethylbenz(a)anthracene; FA, focal adhesion; FACS, flow cytometry; FBLP-1, Fblim1, Filamin-binding LIM protein 1; fl, floxed allele; FN, fibronectin; H/E, Hematoxylin/Eosin; HF, hair follicle; HRP, horse radish peroxidase; IB, immuno blot, IF, immunofluorescence; IR, ionizing radiation; K5, Keratin 5; K14, Keratin 14; LIM, Lin-11/Isl-1/Mec-3; MEF, mouse embryonic fibroblast; n, number of samples; N, number of monoploid chromosomes; NES, nuclear export signal; PBS, phosphate buffered saline; RT, room temperature; SEM, standard error of the mean; TAK1, Transforming growth factor β -activated kinase 1; TBS, Tris-buffered saline; TPA, 12-O-Tetradecanoylphorbol-13-acetate.

Figure Legends

Figure 1. Cre-expression in migfilin-null epidermis leads to a lethal hyperplastic skin defect.

(A) Hematoxylin/Eosin (H/E) stainings of Migfilin^{+/+} and Migfilin^{-/-} back skin at P21 or P28. Bar: 50 μ m. (B) Immunoblot (IB) analysis for Migfilin and Gapdh expression in indicated tissues isolated from Migfilin^{+/+} mice. (C) Immunofluorescence (IF) stainings (green: migfilin, red: vinculin, blue: DNA) of primary keratinocytes with 50 μ M CaCl₂ and 24 hours after induction of cell-cell contacts with 1 mM CaCl₂. Bars: 50 μ m. (D) Image of P8 Migfilin^{fl/+}, Migfilin^{fl/+;K5Cre+}, and Migfilin^{fl/fl;K5Cre+} littermates. (E) Weight gain curve of controls (green, Migfilin^{fl/fl} or Migfilin^{fl/+}; n=14), Migfilin^{fl/+;K5Cre+} (blue, n=5) and Migfilin^{fl/fl;K5Cre+} (red, n=4) pups. Dots indicate mean \pm standard error of the mean (SEM). (F) H/E stainings of P8 Migfilin^{fl/fl} and Migfilin^{fl/fl;K5Cre+} back skin. Bar: 100 μ m. E, epidermis; d, dermis; s, sub-cutis; m, muscle. (G-J) IF stainings of P8 back skin sections of the indicated genotype with the indicated, color-coded antibodies. Bars: 50 μ m. (K) Masson-Fontana stainings of P8 back skin of the indicated genotypes. Melanocytes are dyed black. Hair shafts are indicated by stars (*). Bar: 50 μ m.

Figure 2. Skin defect severity depends on Cre gene dosage.

(A) IB analysis of Cre expression in P4 epidermis of Migfilin^{+/-} mice with the indicated Cre transgenes. Gapdh serves as loading control. (B) Image of P9 Migfilin^{+/-}, Migfilin^{+/-;K14Cre+}, and Migfilin^{+/-;K5Cre+/K14Cre+} littermates. (C) H/E stainings of P4 back skin of the indicated genotypes. Melanocytes are dyed brown. Bar: 50 μ m.

Figure 3. Terminal differentiation and barrier function in Migfilin^{fl/fl;K5Cre+} epidermis are normal.

(A-P) Immunofluorescence (IF) staining of cryo-embedded P8 back skin sections of the indicated genotypes with the indicated, color-coded antibodies. HFs are indicated by white stars (*). Bars: 50 μ m. **(Q)** Surface expression levels of the indicated integrins measured by flow cytometry of freshly isolated keratinocytes of the indicated genotype. 9EG7 recognizes active β 1 integrin, maximal β 1 integrin activation was enforced by addition of 1 mM MnCl₂ for 10 Minutes on ice. Legend: Migfilin^{+/+} (green), Migfilin^{-/-} (red), Migfilin^{-/-;K5Cre+} (blue), isotype control (grey). **(R)** Trans-epidermal water loss (TEWL) measurements with P3 Migfilin^{+/+}, Migfilin^{-/-}, Migfilin^{+/+;K5Cre+}, Migfilin^{-/-;K5Cre+} mice. The mean is indicated by a black line. **(S)** Cryo-sections of P7 Migfilin^{fl/fl} and Migfilin^{fl/fl;K5Cre+} back skin after immersion in LuciferYellow dye (green). Nuclei are stained with DAPI (blue). The basement membrane is indicated by a dashed line. Bar: 50 μ m.

Figure 4. Altered cellularity and apoptosis rates in Migfilin^{-/-;K5Cre+} epidermis.

(A) Upper panel: H/E staining of P6 back skin of the indicated genotypes. Lower panel: IF stainings (green: Itga6, blue: DNA) of epidermal whole mounts and imaged onto the basal surface of epidermis. Arrowheads point to binucleated cells. Bars: 50 μ m. **(B-E)** Epidermal morphometry. Epidermal thickness (B), number of nucleated cell layers (C), number of basal nuclei per mm epidermis (D) and absolute number of Ki67⁺ keratinocytes per mm epidermis (E) by age and genotype of mice. Bars indicate mean \pm SEM. Legend: Migfilin^{+/+} (green), Migfilin^{-/-} (red), Migfilin^{+/+;K5Cre+} (black), Migfilin^{-/-;K5Cre+} (grey). Significance was tested using two-tailed, unpaired Student tests and is indicated if p<0.05. **(F)** Representative IF stainings (green: LM-

322, red: Ki67, blue: DNA) of back skin used for measurements shown in Figure 4B-E. Bar: 50 μ m. **(G)** Quotient of absolute number of Ki67+ keratinocytes (Figure 4E) per mm and respective number of basal nuclei (Figure 4F) by age and genotype. **(H)** Absolute numbers of apoptotic cells per mm epidermis by age and genotype. **(I)** Representative IF stainings (green: cleaved Casp3, red: Itga6, blue: DNA) of back skin used for measurements shown in Figure 4H. Bar: 50 μ m.

Figure 5. Migfilin^{-/-};K5Cre⁺ keratinocytes have increased ploidy levels, but normal DNA damage response and DNA damage levels.

(A) Relative frequencies of freshly isolated P3 basal keratinocytes with respect to DNA contents (2C, 2C to 4C, 4C, or >4C). Significance was tested using two-tailed, unpaired Student tests and is indicated if $p < 0.05$. Legend: Migfilin^{+/+} (green), Migfilin^{-/-} (red), Migfilin^{+/+};K5Cre⁺ (black), Migfilin^{-/-};K5Cre⁺ (grey). **(B)** Representative flow cytometry plots used to generate Figure 5A. Freshly isolated P3 keratinocytes of the indicated genotypes were gated for Itga6-expression, RNase treated and DNA dyed with propidium iodide (PI). Analysis was done with the Watson Pragmatic algorithm and given as number of chromosomal complements C. **(C)** Duration of mitosis (time between dissolution and re-condensation of nuclear membrane) of freshly isolated keratinocytes measured by 24 hour time lapse microscopy. IR, irradiation with 5 Gy 24 hours before start of experiment. **(D)** IF stainings (green: α -Tubulin, red: Aurora B pT232, blue: DNA) of Migfilin^{+/+} and Migfilin^{-/-} keratinocytes during late cytokinesis. IR, irradiation with 5 Gy 24 hours before staining. Bar: 10 μ m. **(E)** Number of pS139-H2ax foci over time in primary keratinocytes after irradiation with 5 Gy IR. **(F)** Flow cytometry analysis of pS139-H2ax levels and side scatter (SSC) in freshly isolated keratinocytes of the indicated genotypes. Legend: Migfilin^{+/+} (green), Migfilin^{-/-} (red),

Migfilin^{+/+;K5Cre+} (black), Migfilin^{-/-;K5Cre+} (blue), isotype control (grey). **(G)** Representative FACS plots used to generate Figure 5F. Freshly isolated P3 keratinocytes of the indicated genotypes were stained for pS139-H2ax. For positive control, Migfilin^{+/+} keratinocytes were irradiated with 5 Gy IR and analyzed after 1 hour (Migfilin^{+/+} IR, green+grey). **(H)** IB analysis of epidermal pS9181-Atm and pS345-Chk1 in triplicate Migfilin^{+/+;K5Cre+} and Migfilin^{-/-;K5Cre+} P3 epidermal lysates. As positive control for pS1981-Atm primary Migfilin^{+/+} keratinocytes were treated for 1 hour with 5 μ M Cisplatin before lysis. As positive control for pS345-Chk1 primary Migfilin^{+/+} keratinocytes were irradiated with 500 J/m² UV/B 24 hours before lysis. Equal loading is indicated by E-cadherin or Gapdh signal intensities. **(I)** IB analysis of epidermal expression of the indicated proteins in triplicate Migfilin^{+/+;K5Cre+} and Migfilin^{-/-;K5Cre+} P3 epidermis. Equal loading is indicated by Gapdh signal intensities.

Figure 6. Loss of p53 aggravates defects in Migfilin^{-/-;K5Cre+} epidermis.

(A) IB analysis of epidermal expression of the indicated proteins in triplicate Migfilin^{+/+;K5Cre+} and Migfilin^{-/-;K5Cre+} P3 epidermis. Equal loading is indicated by Gapdh signal intensities. **(B)** IB analysis of epidermal expression of the indicated proteins in P3 back skin of the indicated genotypes. Equal loading is indicated by Gapdh signal intensities. **(C)** H/E stainings of P3 back skin of the indicated genotypes. Bar: 50 μ m. **(D)** Photograph of P3 pups of the indicated genotype. **(E-H)** Epidermal morphometry. Epidermal thickness (E), number of Ki67+ keratinocytes per mm epidermis (F), number of basal nuclei per mm epidermis (G), and number of apoptotic cells per mm epidermis (H) by age and genotype of mice. Legend: Migfilin^{-/-;Trp53^{fl/fl}} (red), Migfilin^{-/-;K5Cre+;Trp53^{fl/fl}} (white), Migfilin^{-/-;K5Cre+;Trp53^{fl/+}} (grey) and

Migfilin^{-/-;K5Cre+;Trp53^{+/+}} (black). Bars indicate mean±SEM. Significance was tested using two-tailed, unpaired Student tests and is indicated if p<0.05.

Figure 7. Migfilin acts as a tumor suppressor in the DMBA/TPA skin cancer model.

(A) Tumor-free survival over time of C57BL/6 Migfilin^{+/+} (green, n=23) or Migfilin^{-/-} (red, n=29) mice treated by DMBA/TPA regime. Significance was tested with the log rank test. **(B)** Tumor number over time of (A). Dots indicate mean±SEM. Significance was tested by One-way ANOVA. **(C)** Relative numbers of skin papillomas of (A), binned by size as indicated in the legend. **(D-I)** H/E stainings of representative DMBA-initiated skin tumors of Migfilin^{+/+} and Migfilin^{-/-} mice after 32 weeks of TPA-promotion. Representative, well-differentiated Migfilin^{+/+} (D,E) or Migfilin^{-/-} tumors (F,G). (H) Migfilin^{-/-} nodular tumor with high grade of inflammatory infiltration. (I) Migfilin^{-/-} spindle cell carcinoma. Bar: 500 μm (a, c) or 125 μm (b, d-f). **(J)** H/E staining of Migfilin^{+/+} and Migfilin^{-/-} back skin 2 days after triple treatment with TPA or acetone every 2 days. Bar: 50 μm. **(K)** Model for migfilin-mediated suppression of tetraploidy. After Cre-mediated generation of tetraploid cells, these could either further proliferate, arrest in G1/G0, or undergo apoptosis. Migfilin could either facilitate tetraploid cell death (a) or interfere with their proliferation (b).

Tables

Table 1. Mendelian ratios

Intercrossing	No. of offspring	Genotype	Real (ideal) percentage	p(Chi ²)
Migfilin ^{+/-} ;K5Cre ⁺ x Migfilin ^{+/-}	807	Migfilin ^{+/+}	14.5% (12.5%)	} 2.0 * 10 ⁻⁶
		Migfilin ^{+/-}	30.7% (25.0%)	
		Migfilin ^{-/-}	11.9% (12.5%)	
		Migfilin ^{+/+} ;K5Cre ⁺	10.2% (12.5%)	
		Migfilin ^{+/-} ;K5Cre ⁺	25.4% (25.0%)	
		Migfilin ^{-/-} ;K5Cre ⁺	7.3% (12.5%)	

Table 2. Antibodies

Antigen	Source	IB	IF	Flow.
Migfilin	(Moik et al., 2011)	1:2000	1:100	
Kindlin-2	(Montanez et al., 2008)		1:500	
Atm pS1981	Rockland 600-601-400	1:1000		
Aurora B pT232	Rockland 600-401-677		1:200	
clCasp3	Cell Signaling Technology 9661	1:1000	1:100	
Ctnnb1	Sigma C2206		1:1000	
Cyclin A1	Santa Cruz sc751	1:200		
Cyclin B1	Millipore 05-158	1:1000		
Cyclin D1/2	Millipore 05-362	1:1000		
Cyclin E	Millipore 06-459	1:1000		
Desmoplakin	Research Diagnostics, no longer available		1:100	
E-cadherin	Zymed 13-1900		1:200	
Gapdh	Millipore MAB374	1:30000		
H2ax pS139	Millipore 05-636			1:1000
Itgb1	Millipore MAB1997		1:400	1:200
Itgb1 9EG7	BD Pharmingen 550531		1:400	1:100
Itga6	BD Pharmingen 555735		1:200	1:200
Ki67	DakoCytomation M7249		1:800	
Loricrin	Covance PRB-145P		1:400	
Lm322	R14 by Monique Aumailley (University of Cologne, Germany)		1:1500	
Keratin 5	Covance PRB-160P		1:400	
Keratin 6	Covance PRB-169P		1:400	
Keratin 10	Covance PRB-159P		1:400	
p53	Cell Signaling Technology 2524	1:1000		
p53 S18	Cell Signaling Technology 9284	1:1000		
α -Tubulin	Millipore MAB1864		1:400	
Vinculin	Sigma V9131		1:1000	

Figure 1 - Moik et al. 2011b

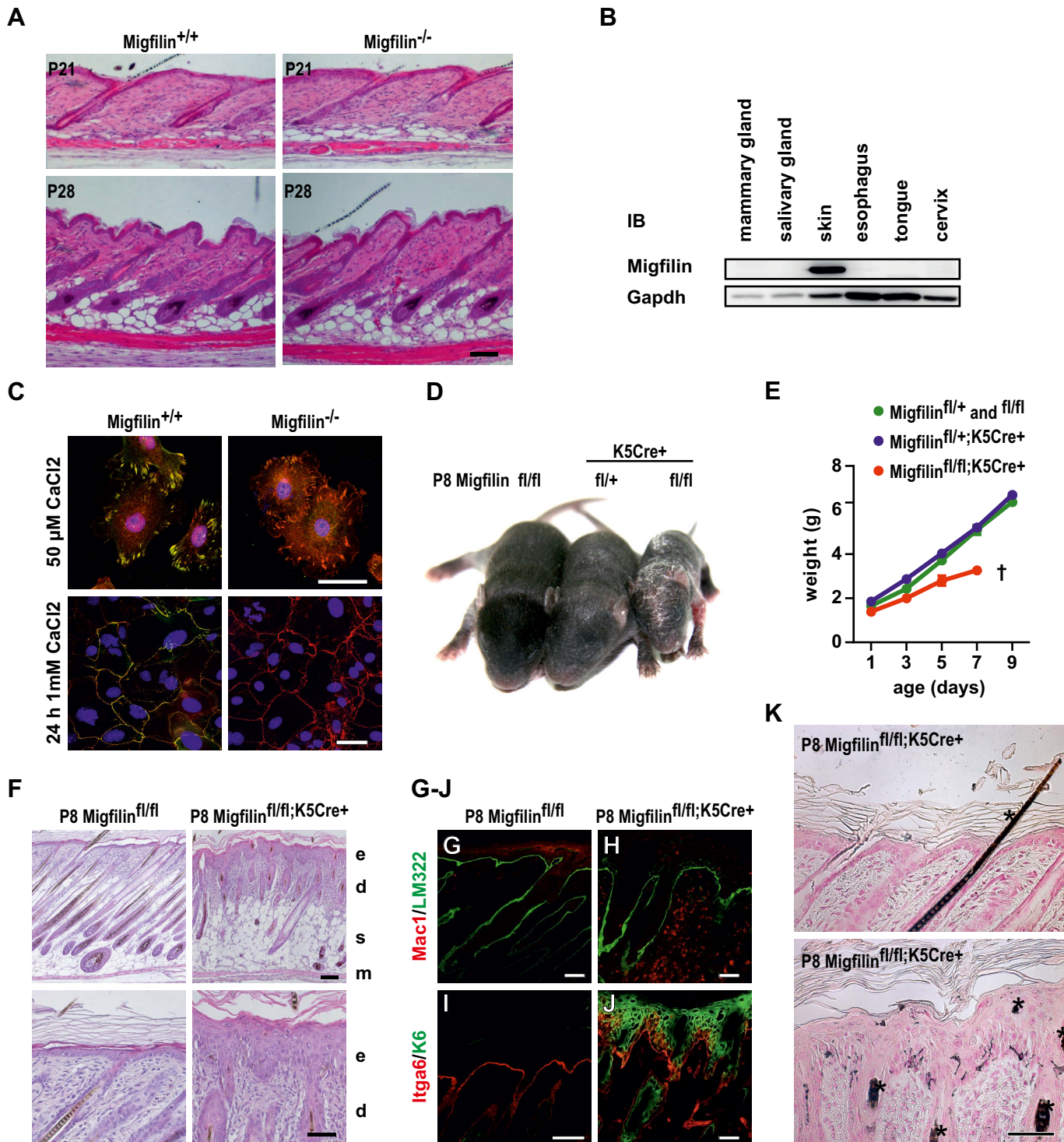
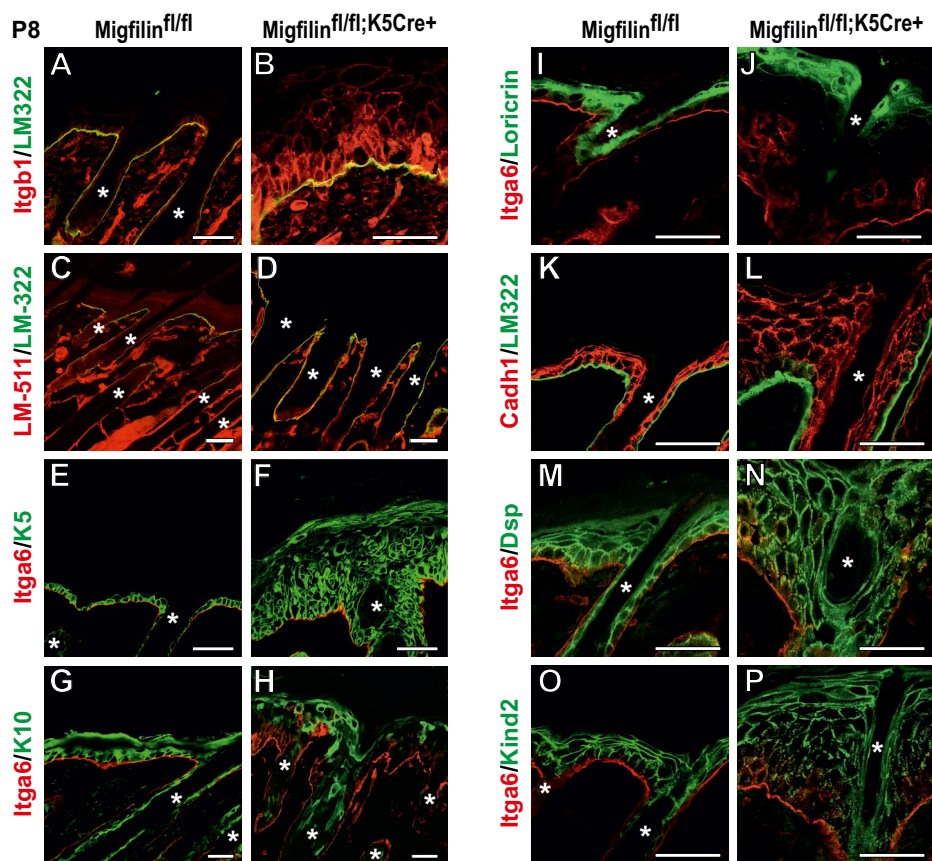
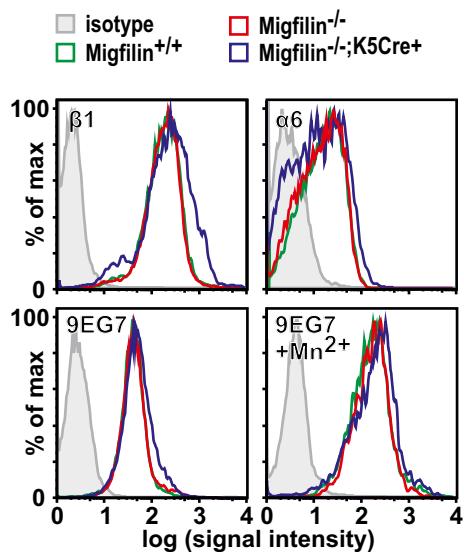


Figure 3 - Moik et al. 2011b

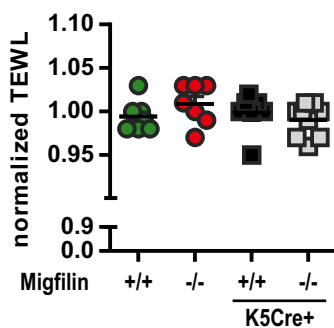
A-P



Q



R



S

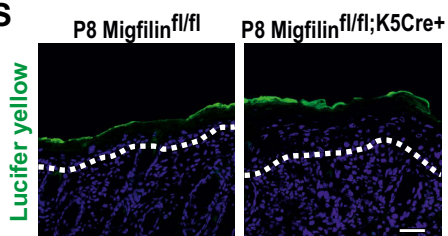
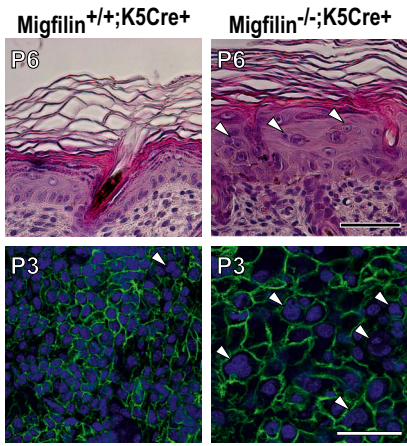
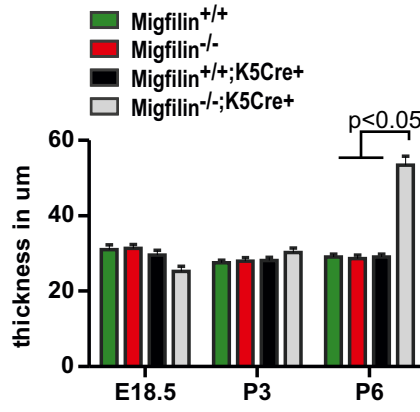


Figure 4 - Moik et al. 2011b

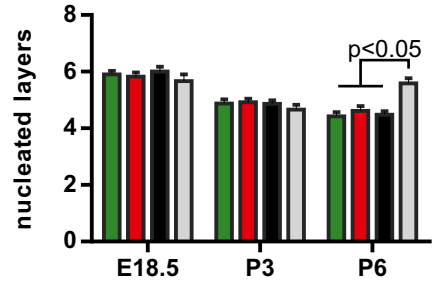
A



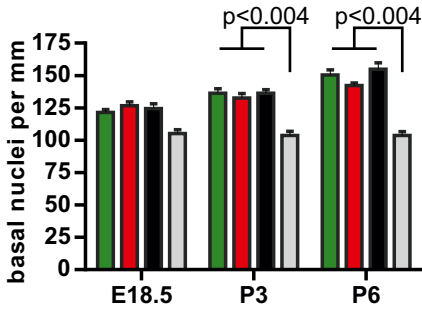
B



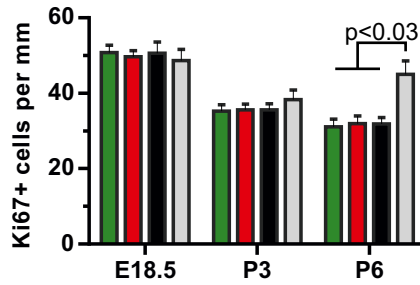
C



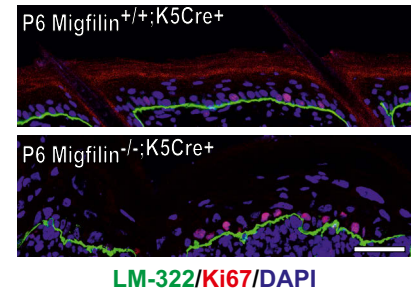
D



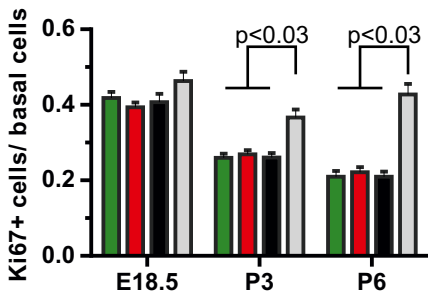
E



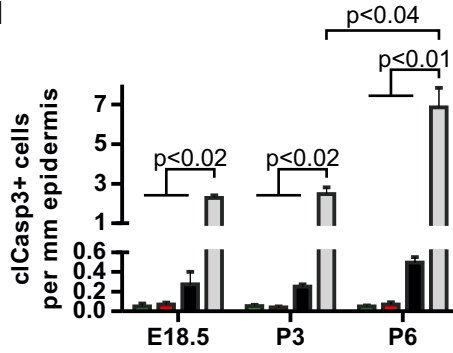
F



G



H



I

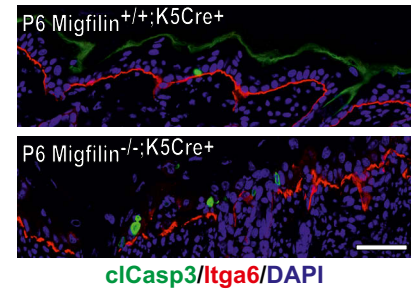


Figure 5 - Moik et al. 2011b

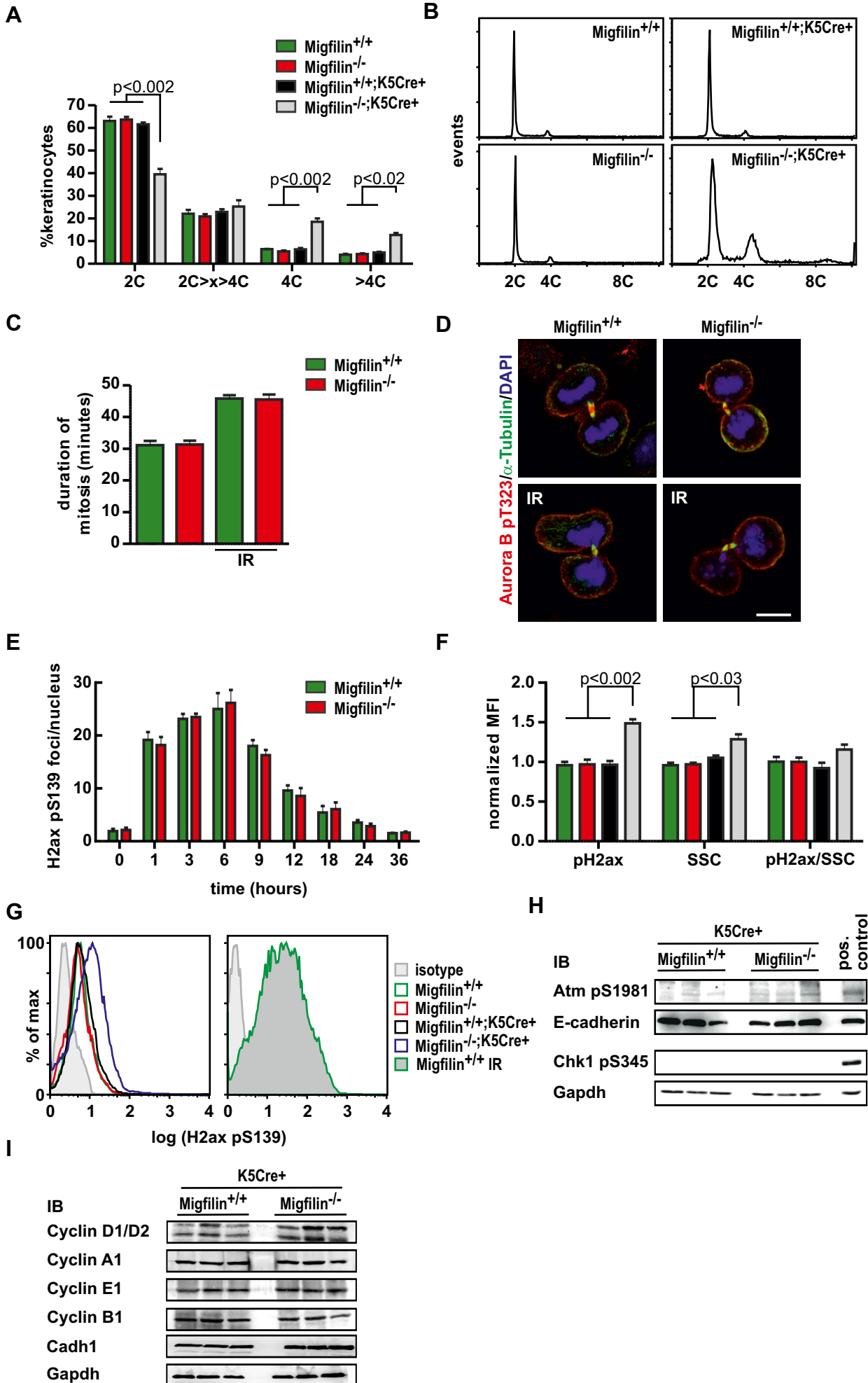


Figure 6 - Moik et al. 2011b

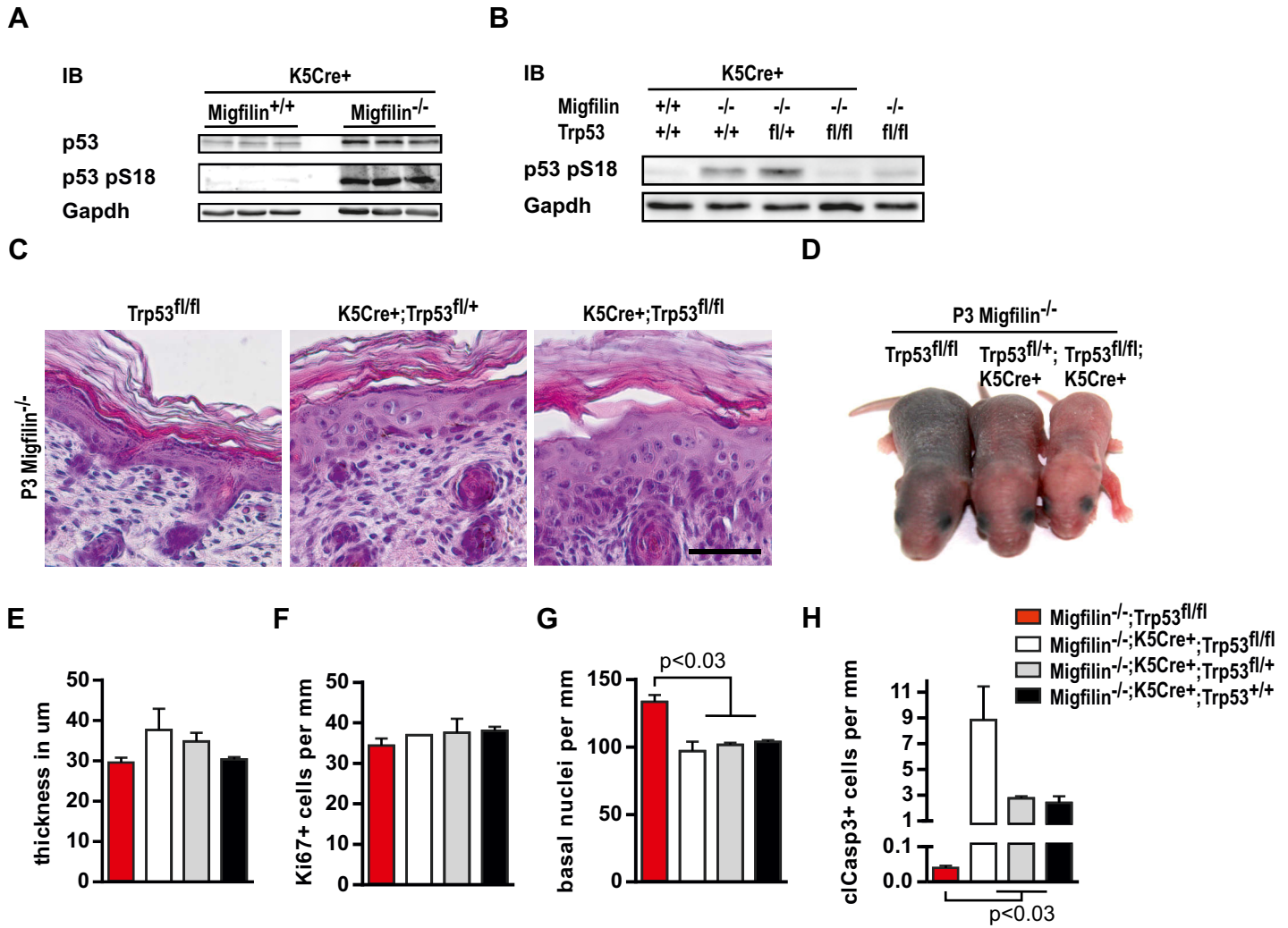


Figure 7 - Moik et al. 2011b

